

2016-03-31

Autonomous Brain-Controlled Functional Electrical Stimulation for Grasp and Release in Complete Cervical Spinal Cord Injury

Katie Gant

University of Miami, gant.katie@gmail.com

Follow this and additional works at: https://scholarlyrepository.miami.edu/oa_dissertations

Recommended Citation

Gant, Katie, "Autonomous Brain-Controlled Functional Electrical Stimulation for Grasp and Release in Complete Cervical Spinal Cord Injury" (2016). *Open Access Dissertations*. 1587.

https://scholarlyrepository.miami.edu/oa_dissertations/1587

This Embargoed is brought to you for free and open access by the Electronic Theses and Dissertations at Scholarly Repository. It has been accepted for inclusion in Open Access Dissertations by an authorized administrator of Scholarly Repository. For more information, please contact repository.library@miami.edu.

UNIVERSITY OF MIAMI

AUTONOMOUS BRAIN-CONTROLLED FUNCTIONAL ELECTRICAL
STIMULATION FOR GRASP AND RELEASE
IN COMPLETE CERVICAL SPINAL CORD INJURY

By

Katie Gant

A DISSERTATION

Submitted to the Faculty
of the University of Miami
in partial fulfillment of the requirements for
the degree of Doctor of Philosophy

Coral Gables, Florida

May 2016

©2016
Katie Gant
All Rights Reserved

UNIVERSITY OF MIAMI

A dissertation submitted in partial fulfillment of
the requirements for the degree of
Doctor of Philosophy

AUTONOMOUS BRAIN-CONTROLLED FUNCTIONAL ELECTRICAL
STIMULATION FOR GRASP AND RELEASE
IN COMPLETE CERVICAL SPINAL CORD INJURY

Katie Gant

Approved:

Abhishek Prasad, Ph.D.
Assistant Professor of Biomedical
Engineering

Jorge Bohorquez, Ph.D.
Associate Professor in Practice of
Biomedical Engineering

Justin C. Sanchez, Ph.D.
Associate Professor of Biomedical
Engineering

Joyce Gomes-Osman, PT, Ph.D.
Assistant Professor of Physical
Therapy

Kim Anderson Erisman, Ph.D.
Research Associate Professor,
The Miami Project to Cure Paralysis

Guillermo Prado, Ph.D.
Dean of the Graduate School

GANT, KATIE
Autonomous Brain-Controlled Functional Electrical
Stimulation for Grasp and Release
in Complete Cervical Spinal Cord Injury

(Ph.D., Biomedical Engineering)
(May 2016)

Abstract of a dissertation at the University of Miami.

Dissertation supervised by Professor Abhishek Prasad.
No. of pages in text. (140)

There are over 33,000 people in the United States living with complete tetraplegia due to traumatic spinal cord injury (SCI). These individuals rely heavily on family and caregivers as they are unable to perform many activities of daily living. People with complete tetraplegia rank restoration of hand and arm function as their highest priority, as it would offer greater independence and improved quality of life. In this study, we show that subjects with chronic (>1-year post-injury) C5/C6-level, motor-complete SCI are able to control a brain computer interface-functional electrical stimulation (BCI-FES) system to perform a hand grasp and release task.

Electroencephalographic (EEG) signals were acquired using a 20-channel wireless EEG system and input to a BCI, which enabled autonomous control over FES of paralyzed muscles for hand grasp and release. A novel stimulation configuration and control paradigms were developed in order to provide reliable activation of the muscles responsible for hand movements. Input features and decoding strategies were evaluated from subjects with SCI, as well as uninjured, control subjects. After optimization of the BCI-FES system and experimental paradigm, 5 subjects with C5/C6, motor complete spinal cord injury and 5 uninjured, control subjects participated in 6 sessions of closed-

loop BCI-FES. Subjects were asked to imagine opening and closing their right hand during the trials for motor imagery. Average power in 5 Hz bins (5-35 Hz) was extracted from C3, C1, Cz, C2, and C4 electrodes and input as features to a Support Vector Machine classification algorithm. When “movement intention” was classified correctly from the motor imagery period, a custom stimulation sequence was delivered to the forearm muscles via surface electrodes to enable opening and closing of the hand for grasp and release. Spinal cord injured subjects produced an average of $21.0\% \pm 3.9\%$ event-related desynchronization and control subjects averaged $13.5\% \pm 3.2\%$. Average decoding accuracy was similar, at $73.3\% \pm 5.6\%$ in the spinal cord injury group and $73.6\% \pm 3.8\%$ in the control group. Over the course of experiments, average event-related desynchronization increased significantly in the SCI group and decoding accuracy improved. This study demonstrates that subjects with motor complete, cervical SCI were able to control a BCI-FES system with performance levels as high as healthy controls with minimal training. Non-invasive BCI-FES systems may have the potential to restore hand function in people with motor-complete SCI, which would increase independence and improve quality of life.

ACKNOWLEDGMENTS

I would like to thank all of the research subjects who volunteered their time to participate in my experiments. They always showed up with positive attitudes, worked hard, and were willing to try new things.

Abhishek Prasad was the best advisor that I could have ever asked for. There were many times throughout this process when I felt discouraged, but his constant support, guidance, and patience always lifted me back up. I would also like to thank Jorge Bohorquez for his encouragement and advice over the years and Justin Sanchez for introducing me to the world of neuroprosthetics research.

I thank my mom, Jane, for the sacrifices she made to provide me with the opportunity to pursue higher education. She modeled strength, compassion, and love throughout my childhood and continues to do so, making positive impacts in many people's lives through her work and personal life.

I would like to thank my husband, Colin, for his love and support throughout this long process. He has always pushed me to do what I love, because life is too short to not enjoy your work. He gives me the strength to take risks, because I know he will always be there to pick me up, dust me off, and push me forward again.

I dedicate my degree to our daughter, Henley, who was born during my time as a PhD student. I wish for her to have the confidence, drive, and grit to forge her own path and keep moving forward when times get tough. "You have brains in your head. You have feet in your shoes. You can steer yourself any direction you choose. You're on your own. And you know what you know. And YOU are the one who'll decide where to go..."

— Dr. Seuss, *Oh, The Places You'll Go!*

TABLE OF CONTENTS

	Page
LIST OF FIGURES	vi
LIST OF TABLES	xiii
Chapter	
1 INTRODUCTION	1
1.1 Spinal Cord Injury.....	1
1.2 Recovery of Hand Function	3
1.3 Functional Electrical Stimulation	6
1.4 Brain-Computer Interface Technology	10
1.5 BCI- FES.....	12
1.5.1 Neural Control Signals.....	13
1.5.2 Previous Studies.....	14
1.5.3 Error Signals	19
1.6 Functional Outcome Measures	22
1.7 Research Goals.....	24
2 GENERAL METHODS	26
2.1 Subject Recruitment and Screening	26
2.2 Neural Data Acquisition	26
2.3 Muscle Stimulation	28
2.3.1 Bioness.....	28
2.3.2 Digitimer	29
2.4 BCI Architecture.....	30
2.4.1 Closed-Loop Control	31
2.4.2 Incorporating Reinforcement Learning.....	32
3 PRELIMINARY BCI-FES EXPERIMENTS.....	34
3.1 Subjects.....	34
3.2 Experiment Protocol	35
3.3 Neural Signal Processing and Decoding.....	37
3.4 Results.....	40
3.5 Conclusion	45
3.6 Lessons Learned.....	47
4 CUSTOM FES CONTROL PARADIGM	50
4.1 Control Paradigm for Delivering Stimulation	50
4.2 Safety and Efficacy of Stimulation Protocol	56
4.3 Conclusion	58

5	FEATURES FOR BCI-FES CONTROL.....	59
5.1	Subjects.....	59
5.2	Experiment Protocol.....	59
5.3	Results.....	61
5.4	Conclusion.....	70
6	ASSESSMENT OF FUNCTION.....	72
6.1	Subjects.....	72
6.2	Experiment Protocol.....	72
6.3	Results.....	75
6.4	Conclusion.....	78
7	BCI-FES FOR GRASP AND RELEASE.....	80
7.1	Subjects.....	80
7.2	Experiment Protocol.....	80
7.3	Results.....	85
7.3.1	Neural Features for Decoding.....	85
7.3.2	BCI Decoding Accuracy.....	92
7.3.3	ERD Changes and Decoder Performance over Time.....	93
7.3.4	Functional Assessment and Muscle Fatigue in SCI Group.....	94
7.4	Conclusion.....	99
	REFERENCES.....	104
	APPENDIX.....	117
	Arduino Code for Muscle Stimulation.....	117
	Matlab Code for Experiment: First Training Block.....	120
	Matlab Code for Experiment: Subsequent Training Blocks.....	129

LIST OF FIGURES

1.1	ASIA standard neurological classification of spinal cord injury.	2
1.2	Function that would most improve the quality of life for people with tetraplegia [1].	3
1.3	Cumulative mean increase in ASIA motor score of ASIA A patients within two years of spinal cord injury. The most rapid improvement occurs within the first 6 months after SCI and is essentially maximal after 12 months [2].	4
1.4	Normalized cortical motor map from right biceps brachii muscle before and after intervention. Left wall of the figure represents the midline of the sagittal plane. Cz represents the point at which the line between the nasion and inion intersects with the interaural line. Note that, during the preintervention test, the majority of the active sites were located posterior to Cz. Following the intervention, the map shifted anteriorly. Note also that motor-evoked potentials (MEPs) could be evoked from a greater number of sites following intervention [3].	6
1.5	Strength duration curves for nerve and muscle. Data from cat tibialis anterior muscle [4].	7
1.6	Stimulus charge/parameter comparisons. Three stimulus trains that have the same total charge, but very different parameters [5].	9
1.7	Basic design and operation of any BCI system. Signals from the brain are acquired by electrodes on the scalp or in the head and processed to extract specific signal features (e.g. amplitudes of evoked potentials or sensorimotor cortex rhythms, firing rates of cortical neurons) that reflect the user's intent. These features are translated into commands that operate a device (e.g. a simple word processing program, a wheelchair, or a neuroprosthesis). Success depends on the interaction of two adaptive controllers, user and system. The user must develop and maintain good correlation between his or her intent and the signal features employed by the BCI; and the BCI must select and extract features that the user can control and must translate those features into device commands correctly and efficiently [6].	11
1.8	Event-related desynchronization and synchronization. Average ERD/ERS time course during slow voluntary movements of the right index finger (movement duration = 1.6 – 2.1 sec) [7].	14

1.9	Signal processing methods utilized in Graz-BCI studies. Bandpass filtered (15-19 Hz) EEG channels C3 and Cz recorded during the first 3 foot movement imaginations (i1, i2 and i3) of one complete grasp sequence (A,C). The vertical lines indicate the start-on of the individual grasp phases. (B, D) Bandpower time courses (15–19 and 20–60 Hz) of EEG channels C3 and Cz averaged over the five grasp phases with movement start at second 0 (amplitudes in arbitrary units) [8].	17
1.10	Location of the anterior cingulate cortex in the human brain.	20
1.11	Error and correct trials. Averages of single trials recorded at FCz with respect to the side where a target appeared for five subjects and the average of them. The four cases are: a) correct trials on left side, b) correct trials on right side, c) error trials on left side, and d) error trials on left side [9].	21
2.1	Electrode configuration for a) X10 and b) X24 headsets.	27
2.2	B-Alert headset transmits neural data via Bluetooth to the external syncing unit, which is linked to the computer by USB port.	28
2.3	a) Control unit and b) neuroprosthetic wrist-hand orthosis of the Bioness H200.	29
2.4	Digitimer DS7a stimulator unit.	30
2.5	Typical BCI architecture. Neural features are extracted and decoded. The subject receives feedback, which is typically displayed on a computer screen.	31
2.6	Actor-critic model of RL BCI architecture, which provides dynamic decoding of neural features.	33
3.1	Experimental setup, including wireless EEG headset, display, and wireless FES. B. A trial consisted of a fixation cross, followed by a cue of either “open” or “close” and then feedback of either “correct” or “wrong”. A magnitude plot also showed the unthreshholded output of the motor potential classifier.	36
3.2	Multilayer perceptron. Weights at the hidden layer (w_h) and output layer (w_o) are updated by Hebbian learning techniques.	39
3.3	Flowchart of the steps of the experiment.	40

3.4	Sample trials from closed-loop sessions for motor signals. Columns show samples for cues of “open” and “close” for both the SCI and control subject. Rows show raw EEG from electrode C3 (top row), PSD (middle row), and Z-scores (bottom row).	41
3.5	Sample trials from closed-loop sessions for error signals. Columns show samples for cues of “open” and “close” for both the SCI and control subject. Rows show raw EEG from electrode Cz (top row), PSD (middle row), and Z-scores (bottom row).	42
3.6	Error potentials for SCI and control subject. EEG signals recorded from Cz following feedback were averaged across all trials and displayed as error-minus-correct for the SCI and control subject.	43
3.7	Motor decoder (actor) weights were updated throughout the 4 days of closed loop BCI-FES training for the A) SCI subject and B) control subject.	43
3.8	Accuracies across days. The first row shows the accuracy of the critic for both the SCI and control subjects. The second row shows the accuracy of the actor. Accuracy for each day is shown in blue. Mean accuracy across days is shown in red. Error bars represent one standard deviation. Mean accuracies were significantly above chance (50%) for both subjects ($p < 0.001$, one sided t-test).	45
4.1	Schematic of printed circuit board for switching stimulation between flexor and extensor muscles.	51
4.2	A) Schematic of printed circuit board for switching stimulation between flexor and extensor muscles. B) Arduino and PCB mounted in a custom enclosure.	52
4.3	Overall stimulation configuration. Custom Matlab programs trigger the Arduino, which is connected to the USB port of the computer. Custom stimulation protocols written to the Arduino microprocessor trigger the Digitimer at 35 Hz via a TTL pulse and switch stimulation between the flexor and extensor muscles responsible for opening and closing of the hand.	53
4.4	Positioning of active (+) and reference (-) over the A) flexor and B) extensor muscles to produce hand closing and opening, respectively.	54

4.5	Stimulation sequence for a grasp and release task. Initially, the coil for the extensor pathway is activated to allow stimulation of the extensor muscles, opening the hand for positioning around the target object. Next, the flexor pathway coil is activated and the flexor muscles are stimulated, closing the hand around the object. Finally, the extensor pathway coil is reactivated, for stimulation of the extensors, which allows the object to be released by the hand.	55
4.6	Test setup for stimulator output waveform measurements.	56
4.7	Output voltage and current waveforms with load resistance of $1k\Omega$, which mimics typical skin contact.	57
4.8	Output A & C) voltage and B & D) current waveforms with load resistance of 510Ω and $5.1k\Omega$, which mimic good skin contact and bad skin contact, respectively.	57
5.1	Timeline of experiment aimed at verifying presence of event-related desynchronization during actual and imagined movements of the right hand.	60
5.2	Discrete fast fourier transform during periods of actual hand movement (blue traces) and periods of rest/idling (red traces) in an uninjured, control subject. Raw EEG signals were averaged over trials and filtered 0.5-75 Hz.	62
5.3	Discrete fast fourier transform during periods of imagined hand movement (blue traces) and periods of rest/idling (red traces) in an uninjured, control subject. Raw EEG signals were averaged over trials and filtered 0.5-75 Hz.	63
5.4	A-C) Fitted dipole positions of clustered independent components (blue dots) for SCI subject 1, SCI subject 2, and control subject 1, respectively. Red dots represent centroids of the clusters. D-F) Scalp maps of each clustered independent component. Upper left maps represent cluster averages.	64
5.5	A-C) Power spectral density during periods of motor imagery and periods of rest/idling for SCI subject 1, SCI subject 2, and control subject 1. D-F) Normalized mean power spectral density calculated by selected independent components for all sessions in each subject. Red region represents the range of \pm one standard deviation.	65
5.6	Time course of ERD during right hand (blue) or bilateral leg (red) motor imagery averaged over the C3, C1, Cz, C2, and C4 electrodes, averaged over 10 trials, with respect to the cue in one subject with SCI.	66

5.7	Normalized power spectral density averaged over over the C3, C1, Cz, C2, and C4 electrodes for SCI subject 1 (left) and SCI subject 2 (right) during right hand and bilateral leg motor imagery, averaged over 100 trials.	67
5.8	Normalized power spectral density averaged over over the C3, C1, Cz, C2, and C4 electrodes for SCI subject 1 (left) and SCI subject 2 (right) during right hand and left hand motor imagery, averaged over 100 trials.	67
5.9	Error signals generated in response to wrong (red) and correct (blue) feedback in an uninjured, control subject. Each trace represents an average of 50 trials.	68
5.10	Two examples of error signals generated in response to wrong feedback in an uninjured, control subject. Each trace represents a single trial.	68
5.11	Error classification rates for two SCI subjects and one control subject using a Guassian mixture model classifier. Accuracy rates were around 50% for all subjects.	69
6.1	The microFET4 dynamometer is used for quantifying grip strength.	73
6.2	Subject readying to perform the Grasp and Release Test. Stimulation is delivered to the muscles responsible for opening and closing of the hand, so that the subject may grasp the object, pick it up, and move it from one side of the table to the other.	75
6.3	Average grip strength/force (\pm standard error) achieved during voluntary contraction of the muscles of the right hand, Bioness stimulation, or stimulation with the custom Digitimer/relay configuration. Stimulation parameters: 35 Hz, 200 μ s, 20-25 mA.	76
6.4	Average grip strength/force (+ standard error) achieved during electrical stimulation of paralyzed hand muscles in SCI subject with Bioness (top) and Digitimer (bottom) stimulators. Stimulation parameters: 35 Hz, 200 μ s, 40 mA.	77
6.5	Average success rate (%) of grasp and release task with a small diameter shot glass, a large diameter, lightweight, empty plastic cup, and a heavy can. The subject performed 5 attempts with each object using voluntary control (blue) and stimulation (red) at the beginning of each session.	78

- 7.1** Experimental setup. A) EEG headset transmits neural data to computer as subject responds to commands displayed on screen. FES is delivered to the muscles via surface electrodes during feedback. B) FES electrodes span the flexor and extensor muscles responsible for hand closing and opening. C) Cue-based experimental timeline for trials classified as correct (i) and wrong (ii). Audio cues sound at the beginning of the rest, motor imagery, and feedback periods. 3 seconds of data from the rest (0-3 seconds following cue) and motor imagery (0.5-3.5 seconds following cue) are used to create features for input to the classifier. **82**
- 7.2** Control signals used for decoding from one SCI (SCI subject #1) and one control subject (Control subject #2). Power spectral density averaged across 5 motor strip electrodes (C3, C1, Cz, C2, and C4) for SCI (A) and control (B) subject, averaged across 720 trials during motor imagery and rest periods (3 sec). Time course of ERD in same subset of electrodes averaged over 720 trials with respect to the motor imagery cue in SCI (C) and control (D) subject. (E,F) Morlet wavelet time-frequency plots showing ERD/ERS during rest and motor imagery. Color scale ranges from 20% ERS to 100% ERD. **87**
- 7.3** Control signals used for decoding from the remainder of SCI and Control subjects. Power spectral density averaged across 5 motor strip electrodes (C3, C1, Cz, C2, and C4), averaged across 720 trials during motor imagery and rest periods (3 sec) (left panel for each subject). Time course of ERD in same subset of electrodes averaged over 720 trials with respect to the motor imagery cue (right panel for each subject). **88-90**
- 7.4** A) Average event-related desynchronization (as a $\% \pm SE$) averaged across 5 motor strip electrodes (C3, C1, Cz, C2, and C4) during motor imagery as compared to rest in each subject (each bar represents an individual subject). B) Average ERD (as a $\% \pm SE$) in SCI and control subject groups, averaged across all subjects during full experiment. **91**
- 7.5** A) Average decoder accuracy (as a mean $\pm SE$) in 5 SCI and 5 control subjects over the entire duration of training (each bar represents an individual subject). B) Average decoder accuracy during closed-loop experiments in SCI and control groups, averaged across subjects. **92**
- 7.6** A) Average ERD (as a $\% \pm SE$) in SCI (blue) and control (red) subjects over the 6 training days (120 trials/day). B) Average decoder accuracy (as a $\% \pm SE$) during closed-loop experiments in SCI (blue) and control (red) subjects. **94**

- 7.7** A) Average grip strength (n=3 trials) in SCI subjects (n=5). A) Force generated during voluntary contractions using residual compensatory mechanisms before BCI training (Pre-BCI). B) Force generated during application of maximal stimulation before BCI-training. C) Force generated during voluntary contractions using compensatory mechanisms after BCI training (Post-BCI). D) Force generated during application of maximal stimulation after BCI-training. **96**
- 7.8** Average success rate (%) of grasp and release task with a large diameter, lightweight, empty plastic cup (A), a heavy can (B), and a small diameter shot glass (C) in one SCI subject. Subjects performed 5 attempts with each object using voluntary control (blue) and stimulation (red) at the beginning of each session. **97**
- 7.9** Average success rate (%) of grasp and release task with a large diameter, lightweight, empty plastic cup (A), a heavy can (B), and a small diameter shot glass (C) in remaining 4 SCI subjects. **98**

LIST OF TABLES

3.1	SCI subject details. Age (in years), sex (M:male, F:female), right side motor level, denervation, time since injury (in years), and whether the person participated in no experiments (-), some experiments (*), or the full protocol (**).	34
5.1	SCI subject details. Age (in years), sex (M:male, F:female), right side motor level, denervation, and time since injury (in years).	59
7.1	SCI subject details. Age (in years), time since injury (in years), cause of injury, and right side motor level. MVA = motor vehicle accident.	80



CHAPTER 1: INTRODUCTION

1.1 Spinal Cord Injury

In the United States, approximately 240,000 to 337,000 people are living with a spinal cord injury (SCI), with about 12,500 new cases occurring each year. The primary causes are motor vehicle accidents (37%), falls (29%), acts of violence (14%), and sports (9%) [10]. The average age at injury is 42 years old, and life expectancy after injury is similar to expectancies found in the general population [11]. Trauma to the spinal cord causes a disruption in the pathways connecting the brain to the muscles, resulting in muscle weakness and paralysis. Other common symptoms include loss of sensation, muscle spasticity, sexual dysfunction, breathing problems, autonomic dysreflexia, and loss of bladder and bowel function.

The level and extent of injury determines which muscles are affected and the amount of voluntary control that remains. Damage to the cervical spinal cord results in paralysis of both the upper and lower limbs to varying degrees, and is called either tetraplegia or quadriplegia. In contrast, damage to the thoracic, lumbar, or sacral cord does not involve the upper limbs and is called paraplegia. Each spinal nerve root receives sensory information from a specific area of the skin called a dermatome and sends motor information to a group of muscles called a myotome. The spinal cord segments affected by the injury can be determined by systematically testing the dermatomes and myotomes on both sides of the body. The American Spinal Injury Association (ASIA) publishes the International Standards for Neurological Classification of Spinal Cord Injury (ISNCSCI), which is revised every few years, most recently in 2011 [12]. The ISNCSCI examination

tests each dermatome and myotome separately to determine sensory and motor levels, single neurological level of injury, completeness of injury, ASIA Impairment Scale (AIS) Grading (A to E), sensory scores, motor scores, and the zone of partial preservation (Figure 1.1).


INTERNATIONAL STANDARDS FOR NEUROLOGICAL CLASSIFICATION OF SPINAL CORD INJURY (ISNCSCI)


Patient Name _____ Date/Time of Exam _____
 Examiner Name _____ Signature _____

RIGHT

MOTOR KEY MUSCLES

UER (Upper Extremity Right)

Elbow flexors C5

Wrist extensors C6

Elbow extensors C7

Finger flexors C8

Finger abductors (little finger) T1

LER (Lower Extremity Right)

Hip flexors L2

Knee extensors L3

Ankle dorsiflexors L4

Long toe extensors L5

Ankle plantar flexors S1

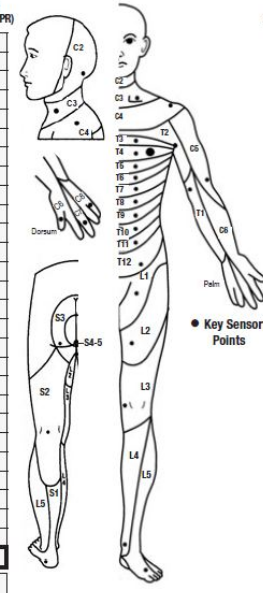
(VAC) Voluntary Anal Contraction (Yes/No)

RIGHT TOTALS (MAXIMUM) (50) (56) (56)

MOTOR SUBSCORES

UER + UEL = **UEMS TOTAL** (50)

LER + LEL = **LEMS TOTAL** (50)



● Key Sensory Points

LEFT

MOTOR KEY MUSCLES

UEL (Upper Extremity Left)

C5 Elbow flexors

C6 Wrist extensors

C7 Elbow extensors

C8 Finger flexors

T1 Finger abductors (little finger)

LEL (Lower Extremity Left)

L2 Hip flexors

L3 Knee extensors

L4 Ankle dorsiflexors

L5 Long toe extensors

S1 Ankle plantar flexors

(DAP) Deep Anal Pressure (Yes/No)

LEFT TOTALS (MAXIMUM) (50) (56) (56)

MOTOR SUBSCORES

LTR + LTL = **LT TOTAL** (56)

PPR + PPL = **PP TOTAL** (112)

NEUROLOGICAL LEVELS (Steps 1-5 for classification as on reverse)

1. SENSORY **R** **L**

2. MOTOR **R** **L**

3. NEUROLOGICAL LEVEL OF INJURY (NLJ)

4. COMPLETE OR INCOMPLETE? (Incomplete = Any sensory or motor function in S4-5)

5. ASIA IMPAIRMENT SCALE (AIS)

(In complete injuries only) **ZONE OF PARTIAL PRESERVATION** **R** **L**

Most caudal level with any intervention **SENSORY** **MOTOR**

This form may be copied freely but should not be altered without permission from the American Spinal Injury Association. REV 11/15

Figure 1.1 ASIA standard neurological classification of spinal cord injury.

Complete cervical level SCIs account for 14% of new cases and causes tetraplegia, which results in paralysis affecting all four limbs. Injuries classified as “complete” indicate that no motor or sensory function is preserved in the sacral segments S4-S5. SCIs classified as “incomplete” indicate preserved sensory function below the

neurological level of injury, as well as sacral sparing. The loss of voluntary control over the hands results in an inability to perform many activities of daily living, which in turn leads to dependence on caregivers and family. When asked to identify the function that would most dramatically improve their life, 48.7% of people with tetraplegia ranked arm/hand function as their highest priority (Figure 1.2) [1]. Restoration of hand function would offer those with high-level SCIs an increased level of independence and greatly improved quality of life.

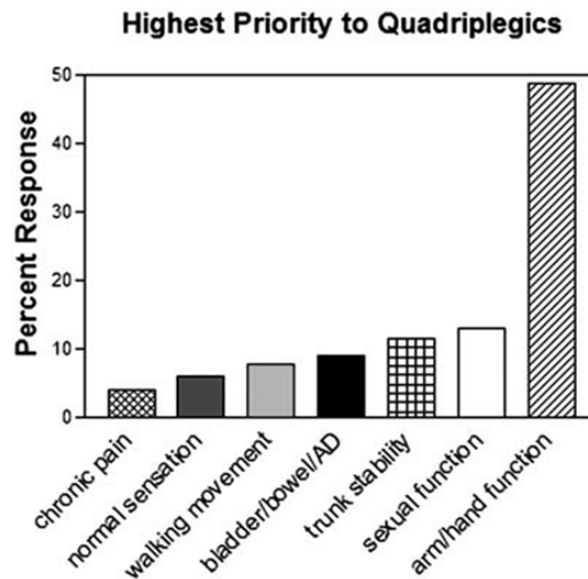


Figure 1.2 Function that would most improve the quality of life for people with tetraplegia [1].

1.2 Recovery of Hand Function

An international panel that examined the spontaneous rate of recovery following SCI [13] found that almost all people experience some recovery of motor function. The most drastic improvements are expected to occur within the first year, with the majority occurring within the first 3 months. However, additional recovery can occur for up to 18

months or more [2, 13] (Figure 1.3). Muscle groups that retain any function at all immediately following injury have a greater likelihood of regaining useful function, and the majority of functional gains occur within the zone of partial preservation. Subjects with incomplete SCI (AIS B, C, or D) experience a higher degree of spontaneous recovery than subjects with complete injuries (AIS A).

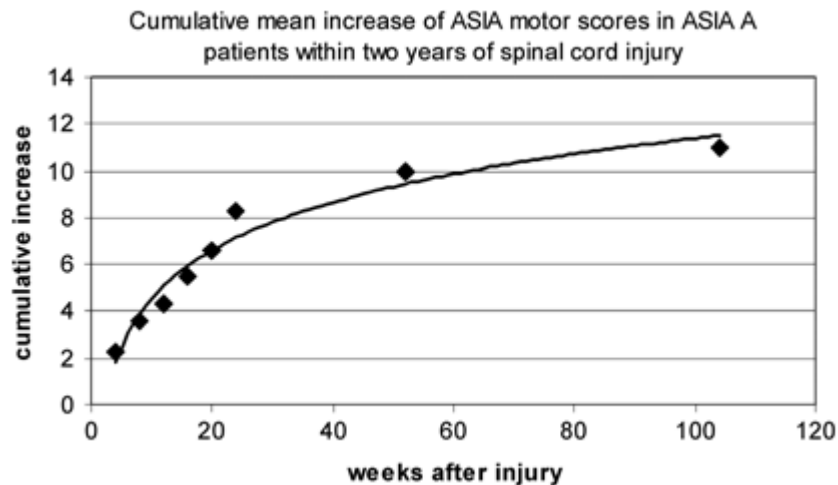


Figure 1.3 Cumulative mean increase in ISNCSCI motor score of AIS A patients within two years of spinal cord injury. The most rapid improvement occurs within the first 6 months after SCI and is essentially maximal after 12 months [2].

In the chronic phase (< 1 year post-injury), functional improvements may be elicited in people with incomplete SCI by training that takes advantage of neuroplasticity. Spared pathways within the central nervous system offer the potential for synaptic strengthening at various levels [14]. In addition, sprouting of new circuits or axonal branching presents new opportunities for functional improvement [15].

Studies of the brain have shown that cortical areas which are responsible for movement and sensation of body parts not affected by the injury tend to take over areas

associated with paralyzed body parts [16-20]. Changes are seen in the location and intensity of activation patterns within the motor cortex following SCI, suggesting a post-injury reorganization of motor control [21-23]. This occurs because “cells that wire together fire together”: the concurrent activation of neurons leads to increased synaptic efficiency [24]. This neuroplasticity can also be exploited during rehabilitation after SCI.

After people with motor incomplete SCIs go through massed practice training programs, the cortical areas that represent affected body parts increase in size and shift back to a more “normal” location. Improvements in hand function also occur [3, 25-27]. In addition, somatosensory stimulation has also been shown to improve motor function and pinch strength following spinal cord injury [25, 28]. When combined, massed practice training and sensory stimulation resulted in greater improvements than either intervention alone [3, 25]. This pairing of “top down” and “bottom up” training paradigms results in strengthened corticospinal connections, as well as increased area and intensity of cortical activation [3, 27, 29]. A study combining massed practice training and sensory stimulation in the biceps muscle showed an anterior shift and increased area in cortical motor maps (Figure 1.4). The pairing of cortical activation and peripheral stimulation is thought to promote cortical reorganization [30, 31] and changes in cortical excitability [32, 33] through long-term potentiation. When signals from the brain and antidromic stimulation from the periphery reach the synapse between upper motor neurons and lower motor neurons at the same time, Hebbian-style synaptic strengthening occurs [24, 34].

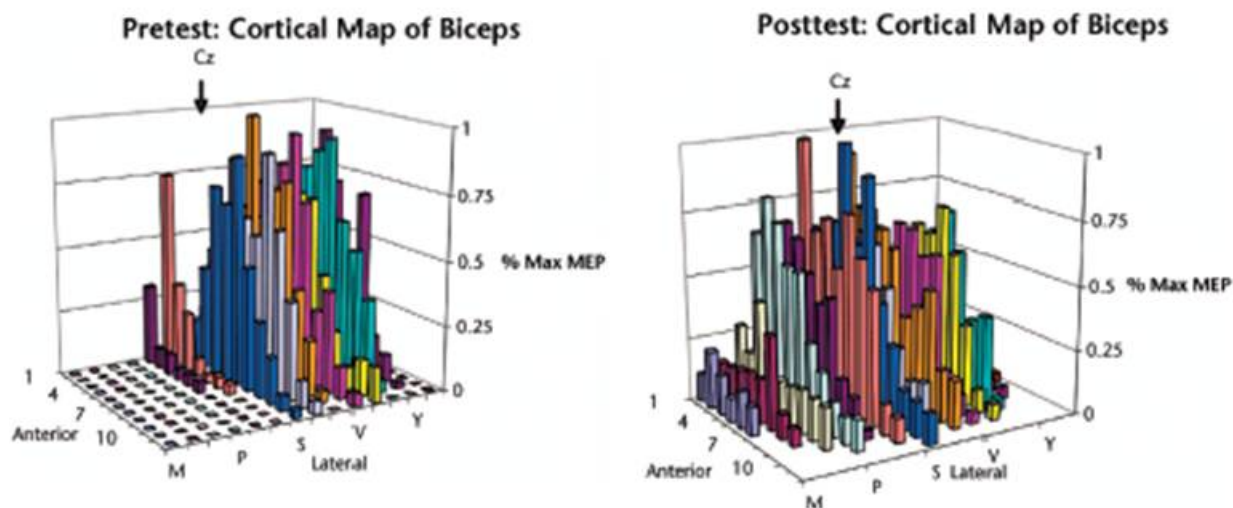


Figure 1.4 Normalized cortical motor map from right biceps brachii muscle before and after intervention. Left wall of the figure represents the midline of the sagittal plane. Cz represents the point at which the line between the nasion and inion intersects with the interaural line. Note that, during the preintervention test, the majority of the active sites were located posterior to Cz. Following the intervention, the map shifted anteriorly. Note also that motor-evoked potentials (MEPs) could be evoked from a greater number of sites following intervention [3].

1.3 Functional Electrical Stimulation

For people with no voluntary control of the hand muscles after SCI, where no retraining strategies will be effective, activation of paralyzed muscles by electrical stimulation is a way to restore function. Functional electrical stimulation (FES) is the application of electrical stimulation to weak or paralyzed muscles to produce an action [35]. For over 50 years, FES has been used extensively for restoration of bladder and bowel function, respiratory and cardiac pacing, therapeutic exercise, and reanimation of skeletal muscle. After incomplete SCI, long-term application of FES has been shown to facilitate voluntary grasping function [36]. Following a complete SCI, FES has been used to restore function that is lost due to complete paralysis.

After traumatic SCI, motor neuron damage and death is common and can extend multiple levels above and below the initial site of injury. Previous studies have reported complete denervation in 39% of triceps muscles [37] and 15% of thenar muscles [38] in subjects with motor complete, C5-C6 SCI. Muscles become denervated when they lose their nerve supply and become difficult to activate by electrical stimulation. People with extensive or complete denervation of the target muscles are generally excluded from FES applications, as the current threshold for initiating an action potential in nerve is much lower than in muscle (Figure 1.5).

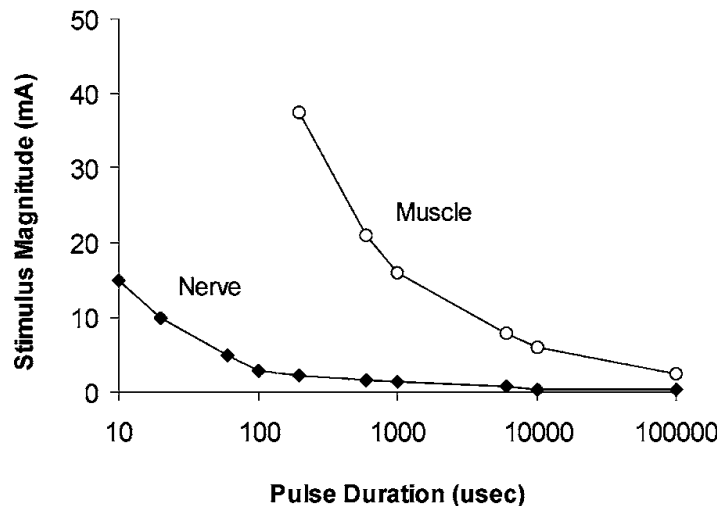


Figure 1.5 Strength duration curves for nerve and muscle. Data from cat tibialis anterior muscle [4].

FES can be delivered to muscle in a variety of ways. Surface systems are the least invasive, as the stimulating electrodes are placed over the motor point of a muscle. Surface systems are relatively inexpensive and easily reversible, but consistent electrode placement and activation of deep muscles can be difficult. In addition, pain receptors in the skin can be activated, making stimulation painful if sensory pathways remain intact.

Fully implantable, intramuscular electrodes are most commonly used in FES systems intended for long term use [35, 39]. All of the components of the system are implanted inside the body. The stimulator is typically implanted in the chest or abdomen and connected to the intramuscular electrodes through subcutaneous cabling. Power and control signals are transmitted by a radio-frequency telemetry link from an external control unit. While both surface and implantable systems have been used with success in people with SCI, surface systems are preferable to implantable systems in cases of early rehabilitation and technology development.

For hand opening, the extensor muscles that contribute to the movement include the extensor digitorum profundus, extensor digitorum superficialis, extensor pollicis longus, and extensor pollicis brevis. To close the hand, the contributing flexor muscles include the flexor digitorum superficialis, flexor digitorum profundus, and thenar muscles [40-42]. Muscles can either be activated individually by placing small electrodes over the motor points of each muscle or more grossly by placing large electrodes across groups of synergistic muscles. Contraction force can be modulated by varying the total charge delivered to the muscle. Many different combinations of amplitude, pulse width, and frequency can result in the same total charge (Figure 1.6).

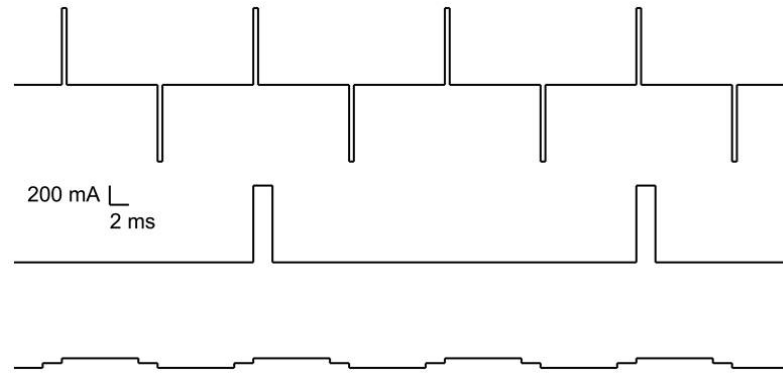


Figure 1.6 Stimulus charge/parameter comparisons. Three stimulus trains that have the same total charge, but very different parameters [5].

In application of surface stimulation to the muscles of the hand, pulse durations of 200-400 μ s and frequencies of 20-40 Hz are commonly used [43, 44]. Frequency is most commonly modulated at the beginning and end of each contraction to produce smooth contractions [44]. To produce full extension of the fingers (hand opening) in able-bodied subjects, typical pulse amplitudes range from 15-20 mA [42]. Full flexion of the fingers (hand closing) in uninjured subjects typically requires pulse amplitudes of 20-26 mA [42]. Higher pulse amplitudes are required to produce hand movements in paralyzed muscles, which are weaker and more fatigable than healthy muscles. In previous studies with SCI subjects, currents necessary for hand opening and closing vary, but are generally less than 40 mA [42]. To determine the optimal stimulation parameters for each subject, particularly those with chronic SCI, a systematic evaluation of the current hand function, muscle excitability, and strength of the target muscle groups is necessary.

Activation of paralyzed muscles by FES has been shown to restore control of hand movements following complete SCI [39, 45, 46]. A variety of control signals have been used to activate FES systems, including voice commands [47], head movements [45],

wrist movements [48], sip and puff [49], contralateral shoulder movements [45, 46, 48, 50] and electromyographic signals from muscles that remain under voluntary control [39, 51]. In addition, muscles below the level of injury have been identified recently as a potential source of command signals [52]. Logical command signals can be used to simply turn the stimulation on or off. Proportional command signals offer graded control of stimulation, so that contractions of different strengths can be achieved.

However, as few muscles remain under voluntary control, movements of the head or arm may interfere with activities of daily living, such as eating and self-care. In addition, the cognitive burden of making unrelated movements could hinder execution of the desired movement. In order to be acceptable to an end user, the command signal task must be easy to perform, inconspicuous, and must not interfere with other tasks [53]. Alternatively, signals from the brain have been identified as potential control signals for FES of paralyzed hand muscles [8, 54-57].

1.4 Brain Computer Interface Technology

Brain computer interfaces (BCIs) may offer a natural method of controlling FES of paralyzed muscles in an intuitive way. A brain computer interface (BCI) provides a link between the brain and an artificial device (Figure 1.7). Natural thoughts can be used to control systems for communication and control [6]. A BCI could be used to provide a control signal for an FES system, which would allow people with cervical SCI restored control over paralyzed hand muscles. Using a BCI to generate voluntary control signals also recreates the normal loop of motor planning, execution, and feedback, otherwise not used in SCI subjects due to paralyzed limbs.

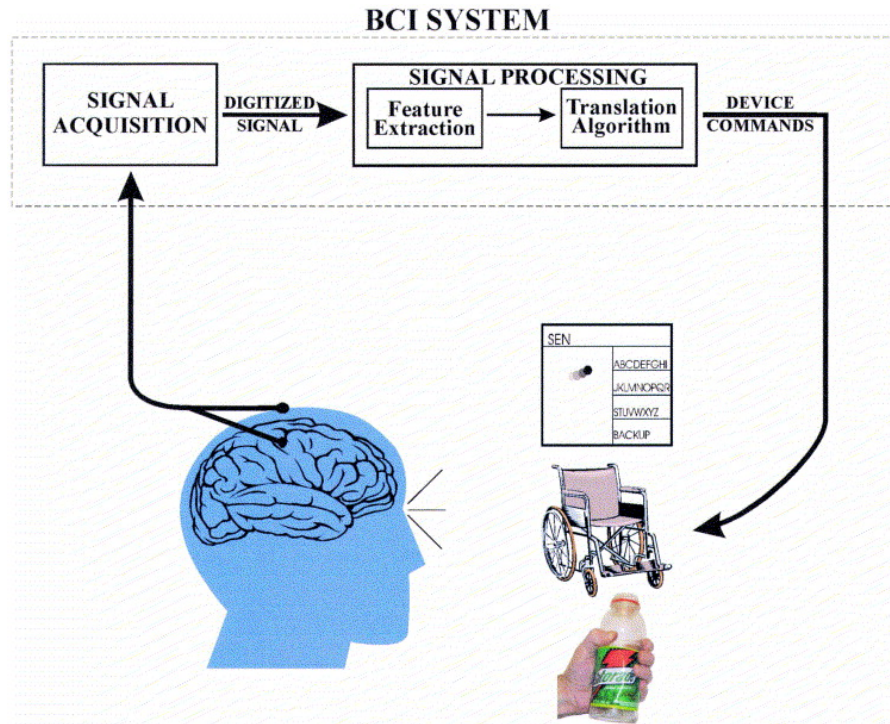


Figure 1.7 Basic design and operation of any BCI system. Signals from the brain are acquired by electrodes on the scalp or in the head and processed to extract specific signal features (e.g. amplitudes of evoked potentials or sensorimotor cortex rhythms, firing rates of cortical neurons) that reflect the user's intent. These features are translated into commands that operate a device (e.g. a simple word processing program, a wheelchair, or a neuroprosthesis). Success depends on the interaction of two adaptive controllers, user and system. The user must develop and maintain good correlation between his or her intent and the signal features employed by the BCI; and the BCI must select and extract features that the user can control and must translate those features into device commands correctly and efficiently [6].

A variety of methods may be used to interface with the brain, which can be either invasive or noninvasive. Microelectrode arrays can be implanted within the brain and record the electrical activation of single neurons, resulting in very high information content. Action potentials, or spikes, from a population of neurons are monitored, and aspects of their firing patterns can be used to control a BCI. Electrocorticography (ECoG) utilizes electrode arrays that are placed on the surface of the brain, which record field potentials from a larger group of localized neurons. Non-invasive BCIs use

electroencephalographic (EEG) electrodes, which are positioned externally on the scalp. EEG electrodes may be placed over areas of the brain involved in motor control and offer a completely non-invasive method of recording electrical activity generated in the motor cortex during imagined movements in subjects with paralyzed limbs due to SCI. This method records field potentials from a very large, distributed group of neurons with relatively low information content. The typical rule of thumb in BCI design is to use the least invasive recording technique that provides the necessary information content. Consideration must also be given to the reliability, safety, long-term stability, and cost-effectiveness [6, 58].

BCIs that aim to restore control of movement to people with paralyzed hand muscles have used both invasive and noninvasive recording methods. Since EEG is noninvasive, portable, cost-effective, and has high temporal resolution [59], it has been used for developing and testing motor neuroprosthetics. Previous studies have used EEG signals to enable communication [60], control avatars within a virtual reality environment [61-63], trigger movement of hand orthoses [64, 65], and deliver FES to weak or paralyzed muscles [8, 55, 57, 66-71].

1.5 BCI-FES

The integration of brain-computer interfaces (BCI) with functional electrical stimulation (FES) systems designed to provide motor rehabilitation may contribute to functional improvements in people following SCI [8, 54, 56, 57, 59, 66, 69-73]. This “top-down, bottom-up” approach is similar to the rehabilitation strategies, where massed practice and sensory stimulation are combined [3, 74]. This strategy offers a potential for

cortical and muscle rehabilitation by actively enabling the user to control their paralyzed limbs for functional tasks using their brain activity. User intent to perform a task is evaluated by the BCI, and electrical stimulation that will activate paralyzed muscles is triggered based on features of neural signals. BCI-FES therapy is designed to counteract the maladaptive cortical reorganization (due to non-use of neural circuits) that occurs post-injury by promoting neural repair and restoration through activation of cortical regions associated with the normal motor behaviors.

1.5.1 Neural Control Signals

One type of EEG signal commonly used in motor neuroprosthetics is the sensorimotor rhythm (SMR), an oscillatory pattern in the electric fields recorded from the sensorimotor cortex. During voluntary or imagined movements, there are reductions in the rhythmic oscillations over the area associated with the target muscle [75-78]. This event-related desynchronization (ERD, Figure 1.8) is thought to be correlated with activated cortical networks [78]. In contrast, event-related synchronization (ERS, Figure 1.8) occurs immediately after a movement [7, 72], which is correlated with deactivated or inhibited cortical networks.

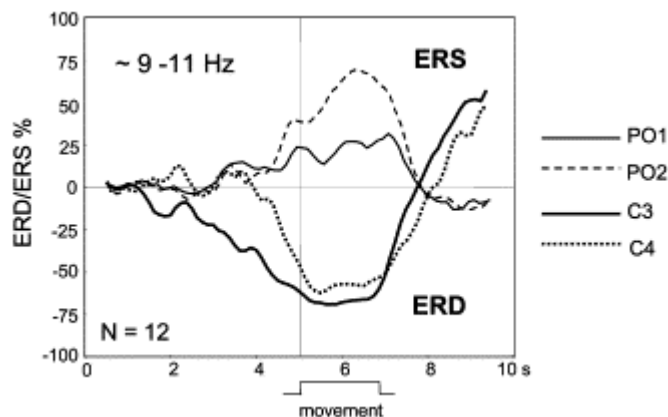


Figure 1.8 Event-related desynchronization and synchronization. Average ERD/ERS time course during slow voluntary movements of the right index finger (movement duration = 1.6 – 2.1 sec) [7].

Although SMRs can be modulated by most adults [79, 80], the ability to use an EEG-based BCI can vary significantly between individuals [81] and sometimes requires extensive training to develop high accuracy control [82, 83]. To make matters worse, after SCI the cortical areas associated with target muscles are often used for control, but may have been taken over by unaffected areas due to neuroplastic remodeling after an injury [16-20]. Changes in the location and intensity of activation patterns within the motor cortex [21-23, 84-87] may make SMR modulation more difficult for people following SCI. Particularly after SCI, ERD/ERS patterns are usually more diffuse and broadly distributed [85].

1.5.2 Previous Studies

Despite changes in cortical activation during motor tasks, previous studies have shown that subjects with SCI have been able to control a BCI using SMRs [85, 88-90]. Most studies that combine BCI with FES include subjects that have experienced either a

stroke or motor incomplete SCI. In these populations, some voluntary control over the target muscles remains, and descending signals from the brain are still able to activate a population of motor units within the target muscle. Previous studies have shown that BCI combined with FES provides an environment for improved rehabilitation through strengthening of descending pathways, resulting in improved upper extremity function in subjects following stroke and incomplete SCI [8, 54, 56, 69, 73]. However, since no descending pathways remain intact after a complete SCI, recovery is not expected and FES is required for activation and movement of paralyzed muscles. A limited number of studies have evaluated EEG-based BCI control of upper-limb FES in subjects with complete, cervical level SCI [8, 55-57, 66, 68].

In 1999, researchers at Case Western Reserve University demonstrated EEG control over an implanted neuroprosthesis for hand opening and closing [55]. One neuroprosthesis user participated in the study, however his injury and function details were not published. The subject sat in front of a computer screen where targets appeared, and a cursor that was controlled by the subjects neural signals moved on the screen. A subset of 5 to 10 electrodes was used to generate cursor movements, while signals from only 1 or 2 electrodes were used to drive cursor movements. The subject participated in 17 weeks of training, with 1-3 sessions per week, where he learned to control the amplitude of the beta rhythm in the frontal and somatomotor cortices (F3). FES for hand opening/closing was activated when a preset threshold amplitude was met. The subject performed some grasp and release tasks, such as moving a weight and grasping and releasing a fork and cup. During the first 6 sessions (2 weeks), there was a learning period during which the accuracy increased from 50% to 90%. Over the remainder of the

17 weeks of training, the subject was able to control the frontal beta rhythm with consistent accuracy (>90%). This study provided one of the first “proof-of-concept” examples of FES controlled by a BCI. After a short period of time, the neuroprosthetic user was able to control the system with high accuracy. However, a later publication from this group reported that the frontal EEG signals were found to be contaminated by EMG [91].

The first group to control surface-based FES using EEG was the Graz laboratory [8]. A subject with a complete C4/C5 SCI participated in the study. He received FES for 10 months (45 min/day, 5 days/week) in order to strengthen his muscles and reduce fatigability in the arm and shoulder. At the beginning of the study, the researchers experimented with different types of motor imagery (foot, right hand, left hand) and found that foot motor imagery resulted in stable beta oscillations in the C3 and Cz electrodes, with a dominant frequency of 17 Hz (Figure 1.9) [92]. A linear-discriminant analysis (LDA) classifier was trained using 160 trials of foot movement imagery. Surface electrodes were applied to the forearm to enable opening and closing of the hand, and FES was triggered when the classifier output reached a preset threshold. No accuracy data were published. This study showed that a subject with high-level SCI could control his neural signals over an extended period to trigger surface FES.

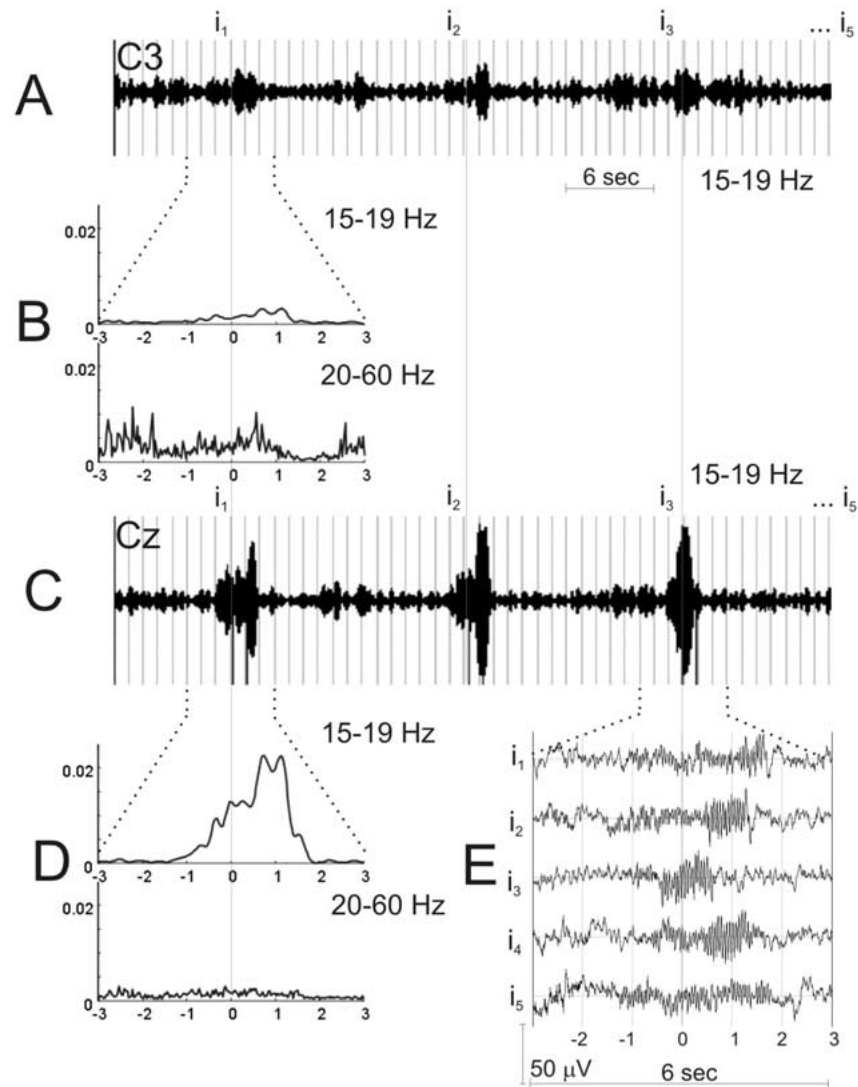


Figure 1.9 Signal processing methods utilized in Graz-BCI studies. Bandpass filtered (15-19 Hz) EEG channels C3 and Cz recorded during the first 3 foot movement imaginations (i_1 , i_2 and i_3) of one complete grasp sequence (A,C). The vertical lines indicate the start-on of the individual grasp phases. (B, D) Bandpower time courses (15–19 and 20–60 Hz) of EEG channels C3 and Cz averaged over the five grasp phases with movement start at second 0 (amplitudes in arbitrary units) [8].

Another case study from the Graz group demonstrated control of a Freehand system using an EEG-based BCI [56]. Since the above two “proof of concept” studies took place over long training periods, the goal of this study was to demonstrate control in a very short period of time (3 days). The subject, who had a C5 motor complete SCI, had

a Freehand system implanted in his right hand and arm. Signals from 14-16 Hz and 18-22 Hz from channels Cz and C4 during left hand motor imagery were used to create features for input to an LDA classifier. Signals from channel C3 (electrode most closely related to right hand movements) were not considered because of potential contamination from active movements of the right arm. Each trial consisted of a ball dropping from the top of the screen to the bottom within 3 seconds. Baskets were positioned either on the left or right side of the screen, and the subject had to “steer” the ball into the correct basket. One run consisted of 40 trials, and the highest accuracy achieved during a single run on day one was 73%. On day 2, the best accuracy achieved was 68%. FES was delivered to the right hand via the Freehand system when signals were decoded correctly. On day 3, the subject performed a grasp and release sequence, during which he was instructed to move a paperweight from one position to another, with the system operating freely, not in a cue-based mode.

Another recent publication from the Graz group evaluated a BCI-FES system in a different subject with a complete cervical-level SCI [57]. The subject underwent two months of FES training in order to strengthen the muscles of the hand and reduce fatigability. A custom neoprene sleeve was used to attach the FES electrodes. The standard Graz-BCI training protocol was performed to find subject-specific frequency-based features and an LDA classifier was used. Over one year of BCI-FES training, accuracies varied from 50 to 93%, with an average of 70.5%. The subject’s average performance did not improve over the year of training, and no training effects were seen.

All of the studies described above were case studies of a single subject with SCI over varying time periods. Training periods lasted over a year in some studies [8, 57, 66],

while one lasted only 3 days [56]. Typically, user-specific features were determined from an initial evaluation period and features were chosen from only the most reactive frequency bands and electrode locations for each particular subject [8, 56, 57, 66]. Since SCI presents with such variability across subjects, it is difficult to generalize results from case studies. In addition, daily calibration of decoders can be time-consuming [93-95] to achieve a high level of accuracy across subjects.

1.5.3 Error Signals

Optimization of data collection methods, signal processing, and decoding algorithms have resulted in classification accuracy of 80-97% after 6-10 20-minute sessions [80, 96-98]. However, EEG-based BCI classification rarely achieves 100% success. For this reason, methods for verifying user intent have been explored [99].

A particular neural signal called the error potential (errP) may be useful for identifying when mistakes are made in the classification of user intent [9, 100, 101]. An errP is elicited when a person recognizes that an error has been made [102-104]. The main components of errPs have been shown to originate in the anterior cingulate cortex (ACC, Figure 1.10), a deep brain structure that is involved in attention, motivation, modulation of emotional responses, anticipation of tasks, and error detection [102]. Different types of errPs have been identified, which vary slightly in presentation depending on the task being performed by the user.

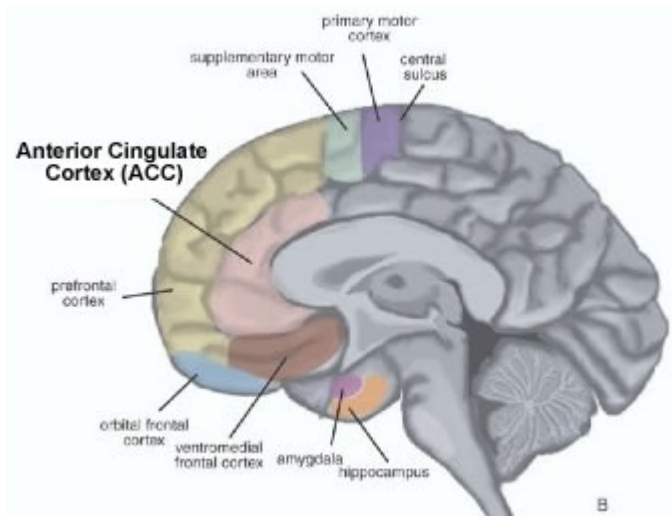


Figure 1.10 Location of the anterior cingulate cortex in the human brain.

The specific type of errP that results when errors are made at a BCI interface is called “interaction errP”[9]. These errPs have a fronto-central distribution along the midline of the brain and are characterized in EEG by a negative wave (error negativity, N_E) followed by a broader positive peak (error positivity, P_E , [101, 102]. Ferrez and Milian [9] detected interaction errPs from subjects during BCI use. A target appeared on the left or right side of the screen, and the subject controlled a cursor using their brain signals. If the cursor moved in the direction of the target, it was considered a correct trial. If it moved in the wrong direction, it was considered to be an error trial. Subjects performed ten sessions of 3 minutes on two different days, corresponding to about 75 single trials per session. Figure 1.11 shows averages of single trials recorded from electrode FC_z for 5 different subjects, as well as a group average. Averages for correct trials on the left (Figure 1.11 a) and right (Figure 1.11 b) and for wrong trials on the left (Figure 1.11 c) and right (Figure 1.11 d) are shown. Each trace for individual subjects represents an average of approximately 1500 trials, and the grand average trace

represents an average of around 7500 trials. The left and right correct averages are very similar and the left and right wrong averages are very similar. In contrast, the left correct and wrong as well as the right correct and wrong are very different.

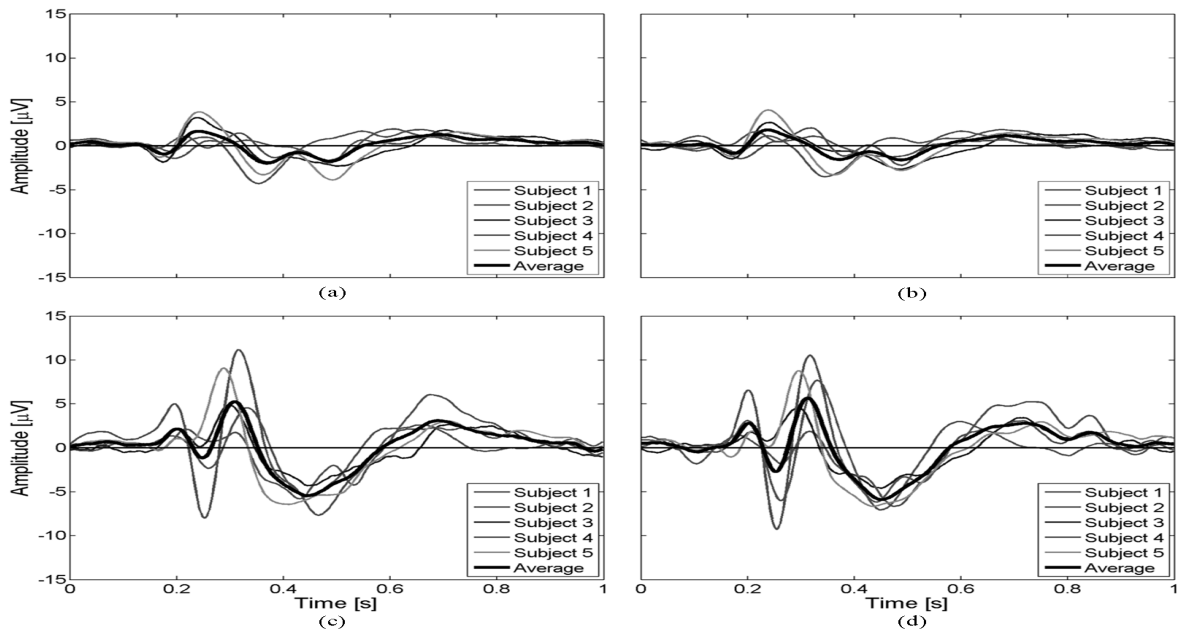


Figure 1.11 Error and correct trials. Averages of single trials recorded at FCz with respect to the side where a target appeared for five subjects and the average of them. The four cases are: a) correct trials on left side, b) correct trials on right side, c) error trials on left side, and d) error trials on right side [9].

In order to be effective in a BCI application, errPs must be able to be identified in single trials. Previous studies have attempted to classify errors made in closed loop BCI experiments [9, 105-107]. Signals from channels F_z , C_z , and FC_z are used to create features for input to a Gaussian classifier. Gaussian classifiers estimate the posterior probability that a single trial corresponds to either “error” or “correct” [9]. With a 40% error presentation rate, classification accuracy was 59%. When the error presentation rate was reduced to 20%, classification accuracy rose to 63% [105]. Identification of errors

from single trials can be improved, with up to 85% accuracy, when a combination of error waveforms and brain connectivity features are used [106]. If high classification accuracies can be attained for identifying errPs from single trials, they could be useful in BCI applications.

1.6 Functional Outcome Measures

Within the research community, there is no general consensus regarding assessment of hand function in people with cervical level injuries due to the difficulty of identifying valid, reliable, and sensitive measures [108, 109]. When assessing hand function in people using a neuroprosthetic, matters become even more complicated. The tests that have been most commonly used in previous studies include the Jebsen-Taylor Test of Hand Function, the Sollerman Hand Function Test, the Grasp and Release Test (GRT), and the Activity of Daily Living Abilities Test (ADLAT).

The Jebsen-Taylor hand function test is a quantitative assessment of grasp and release and object manipulation [110] and is commonly used to assess hand function following interventions in people with SCI [3, 25, 29], but less commonly used during FES neuroprosthetic use [109]. The subject completes 7 subtests, following standardized instructions, while being timed. The tasks include 1) writing a short sentence, 2) simulated page turning, 3) lifting small, common objects (bottle caps, pennies, paper clips), 4) simulated feeding, 5) stacking checkers, 6) lifting large, light objects (empty cans), and 7) lifting large, heavy objects (full cans).

The Sollerman hand function test consists of 20 activities of daily living that require common hand gripping strategies [111], such as using a key, picking up coins,

using a phone, and pouring water from a jar. The test was designed with tetraplegic patients in mind, so it may reflect the needs of the SCI population better than other hand function tests. However, most of the movements performed during the Sollerman Test require contributions from muscles that are proximal to the hand, which can confound interpretation of the results.

The Grasp and Release Test (GRT) measures pinch strength, grasp strength, and hand function in people with cervical SCIs [67, 112]. The subject is asked to pick up and release five different objects of various weights and sizes using only one hand, and pinching ability is evaluated by grabbing a fork handle and stabbing food. One of the benefits of this test is that the objects do not need to be moved across the body, from one side to the other. Because of this, the GRT more accurately reflects hand function alone, rather than more proximal muscle function [109]. The GRT has been used in previous studies to assess hand function following tendon transfers and during use of FES neuroprosthetics [67, 113].

The Activities of Daily Living Abilities Test (ADLAT) quantifies changes in hand function and is appropriate for assessing performance in people with cervical SCIs [114]. The ADLAT consists of six activities, including eating with a fork, drinking from a glass, writing with a pen, dialing a phone, using a CD, and brushing the teeth. The test accounts for subject preference, assistance required, and quality of movement. The ADLAT has been used to measure performance in hand function in people with tetraplegia while using a FES neuroprosthetic for hand opening and closing [109].

1.7 Research Goals

The overall goal of this project is to give people with motor complete, cervical SCI a restored control over paralyzed muscles in the hand through autonomous brain-controlled stimulation control paradigms for grasping and releasing an object. After completion of preliminary experiments (chapter 3), the following aims guided this project:

AIM 1: Develop stimulation control paradigms for functional activation of hand muscles for grasp and release (chapter 4). The first step was to design a control paradigm for delivering stimulation to the muscles of the arm and hand that produced movements for grasping and releasing an object. Next, the efficacy and safety of the stimulation protocol was evaluated by bench testing in an electronics lab, and then in a few healthy subjects.

AIM 2: Closed-loop brain controlled FES of paralyzed muscles to perform a functional grasp and release task (chapter 5). The neural features that are optimal for triggering muscle stimulation sequences synchronously were determined. Next, an experimental paradigm for brain-controlled activation of paralyzed muscles to perform a grasp and release task was developed.

AIM 3: Quantify function of hand muscles in chronic SCI subjects (chapter 6). Maximal grip strength produced by electrical stimulation of hand muscles was assessed at the beginning of each experiment day. The Grasp and Release Test was used to assess function during performance of a grasp and release task. Improvement in strength and task performance was assessed over the duration of the experiment.

Following the completion of these aims, a BCI-FES system was evaluated in 5 subjects with SCI and 5 uninjured, control subjects (chapter 7) over 6 days of training. The system was designed based on the results from the above aims and gave subjects with motor-complete SCI the ability to control FES for grasp and release using natural signals generated in the brain.

CHAPTER 2: GENERAL METHODS

2.1 Subject Recruitment and Screening

Subjects with SCI were recruited from The Miami Project to Cure Paralysis database. To be considered for participation in any phase of the study, a potential SCI subject had to meet the following inclusion criteria: 18-50 years old, chronic injury (longer than 1 year) but no more than 15 years post-injury, C5 or C6-level motor complete SCI as classified by ISNCSCI standards [115], and no extensive denervation of target muscles. The excitability and strength of paralyzed hand muscles were assessed during the first visit, by applying surface stimulation. Trains of pulses were delivered via surface electrodes to the flexor and extensor muscles of the right hand, in turn. Able-bodied subjects were recruited from within the Neuroprosthetic Research Group at the University of Miami. All were healthy with no history of serious medical issues. All subjects provided written informed consent and study procedures were approved by The University of Miami Institutional Review Board (ID: 20120596).

2.2 Neural Data Acquisition

Two different wireless EEG systems were used to acquire EEG signals from the subjects. Either a 9-channel (Fz F3, F4, Cz, C3, C4, P3, P4, POz, X10 headset) or 20-channel (Fz, F1, F2, F3, F4, Cz, C1, C2, C3, C4, CPz, Pz, P1, P2, P3, P4, POz, Oz, O1, O2, X24 headset) EEG system (256 Hz sampling rate, 16-bit resolution, Advanced Brain Monitoring, Carlsbad, CA) with linked-mastoid reference electrodes was fitted to the subject's head (Figure 2.1). Continuous EEG signals were acquired in real-time from

electrodes arranged on headstrips according to the International 10-20 system standards. Foam sensors were attached to the electrode sites and saturated with Synapse (Kustomer Kinetics, Arcadia, CA) conductive electrode paste. Corresponding sites on the subject's head were abraded and cleaned with alcohol before placing the sensors on the scalp. Electrode impedances were tested before and after each session using the manufacturer provided software. Sensors were individually readjusted on the scalp for proper placement if impedance values exceeded $40\text{ k}\Omega$.

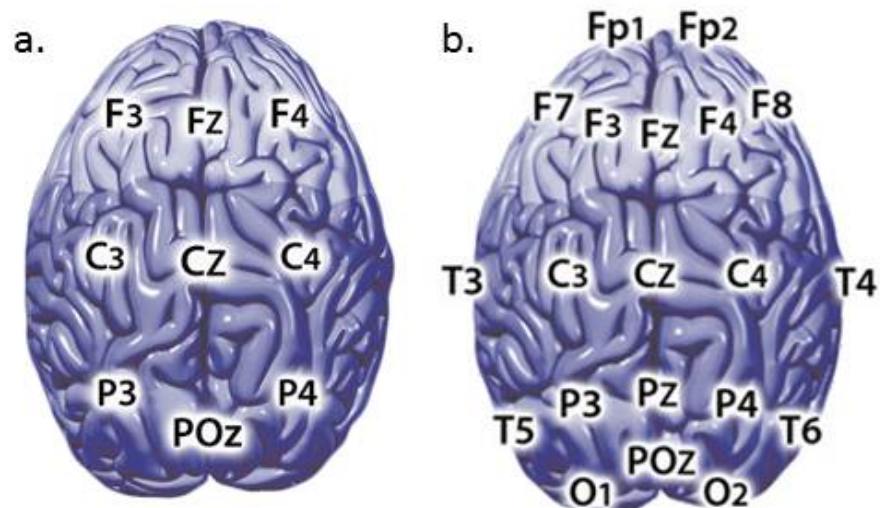


Figure 2.1 Electrode configuration for a) X10 and b) X24 headsets.

A wireless headset, attached to an elastic headband, was positioned at the back of the subject's head and interfaced with the electrode strip (Figure 2.2). Signals were wirelessly transmitted via Bluetooth from the headset to the external syncing unit (Figure 2.2), which was connected to the computer by USB. Matlab (MathWorks, Natick, MA) was used for processing and decoding of neural signals.

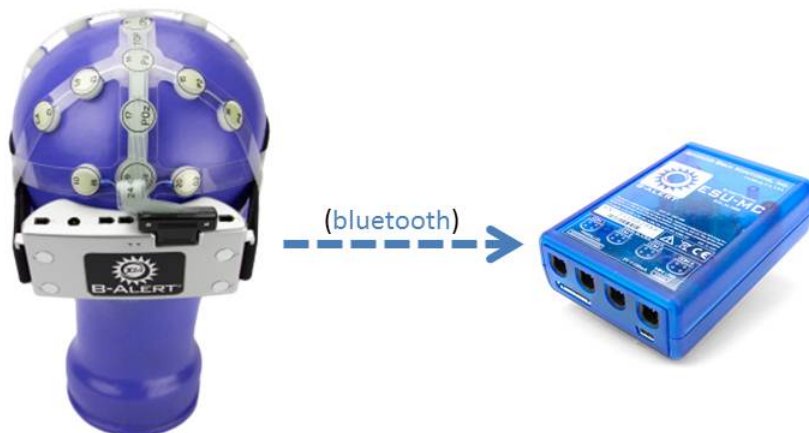


Figure 2.2 B-Alert headset transmits neural data via Bluetooth to the external syncing unit, which is linked to the computer by USB port.

2.3 Muscle Stimulation

2.3.1 Bioness

For the preliminary BCI-FES experiments (Chapter 3), a Bioness H200 neuroprosthetic wrist-hand orthosis (Bioness Inc, Valencia, CA, Figure 2.3) was used to deliver electrical stimulation to the muscles controlling movements of the hand. During the first visit, a neuroprosthetic wrist-hand orthosis (NESS H200, Bioness Inc, Valencia, CA) was fitted to the right hand of the subject. FES was delivered to the extensor (extensor digitorum communis and extensor pollicis brevis) and flexor (flexor pollicis longus and thenar) muscle groups alternately to produce opening and closing movements of the fingers and hand. Stimulation intensity was set by holding the pulse duration (300 μ s) and frequency (35Hz) constant, while slowly increasing the current amplitude. Once a maximal muscle contraction was attained (increases in current intensity do not

produce additional muscle contraction), the current amplitude was increased an additional 25% in order to maintain consistent muscle contractions throughout the experiment.

Trigger signals were sent wirelessly from the control unit to the orthosis. The control unit is like a remote control, which has buttons to trigger a stimulation program (“on” or “off”), increase or decrease the stimulation intensity, and toggle between two preset programs. The company provided us with a “hack in” to the control unit, so that the stimulation could be triggered on/off at the control unit, using a TTL pulse sent from the computer to a relay.



Figure 2.3 a) Control unit and b) neuroprosthetic wrist-hand orthosis of the Bioness H200.

2.3.2 Digitimer

For all other experiments in which stimulation was incorporated (Chapters 4, 6, and 7), a Digitimer DS7a stimulator (Digitimer LTD, Hertfordshire, England, Figure 2.4) was used. The DS7a stimulator was ordered with the M288A modification, which allows the delivery of pulses of alternating polarity between successive stimuli. This type of

stimulation is most commonly used for FES applications to reduce tissue polarization. Surface electrodes can be trimmed to fit the subject's arm and allow custom placement across the extensor and flexor muscle groups. Further details regarding the stimulation control paradigm can be found in Chapter 4.



Figure 2.4 Digitimer DS7a stimulator unit.

2.4 BCI Architecture

BCI studies differ from basic neuroscience studies, which are typically observational. In basic science research, neural signals are recorded in a passive, open-loop way, with no feedback from the recording system. BCIs record activity from the nervous system and produce an output that is given to the user as feedback in real time. In this way, a BCI can affect the signals being recorded from the nervous system.

2.4.1 Closed-Loop Control

Most BCI systems operate with closed-loop architecture (Figure 2.5), in which the electrical activity in the brain is detected by EEG, and neural features are classified by a decoder to determine the user's intent. Feedback is then given to the user, typically through a visual display on a computer monitor. The decoder is often trained by supervised learning algorithms, which map neural features (inputs) to desired outputs [116]. Many examples of input-output pairs are required to train the decoder, so that it will be able to correctly classify future unmapped neural features. The decoder is static, so that after training, specific inputs are mapped to specific outputs. The mapping will not change during use of the BCI, unless the decoder is retrained using different data. This static architecture may be problematic, as neural features are expected to change as the user adjusts to the BCI system. Frequent retraining of the motor decoder or decoder adaptation may improve performance as neural signals adapt during training [94, 117, 118].

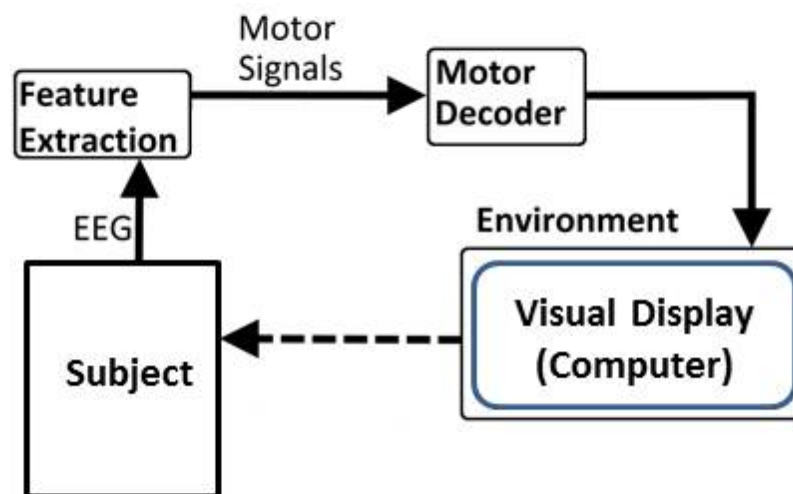


Figure 2.5 Typical BCI architecture. Neural features are extracted and decoded. The subject receives feedback, which is typically displayed on a computer screen.

2.4.2 Incorporating Reinforcement Learning

A BCI architecture that incorporates reinforcement learning (RL) could be useful for dealing with the neuroplastic changes expected during BCI use. The goal of RL is to maximize rewards for an environmental state by comparing actual outcomes to expectations. The most appropriate RL scheme is the actor-critic model, in which the agent is composed of an actor and a critic [119]. The actor is a policy (π) with parameters (θ) that maps user's brain states (s_t) to actions (a_t).

$$\pi(a | s ; \theta) = \Pr(a_t = a | s_t = s)$$

The critic provides a reinforcement signal to adapt the actor's parameters (θ) by estimating reward at each time step to form the reward expectation (V).

$$v_t(s, a) = E[r_{t+1} | s_t = s, a_t = a], \forall s \in S, \forall a \in A$$

The actor-critic RL architecture (Figure 2.6) is a semi-supervised learning technique that modifies the actor's decoding strategies based on feedback from the critic. The actor decodes the motor/action signals, mapping the neural features to outputs. Then, the critic decodes the error signals and uses them to improve the performance of the actor [103]. Incorporating this model into the BCI architecture may allow continuous coadaptation of the BCI to the user and of the user to the BCI, accounting for future learning and neuroplasticity.

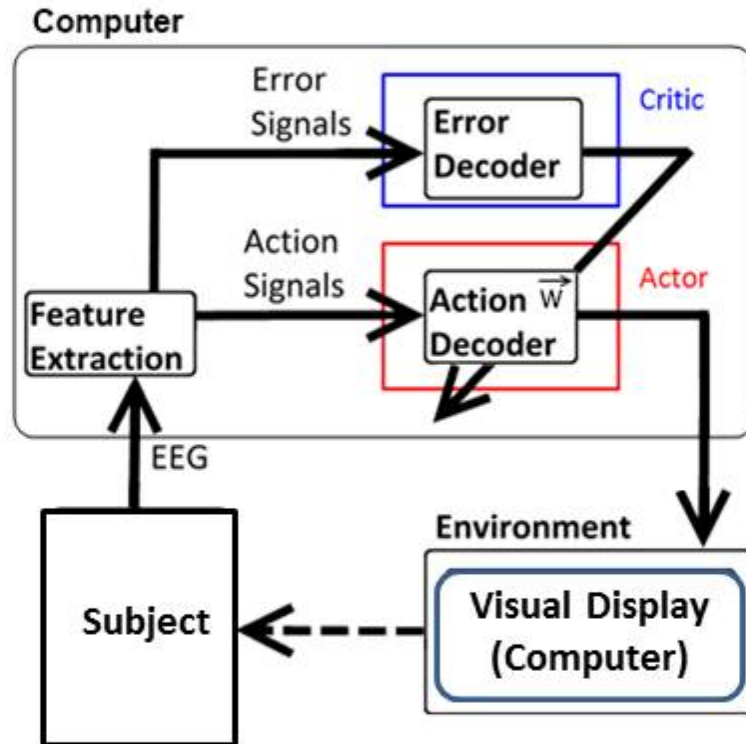


Figure 2.6 Actor-critic model of RL BCI architecture, which provides dynamic decoding of neural features.

CHAPTER 3: PRELIMINARY BCI-FES EXPERIMENTS

3.1 Subjects

Seven subjects with SCI (Table 3.1) were recruited and screened as described in Section 2.1. Four of those had hand muscles that were unresponsive to electrical stimulation with the Bioness. Three of the 4 were excluded from further study, and 1 subject with unresponsive muscles participated in some experiments. Four subjects participated in some part of the experiments, and 2 subjects completed the full protocol. Both subjects who completed the full protocol had hand muscles that were responsive to stimulation. Three able-bodied subjects participated in the full training protocol. Data in this chapter are presented for one SCI subject (SCI subject #3) and one uninjured, control subject.

Subject #	Age	Sex	R motor level	Hand muscles responsive to Bioness stimulation?	Time since injury	Participation
1	36	M	C5	NO	9	*
2	49	F	C6	YES	4	*
3	30	M	C6	YES	15	***
4	28	M	C5	NO	2	-
5	27	M	C6	NO	4	-
6	25	M	C6	YES	2	***
7	31	M	C5	NO	5	-

Table 3.1 SCI subject details. Age (in years), sex (M: male, F: female), right side motor level, denervation, time since injury (in years), and whether the person participated in no experiments (-), some experiments (*), or the full protocol (***).

Both subjects were 30 year old males. The subject with SCI was injured playing football, and his injury (duration = 15 years) was classified by ISNCSCI as incomplete

(AIS B), with bilateral motor levels of C6. Motor scores of 5 (normal function) were attained at the C5-level bilaterally, with scores of 5 (right) and 3 (left) at the C6-level. All motor scores below level C6 were zero. The subjects had no history of other serious medical issues.

3.2 Experiment Protocol

The experimental setup is shown in Figure 3.1A. The ABM X10 headset was used to record neural signals from subjects during these experiments. All commands and feedback were displayed on an Arduino UNO microcontroller board with a display shield (1.8" 18-bit Color TFT Shield with microSD and Joystick, Adafruit.com), which was interfaced to the system through a serial port of the ESU. The Bioness wrist-hand orthosis was used to deliver stimulation to the extensor muscles responsible for opening the hand. No stimulation was delivered for hand closing, as the Bioness was not capable of delivering this type of stimulation in isolation.

Each subject participated in four days of closed-loop BCI-FES training over 2 weeks. The subjects performed 300 trials on the first day, 450 trials on the second and third day, and 300 trials on the fourth day. Subjects sat either in their wheelchair (SCI) or in a stable armchair (control) facing a display, with their right forearm resting on a table. At the beginning of each trial, a fixation cross was displayed for 1 second to minimize eye movements (Figure 3.1 B, row 1). Then, cues of either "open" or "close" were displayed for 1 second, instructing the subject to imagine either opening or closing the right hand (Figure 3.1 B, row 2). Feedback of either "correct" or "wrong" was then given

to the subject, accompanied by a plot of the unthresholded output of the system (Figure 17 B, row 3).

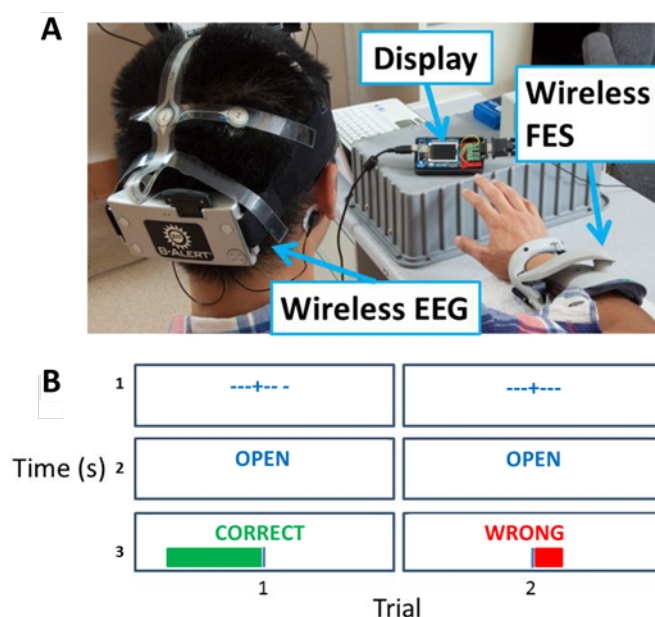


Figure 3.1 A. Experimental setup, including wireless EEG headset, display, and wireless FES. B. A trial consisted of a fixation cross, followed by a cue of either “open” or “close” and then feedback of either “correct” or “wrong”. A magnitude plot also showed the unthresholded output of the motor potential classifier.

During the first 120 trials on the first day of training, random feedback was given to the subject, so that 50% of trials resulted in a “wrong” outcome and 50% of trials displayed a “correct” outcome. When the user perceives that the outcome of the action decoder was incorrect (“wrong” feedback), error potentials should be generated. The neural signals recorded in response to a “wrong” outcome during these 120 trials were used to develop the error potential classifier. During all subsequent trials, closed-loop feedback was given to the subject that matched the output of the motor classifier. For example, when the “open” command was displayed, “correct” feedback would be

displayed if the motor signals were classified correctly (ie. motor classifier determined that the subject was imagining opening the hand). If the motor classifier determined that the subject was imagining closing the hand, a “wrong” feedback would be displayed. Stimulation accompanied all outputs corresponding to hand closing, and no stimulation was delivered for hand opening.

3.3 Neural Signal Processing and Decoding

Motor potentials for imagery of hand movements were recorded from the C3 electrode, corresponding to the area of the motor cortex involved in movements of the right hand. Error potentials were recorded from the Cz electrode, which is the electrode located nearest the anterior cingulate cortex, where errPs are generated. EEG signals generated between 0.15 and 1.0 seconds following the commands of “open” or “close” were used for the motor classifier. For the error classifier, EEG signals generated between 0.15 and 0.70 seconds following the feedback command were used. Raw EEG signals were transformed in to the frequency domain using the fast Fourier transform (FFT) to obtain a power spectral density (PSD) in 1 Hz bins. Normalized z-scores of the PSD [120] were used as input features to both decoders. These were found by subtracting the mean of all previous trials at each frequency and dividing by the standard deviation of all previous trains for that particular frequency. A negative z-score indicates that the power was below the mean for that particular trial and frequency bin.

The motor classifier (actor) and error classifier (critic) were modeled by multilayer perceptrons (MLP) and are incorporated in to the RL BCI architecture. Each MLP consists of a 3-layer fully connected feedforward neural network (Figure 3.2) that

maps inputs to outputs [121]. The inputs to the actor classifier were z-scores from 1-50 Hz, and inputs to the critic classifier were z-scores from 1-12 Hz [9, 122]. The actor has 50 inputs and 5 hidden nodes, while the critic has 12 inputs and 5 hidden nodes. The hidden and output layers perform a weighted sum on their inputs, which is then passed through a hyperbolic tangent (tanh) function with an output from -1 to 1. The tanh function is often used in neural networks because of its biological realism. The output of the MLP is found by:

$$r_h = \varphi (w_h * r_i)$$

$$r_o = \varphi (w_o * r_h)$$

where r_i is the input to the MLP, r_h is the output of the hidden layer, r_o is the output of the MLP, φ is the activation function, w_h are the weights of the hidden layer, and w_o are the weights of the output layer.

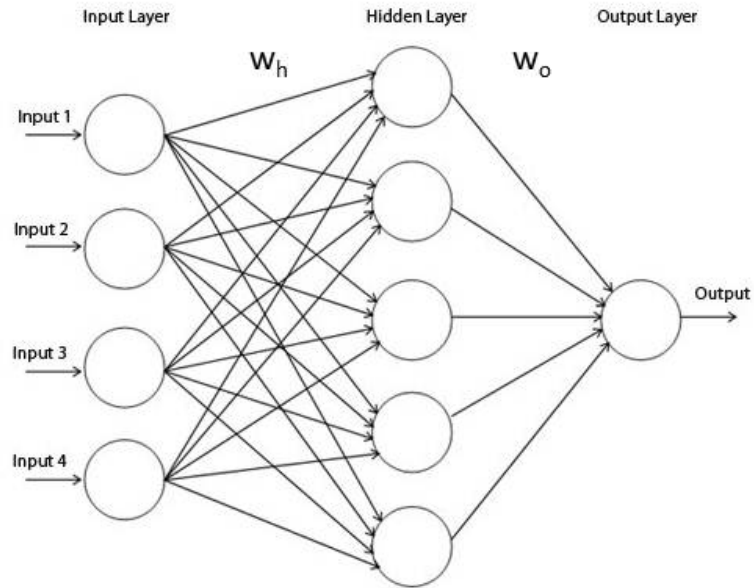


Figure 3.2 Multilayer perceptron. Weights at the hidden layer (w_h) and output layer (w_o) are updated by Hebbian learning techniques.

The critic weights were established by supervised learning techniques (Figure 3.3, box 2), where the network learns from the data collected during the first 120 trials (Figure 3.3, box 1). The data consists of input/desired output pairs, which are split into two sets: the training and test sets. The training set is used to optimize the weights at the hidden layer (w_h) and output layer (w_o), and the test set is used to validate the weights. Weights were assessed by applying them to the test set and classification accuracies were calculated. The weights with the highest classification accuracies were used for the critic classifier during subsequent training blocks.

The actor weights were randomly initialized (Figure 3.3, box 3) and then updated after each trial (Figure 3.3, box 4). Weights are updated using Hebbian-style learning methods, and weight modification updates are expressed by:

$$\Delta w_{ij} = \gamma (x_i (p_j - x_j)) + \gamma (1 - f)(x_i (1 - p_j - x_j))$$

where Δw_{ij} is the change of the weight between nodes i and j , γ is the learning rate, x_i is the input to node j from node i , x_j is the output of node j , p_j is a sign function of x_j (where positive values become +1 and negative values become -1), and f is the current feedback of the critic (which is -1 if an errP is detected and +1 if an errP is not present). The weight update equation is based on Hebbian style learning [119, 123].

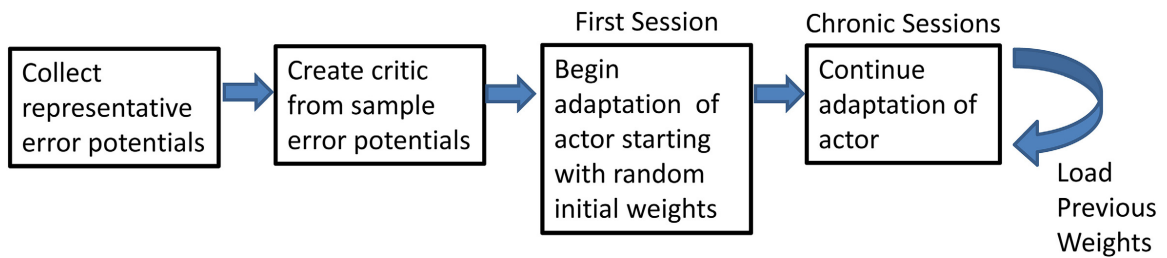


Figure 3.3 Flowchart of the steps of the experiment.

3.4 Results

Figure 3.4 shows sample motor signals from the SCI and Control subject in response to cues of “open” and “close”. Raw EEG (C3 EEG, top row) signals are transformed by FFT to create PSDs (C3 PSD) and then normalized z-scores (Z-score) are input to the motor decoder. In general, the features for the “close” cue corresponded to

lower power than the features for the “open” cue. Forty-four of the 50 frequency bins had lower power for the “close” cue.

A similar procedure was used to create error decoder input features, and representative samples are shown in Figure 21. Raw EEG signals from Cz are shown for the SCI and Control subject following “correct” or “wrong/error” feedback (Figure 3.5, row1). PSDs (Figure 3.5, row 2) and normalized z-scores (Figure 3.5, row 3) are also shown. The features for “correct” feedback corresponded to lower power compared to features generated following “wrong” feedback in 8 of the 12 bins (2-7 and 9-10 Hz bins).

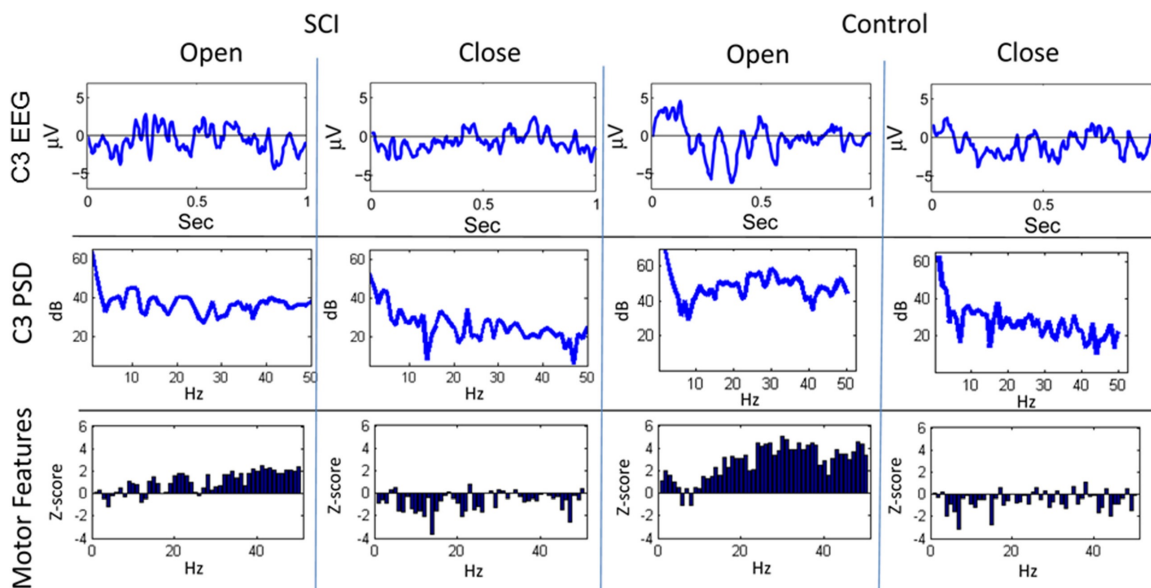


Figure 3.4 Sample trials from closed-loop sessions for motor signals. Columns show samples for cues of “open” and “close” for both the SCI and control subject. Rows show raw EEG from electrode C3 (top row), PSD (middle row), and Z-scores (bottom row).

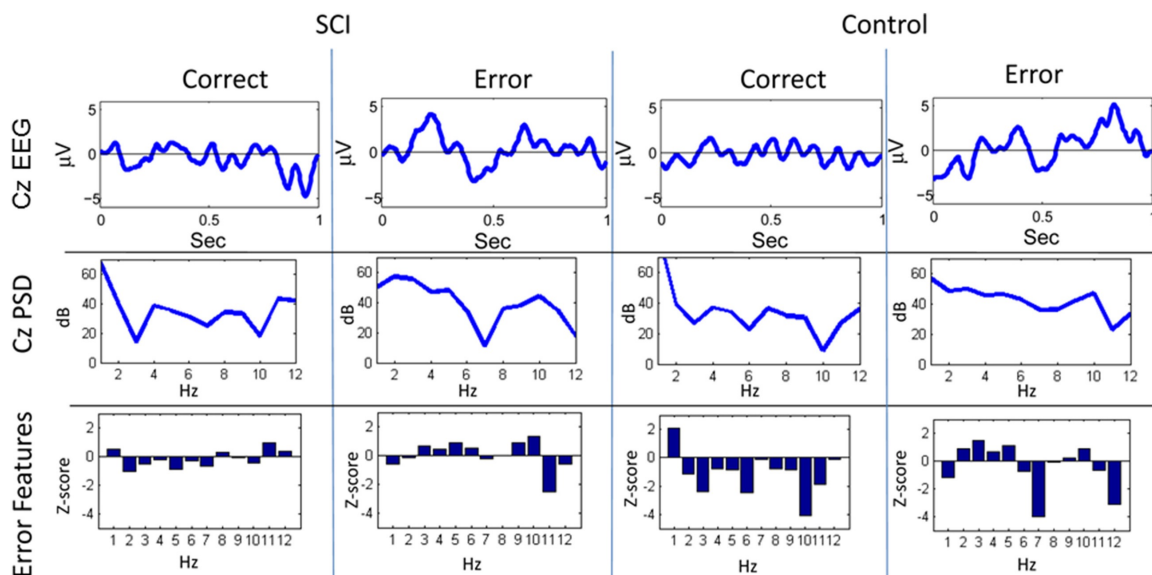


Figure 3.5 Sample trials from closed-loop sessions for error signals. Columns show samples for cues of “open” and “close” for both the SCI and control subject. Rows show raw EEG from electrode Cz (top row), PSD (middle row), and Z-scores (bottom row).

Although error potentials were not clearly identifiable from single trials (Figure 3.5, row 1), their biphasic shape became clearer when averaged over all trials performed by each subject throughout the full experiment. The average of EEG signals recorded from the Cz electrode in the 1 second following “wrong” and “correct” feedback was calculated. Figure 3.6 shows average error trials minus the average during correct trials for the SCI and Control subject. The waveform shape and temporal features are similar to previously published results [9].

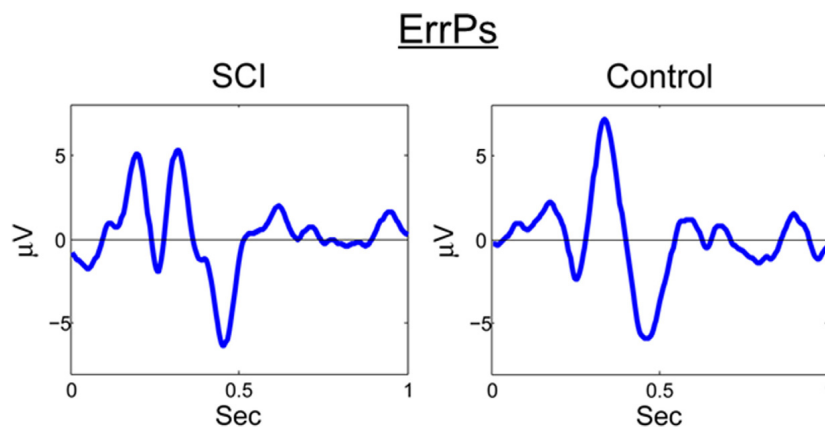


Figure 3.6 Error potentials for SCI and control subject. EEG signals recorded from Cz following feedback were averaged across all trials and displayed as error-minus-correct for the SCI and control subject.

Weights within the actor adapted throughout the 4 days of closed-loop BCI-FES testing, based on the feedback from the critic (Figure 3.7). As expected, weights adapted quickly during the first session, due to the random initialization of the actor weights. Weights adapted less quickly as subsequent experiments progressed, since weights from previous experiments were loaded in at the beginning of each session.

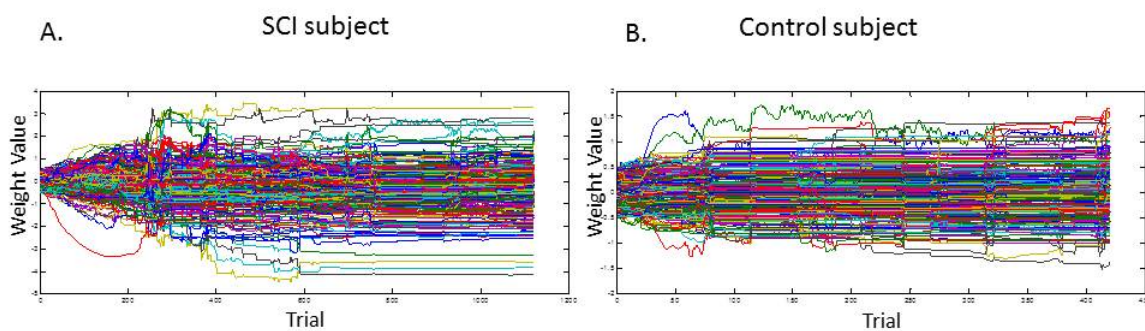


Figure 3.7 Motor decoder (actor) weights were updated throughout the 4 days of closed loop BCI-FES training for the A) SCI subject and B) control subject.

Initially, classification accuracy started at or below 50%, due to the random initialization of the actor weights. As the actor weights adapted in response to feedback from the critic, the overall classification accuracy improved. Accuracies for both the SCI and control subjects improved more rapidly during the first two sessions, similar to the actor weight adaptation behavior. In later sessions, the weights adapted less quickly and the classification accuracy continued improving, but less rapidly than during the first two sessions.

The actor and critic performance is shown in Figure 3.8. The Control subject performed slightly better than the SCI subject during the first session, which may be explained by the random initialization of the weights. Over the 4 days of training, the average overall classification accuracy of the actor (motor classifier) was similar between the two subjects, at just over 63.3% in the SCI subject and 64.2% in the Control subject. The average overall classification accuracy of the critic (errP classifier) was higher for the Control subject (68.8%) than for the SCI subject (64.2%) ($p < 0.005$). The performance of the actor improved over successive days until it reached the accuracy level of the error classifier (critic).

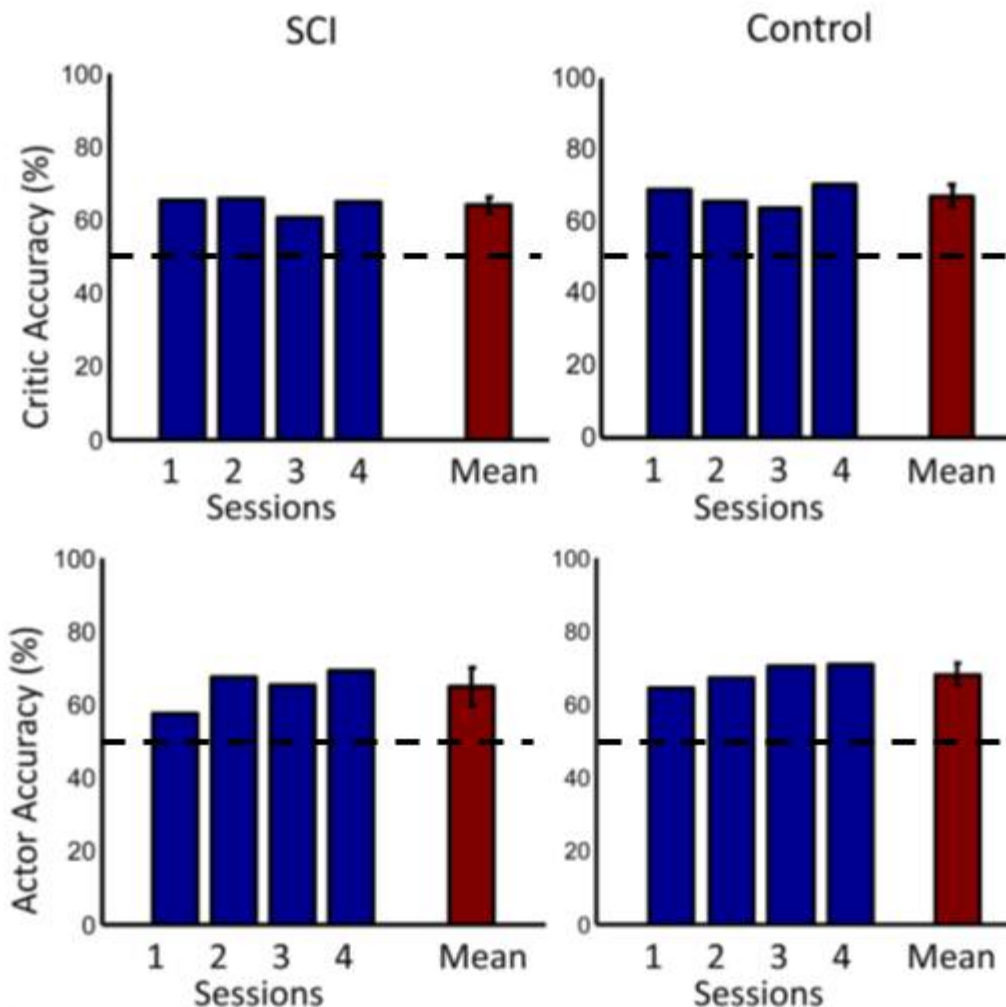


Figure 3.8 Accuracies across days. The first row shows the accuracy of the critic for both the SCI and control subjects. The second row shows the accuracy of the actor. Accuracy for each day is shown in blue. Mean accuracy across days is shown in red. Error bars represent one standard deviation. Mean accuracies were significantly above chance (50%) for both subjects ($p < 0.001$, one sided t-test).

3.5 Conclusion

These experiments demonstrated that a subject with SCI could control an EEG-based BCI-FES system as well as an uninjured, control subject. An actor-critic decoding architecture was implemented in order to provide continuous feedback for adaptation throughout the experiments, and the actor weights were continuously modified, based on

the output from the critic. Continual adaptation of a BCI-FES system may be beneficial, as it would not require time-consuming offline training beyond the first session. In addition, the system would be capable of adapting along with the user, as changes occur in the motor cortex in response to motor imagery training [124].

The ability to rehabilitate the motor cortex by motor imagery is meaningful in the context of BCI systems, as changes in sensorimotor rhythms are most often used for control. Motor imagery has been used for control in BCI-FES systems following spinal cord injury in only a few previous studies ([8, 56, 57, 66, 68]. After stroke, motor imagery training with a BCI-FES was shown to improve finger extension following only 3 sessions of training for 3 weeks [54]. In fact, following only a single session of motor imagery controlled BCI-FES in a stroke patient, electromyographic amplitudes from a leg muscle were significantly increased when compared to FES alone. The coupling between motor imagery BCI and FES is thought to affect neural plasticity. A system that is capable of adaptation should perform better than a static system.

Off-line analysis was performed with the data to compare performance levels from online experiments to levels acquired with static weights trained by supervised learning. During the first session, performance of the decoder was higher when using static weights, because the classifier was pre-trained, rather than having weights that were randomly initialized. However, the accuracies achieved during later sessions when using a system with static weights performed worse than the adaptive closed-loop system.

3.6 Lessons Learned

During these experiments, the Bioness H200 was used to deliver stimulation for opening the hand. Over time, we discovered that the Bioness had numerous limitations, which make it less than ideal for use during future BCI-FES experiments. First, the unit is not capable of sending more than one type of stimulation during a training block. In the way the wireless control unit functions, we were only able to send a signal for triggering stimulation either “on” or “off”. We were not able to toggle between different stimulation protocols using trigger pulses. This could only be accomplished manually, through a process requiring the programmers tablet. In addition, we were not able to create custom stimulation protocols with the Bioness, and we therefore were only able to use pre-existing stimulation programs set up by the company. There were no programs that delivered stimulation enabling closing of the hand in isolation. For this reason, stimulation was only sent for the “open” case in the experiments described in Chapter 3. We also experienced problems with the wireless communication between the control unit and the orthosis. Although the TTL pulse trigger was received by the control unit (confirmed by a light flash and audible tone), the signal was often not received by the orthosis, which resulted in confusing feedback to the user. Furthermore, the orthosis was found to be uncomfortable and limiting to some subjects, as a wrist bar spans across the back of the wrist, limiting voluntary movement at the wrist. For these reasons, we determined that a new stimulation paradigm was needed to optimize activation of the hand muscles in future BCI-FES experiments to enable grasp and release (Chapter 4).

Although the decoder used in this experiment did perform at a level significantly higher than chance, the overall performance in the SCI and Control subjects did not reach

70%, which is the level of control considered necessary for acceptance by the user [125, 126]. In order to improve performance, we decided to explore different methods for extracting features from the EEG data, as well as different decoding strategies. In these experiments, only raw signals from the C3 and Cz electrodes were used to create input features to the actor and critic, respectively. We decided to explore a greater number of electrodes where frequency modulation may be occurring during motor imagery. EEG signals were recorded with the ABM X10 headset, which has 9 electrode recording sites. The ABM X24 headset, which has 20 electrode recording sites, will be used for future BCI-FES experiments. Also, only 1 second of time was given between the display of the command and the display of feedback. Longer time periods will be explored, which would allow subjects more time to modulate neural activity. In addition, online filtering of the EEG signals may allow us to better utilize the small signal sources in inherently noisy EEG recordings. Signals will be filtered to focus on the mu (8-12 Hz) and beta (16-31 Hz) frequency ranges. ERD was most obvious within the mu range, however smaller changes within the beta range may be used to further discriminate between periods of motor imagery and rest. Z-scores of the power spectral density from 1-50 Hz and 1-12 Hz were used as neural features to the actor and critic, respectively. We will create new features and feed them to the decoder for comparison. The actor features will be based on frequency characteristics and may include either average or maximum power within the time window, the energy within individual frequency bins, or variances in power/energy. IC and principal component analysis may be used to localize sources during motor imagery. For the critic, a Gaussian classifier may better identify error potentials in single trials. These proposed changes will be explored in Chapter 5.

Finally, function was not assessed during these preliminary experiments. In order to be acceptable to the end user, a BCI-FES system must allow the person to accomplish a task that could not be accomplished without the device. During future experiments, function will be assessed by the Grasp and Release Test (GRT). Grip strength will be assessed using a grip force gauge dynamometer. The initial testing of these methods in uninjured, control subjects will be explored in Chapter 6.

CHAPTER 4: CUSTOM FES CONTROL PARADIGM

Aim 1 of this project was to investigate stimulation paradigms for electrical activation of hand muscles for a functional task. In order to accomplish this, two main objectives were established: 1) design a control paradigm for delivering stimulation, and 2) test efficacy and safety of stimulation protocol.

4.1 Control Paradigm for Delivering Stimulation

In order to perform the grasp and release task, a custom stimulation configuration and control paradigm were developed for delivering stimulation to the muscles using a Digitimer stimulator. Custom stimulation protocols were programmed in the Arduino integrated development environment (IDE 1.0.5) software and then uploaded to an Arduino UNO microcontroller board. The Arduino code is provided in the Appendix material. Trigger inputs (20 μ s pulse duration) were sent from the Arduino to the Digitimer, through custom cables (Cooner Wire), at a frequency of 35 Hz. The stimulation pulse duration (200 μ s) and current amplitude (10-30 mA) were set manually at the Digitimer stimulation unit. Current amplitudes were varied between subjects to produce full contraction of the target muscles.

A custom relay switch was designed on a printed circuit board (PCB) to allow consecutive stimulation of the flexor and extensor muscles of the hand (Figure 4.1). The PCB was designed using CAD software and fabricated (ExpressPCB) (Figure 4.2 A). The stimulation was split on the board and sent through two integrated circuit high voltage relays (Coto Technology). Flyback diodes (Fairchild Semiconductor) were connected in

parallel to the coil of each relay. When current to the coil (an inductor) is switched off, the diode provides a path for the current. Without the diode, the energy would have no place to go and could cause large, destructive voltage spikes. Circuit elements were soldered to the board, and the circuit was integrated with the Arduino microprocessor. The Arduino and PCB were cabled together and mounted within a custom enclosure (Figure 4.2 B). Multi-conductor shielded cables (Cooner Wire) and push-pull circular connectors (LEMO) were chosen to connect the Arduino and PCB to the USB port of the computer, Digitimer stimulator, and muscles to provide reliable application of stimulation. The stimulation is triggered through serial port commands sent from Matlab to the Arduino (Figure 4.3).

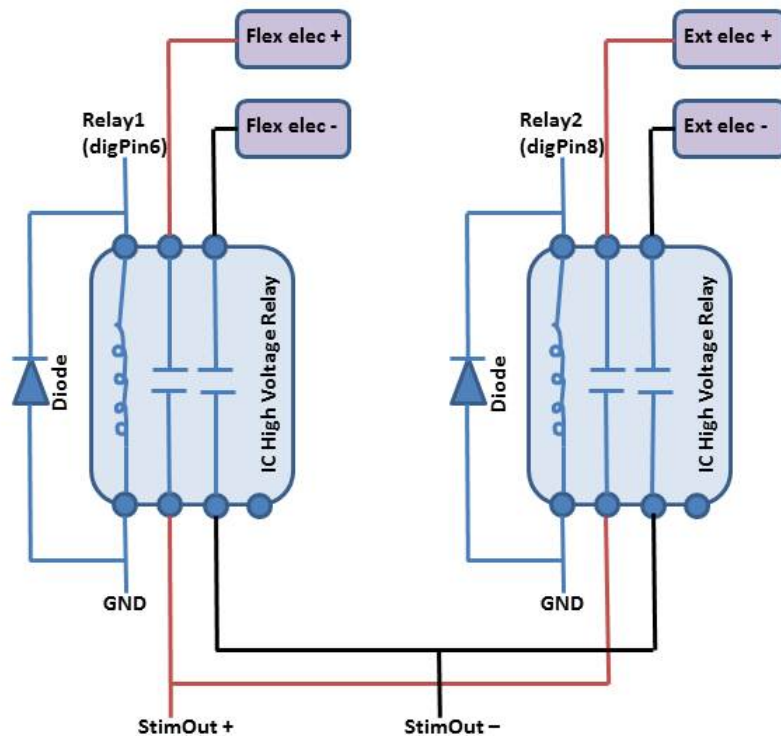


Figure 4.1 Schematic of printed circuit board for switching stimulation between flexor and extensor muscles.

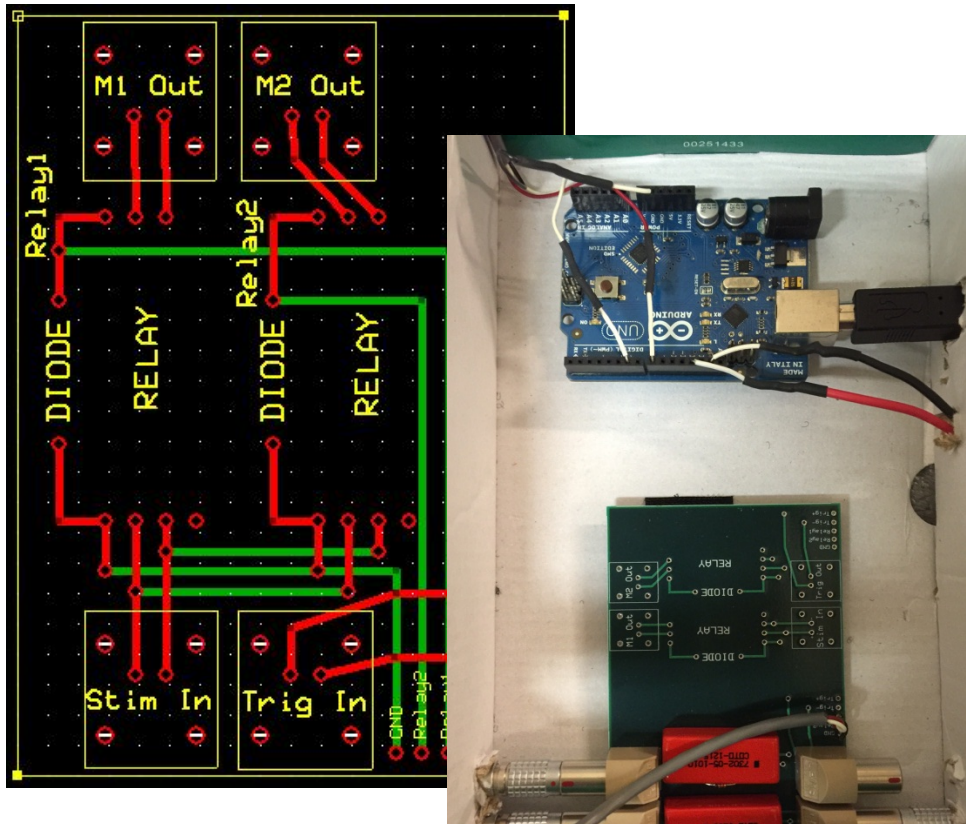


Figure 4.2 A) Printed circuit board designed for switching stimulation between flexor and extensor muscles. B) Arduino and PCB mounted in a custom enclosure.

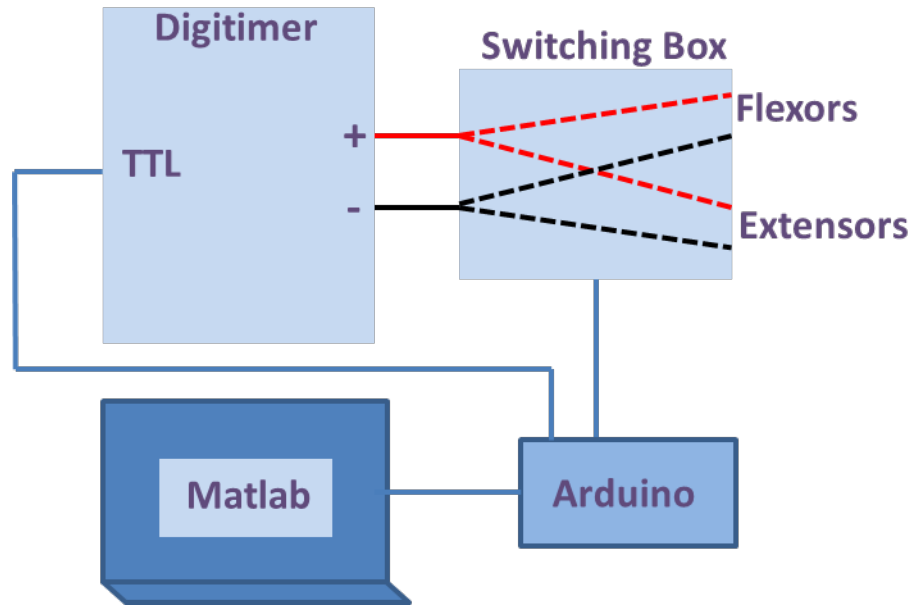


Figure 4.3 Overall stimulation configuration. Custom Matlab programs trigger the Arduino, which is connected to the USB port of the computer. Custom stimulation protocols written to the Arduino microprocessor trigger the Digitimer at 35 Hz via a TTL pulse and switch stimulation between the flexor and extensor muscles responsible for opening and closing of the hand.

Surface electrodes were applied to the muscles responsible for producing extension (opening) and flexion (closing) of the fingers for a grasp and release task (Figure 4.4). For extension, the active electrode was placed across the extensor digitorum profundus, extensor digitorum superficialis, and extensor pollicis longus. For flexion, the active electrode spanned the flexor digitorum superficialis and flexor digitorum profundus.

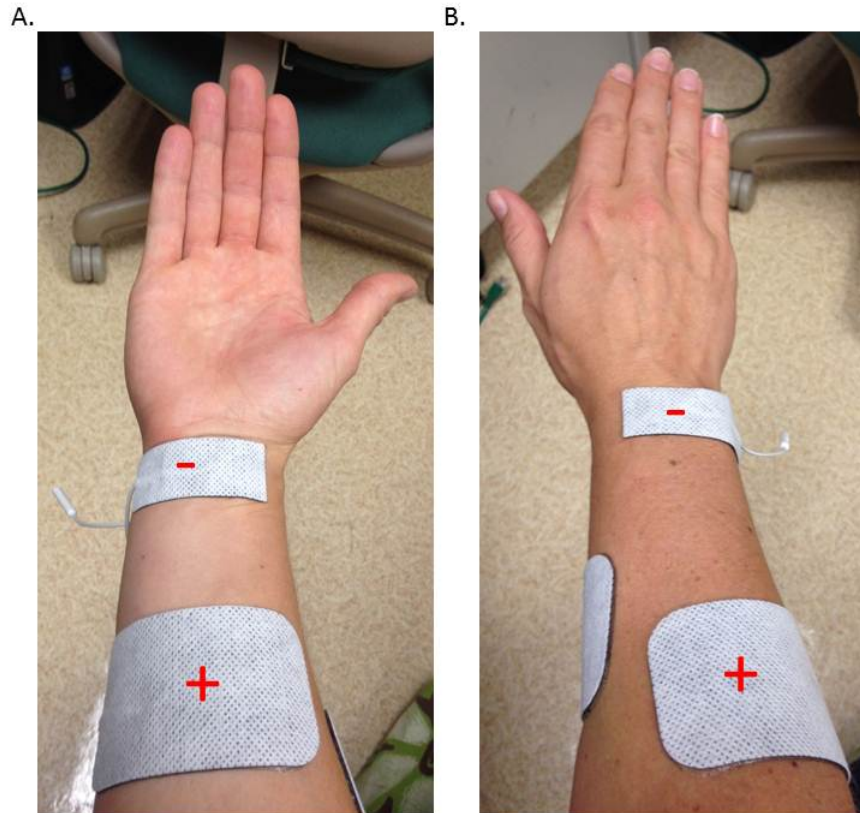


Figure 4.4 Positioning of active (+) and reference (-) over the A) flexor and B) extensor muscles to produce hand closing and opening, respectively.

Stimulation was delivered to the extensors and flexors in a pre-programmed sequence (Figure 4.5) so that the subject could pick up and move an object from one position on a tabletop to another with no voluntary contribution. This is achieved by opening the hand (to allow positioning around the object) for 4 seconds, then closing the hand (to grasp the object) for 4 seconds, and opening the hand again (to release the object) for 2 seconds. When the movement sequence is triggered, the coil activating the extensor pathway is activated. Then, stimulation from the Digitimer is sent through the extensor pathway such that the current is ramped up from 0 to 35 Hz over a period of 200 ms, held at 35 Hz for 3.6 seconds, and then ramped down from 35 Hz to 0 Hz over 200 ms, which opens the hand to allow positioning around the object. The extensor pathway

coil is then deactivated and the flexor coil becomes active. Current is ramped up to the flexor muscles (0-35 Hz, 200 ms), remains active for 3.6 seconds, and then ramped down (35-0Hz, 200 ms), which closes the hand around the object. The flexor pathway coil is deactivated and the extensor pathway is activated, allowing current to ramp up (0-35 Hz, 200 ms), hold constant (35 Hz) for 1.6 seconds, and then decrease (35-0 Hz) over 200 ms, allowing the hand to open and release the object.

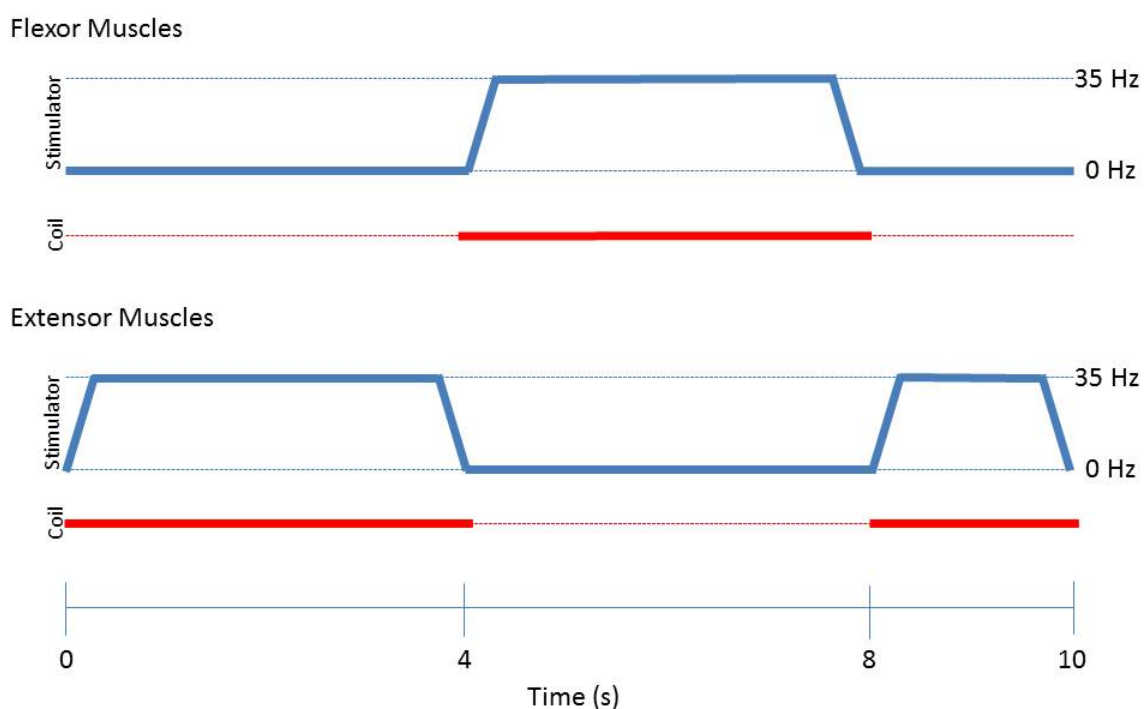


Figure 4.5 Stimulation sequence for a grasp and release task. Initially, the coil for the extensor pathway is activated to allow stimulation of the extensor muscles, opening the hand for positioning around the target object. Next, the flexor pathway coil is activated and the flexor muscles are stimulated, closing the hand around the object. Finally, the extensor pathway coil is reactivated, for stimulation of the extensors, which allows the object to be released by the hand.

4.2 Safety and Efficacy of Stimulation Protocol

The safety and effectiveness of the stimulation was assessed before use with human subjects. The Digitimer stimulator/PCB/Arduino configuration was bench tested in an electronics lab and output characteristics were assessed on an oscilloscope (Figure 4.6). A simulated body impedance circuit was designed to test the output parameters of the flexor and extensor circuits. A resistive-capacitive load made up of a $1\text{k}\Omega$ resistor in parallel with a $.047\mu\text{F}$ capacitor was used for voltage output measurements. A $1\text{k}\Omega$ shunt resistor was used for current measurements. To mimic variations in electrode impedance, the value of the load resistor was varied from $1\text{k}\Omega$, to 510Ω and $5.1\text{k}\Omega$. Pulse duration was set constant at $200\ \mu\text{s}$ and current amplitude was $5\ \text{mA}$.

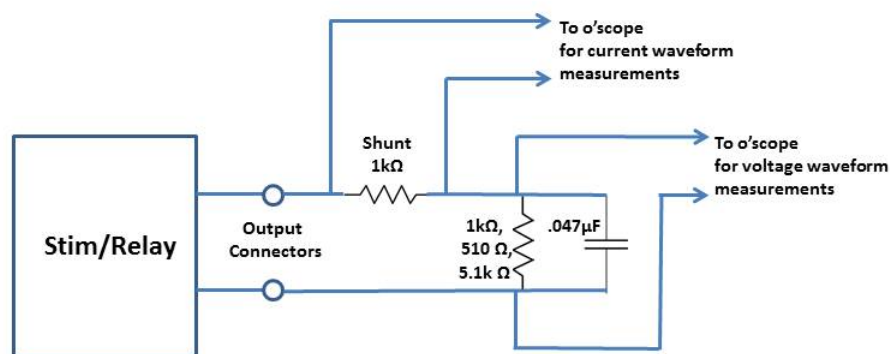


Figure 4.6 Test setup for stimulator output waveform measurements.

Output waveforms corresponding to the voltage and current output measurements are shown (Figure 4.7). No significant differences were seen in the current output when the load resistor was changed from $1\text{k}\Omega$ (typical), to 510Ω (good skin contact), and $5.1\text{k}\Omega$ (bad skin contact) (Fig 4.8). Even though the voltage waveforms display significant changes (Figure 4.8 A, C), the current that reaches the subject remains

constant (Figure 4.8 B, D). This ensures that changes in skin electrical impedance, which are expected to vary between subjects, will not affect the current delivered to the muscles. In addition, no voltage spikes were created during relay switching between flexor and extensor channels.

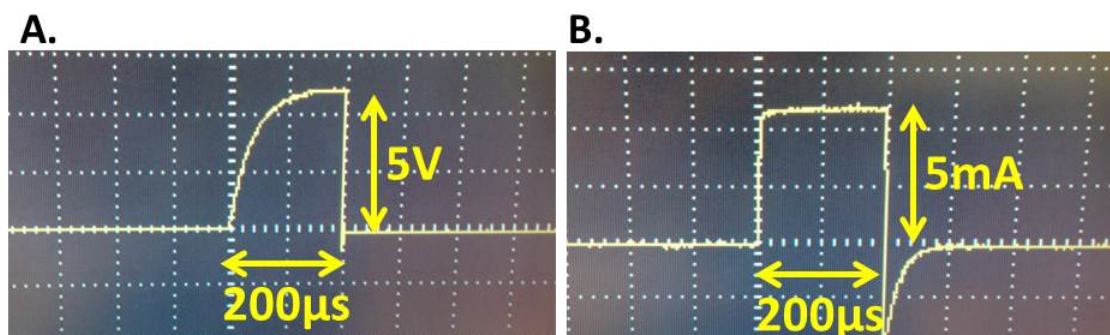


Figure 4.7 Output A) voltage and B) current waveforms with load resistance of $1\text{k}\Omega$, which mimics typical skin contact.

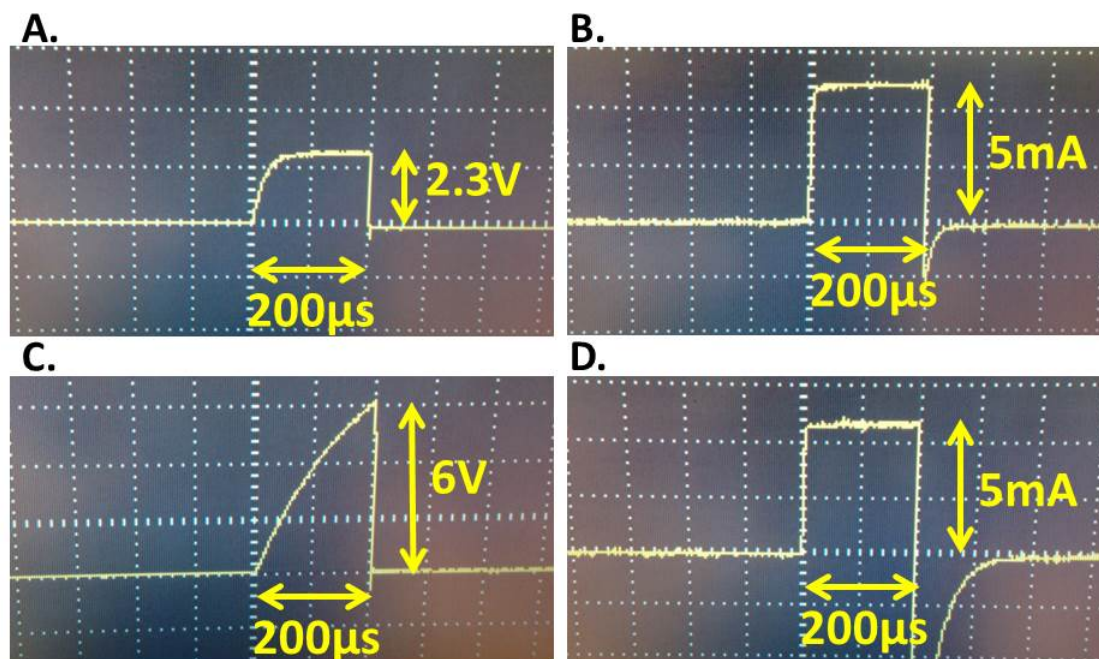


Figure 4.8 Output A & C) voltage and B & D) current waveforms with load resistance of 510Ω and $5.1\text{k}\Omega$, which mimic good skin contact and bad skin contact, respectively.

4.3 Conclusion

A custom stimulation paradigm was successfully designed for sending stimulation to the flexor and extensor muscles to enable grasp and release of an object. This process required the design, production, and assembly of a printed circuit board. Custom code was written to send trigger signals from the Arduino/PCB to the Digitimer stimulator. Custom cables and connectors were designed, soldered, and tested to provide consistent and reliable stimulation to the flexor and extensor muscles to enable closing and opening of the hand for a grasp and release task.

CHAPTER 5 FEATURES FOR BCI-FES CONTROL

Aim 2 of this project was to enable closed-loop brain control of FES to paralyzed muscles in order to perform a functional task. In order to accomplish this, two main objectives were established: 1) determine neural features that are optimal for triggering muscle stimulation sequences synchronously, and 2) develop an experimental paradigm for brain-controlled activation of paralyzed muscles to perform a functional task.

5.1 Subjects

Two subjects with SCI and 1 uninjured, control subject participated in these experiments. SCI subject details are included in Table 2. The control subject was a healthy 32 year old female.

Subject #	Age	Sex	R motor level	Time since injury (years)
1	30	M	C6	15
2	25	M	C6	2

Table 5.1 SCI subject details. Age (in years), sex (M:male, F:female), right side motor level, and time since injury (in years).

5.2 Experiment Protocol

Since event-related desynchronization was not clear in earlier experiments (Chapter 3), when only 1 second was given for subjects to imagine either opening or closing of the hand, it was determined that a longer period of time should be allowed. In order to verify the presence of ERD during actual and imagined movements of the hand, control subjects were instructed to spend 10 seconds idling/resting, followed by 10 seconds moving their right hand (cycling slowly between opening and closing the hand),

10 seconds idling/resting, and then another 10 seconds of imagining moving the right hand (Figure 5.1). This cycle was repeated so that each subject completed at least 30 trials each of actual and imagined movements of the right hand. The SCI subjects cycled between 10 second periods of idling/resting and 10 seconds of motor imagery. In addition, subjects were asked during other trials to imagine movements of the left hand or movements of the legs. The ABM X10 headset was used to record EEG signals, which were wirelessly transmitted to the computer and stored for later analysis.

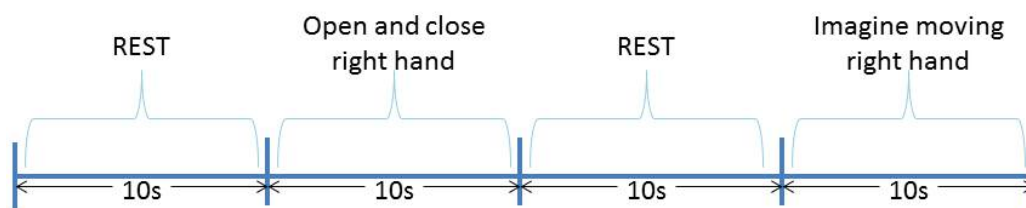


Figure 5.1 Timeline of experiment aimed at verifying presence of event-related desynchronization during actual and imagined movements of the right hand.

In attempts to verify the presence of error potentials in response to trials in which the outcome did not match the intent (“wrong” feedback), subjects participated in closed-loop experiments, similar to those described in Chapter 3. In those experiments, errors were randomly presented during the first training block at a rate of 50%, such that half of all trials resulted in “wrong” feedback. During this round of experiments, errors were presented at a rate of only 20%. Since error signal amplitudes have been shown to be inversely proportional to the error presentation rate [9], we expect that error signals will be elicited better with this lower presentation rate. Each subject completed 40 trials a day

of closed-loop BCI-FES training with an error presentation rate of 20%. Error signals (20%) were then compared to the error signals collected in Chapter 3 (50%).

In addition, error signals were classified offline using the methods described in Chapter 3 (z-scores, 1-12 Hz, MLP). Then, error signals were classified using a Gaussian mixture model [9], which has been shown to produce better outcomes in single trial identification of errPs. First, raw EEG signals from the Cz electrode were spatially filtered by subtracting the average EEG from each electrode at every time step. This removes background activity, to ensure the information of interest is coming from local sources close to each electrode. Then, a 1-10 Hz bandpass filter was applied, since errPs are slow cortical potentials. The input features were made up of 150 ms of data (downsampled to 64 Hz), starting 250 ms after the feedback. Two different classes, “error” or “correct” were recognized by the Gaussian classifier. Each Gaussian unit represents a prototype of one of the classes, and several prototypes are used per class. During training, the centers of the classes are pulled towards the trials of the class that they represent and pushed away from the trials of the other class.

5.3 Results

During actual movements of the right hand, event-related desynchronization (ERD) was apparent at the C3, Fz, and F3 electrodes (Figure 5.2) within the 8-20 Hz range. No difference was seen between the two conditions above 20 Hz, except for in electrode F3. During imagined movements of the right hand, ERD was present along a wider frequency range over a greater number of electrodes (Figure 5.3). ERD occurred

across the spectrum in the C3 and C4 electrodes and above 20 Hz in the Fz, F3, F4, P3, P4, and POz electrodes.

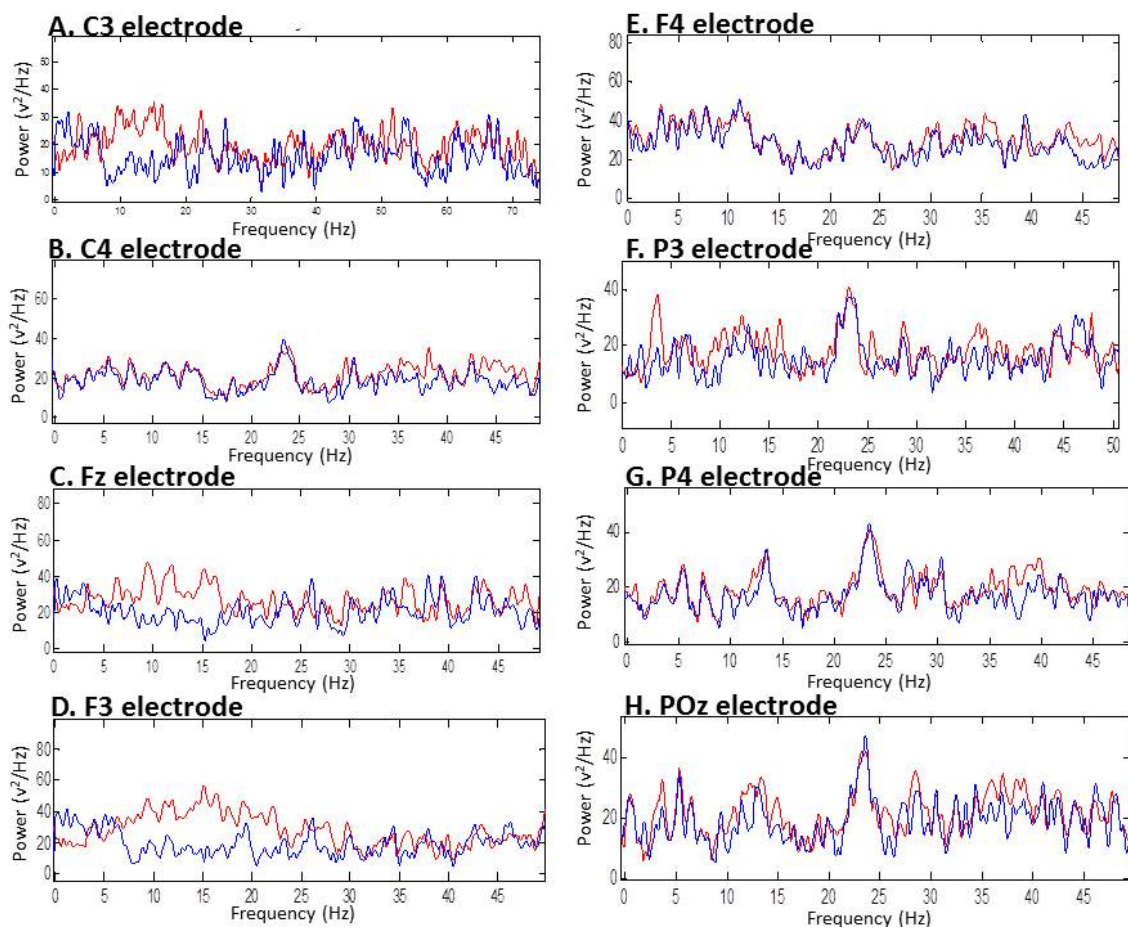


Figure 5.2 Discrete fast fourier transform during periods of actual hand movement (blue traces) and periods of rest/idling (red traces) in an uninjured, control subject. Raw EEG signals were averaged over trials and filtered 0.5-75 Hz.

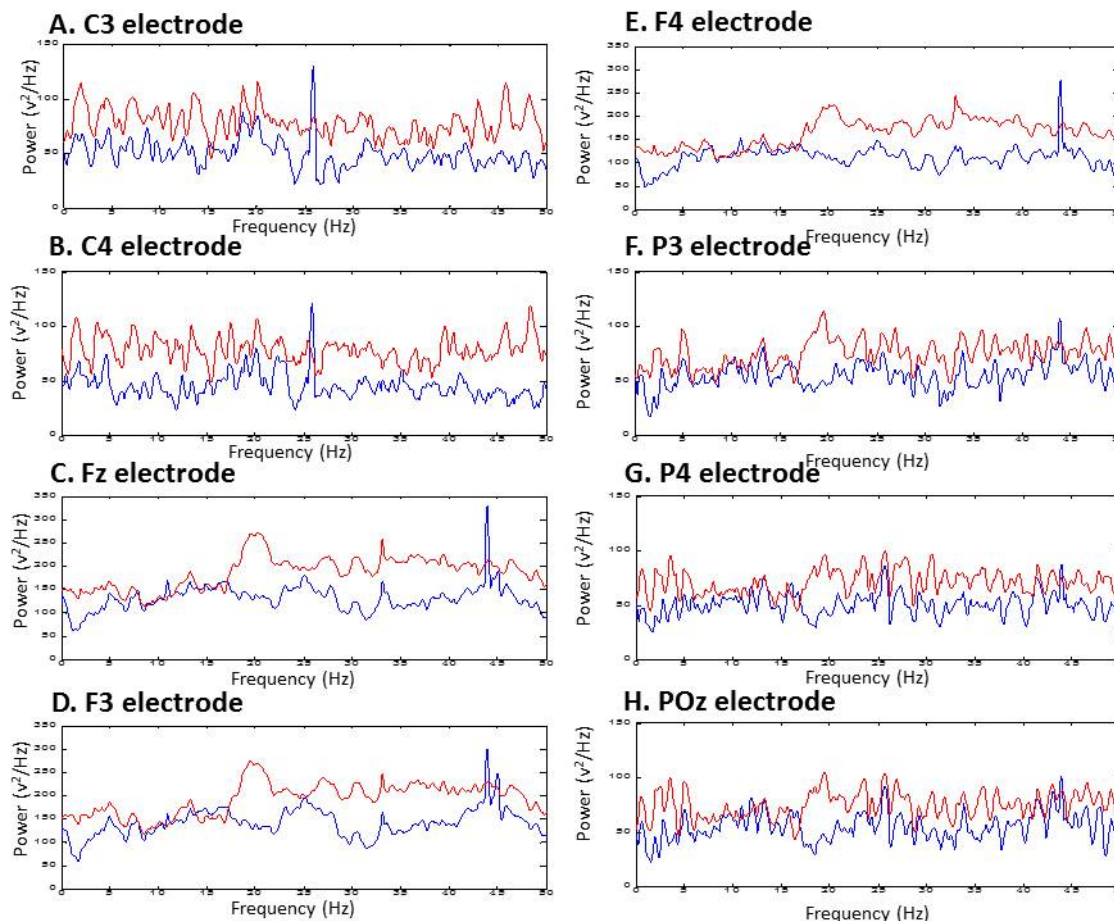


Figure 5.3 Discrete fast fourier transform during periods of imagined hand movement (blue traces) and periods of rest/idling (red traces) in an uninjured, control subject. Raw EEG signals were averaged over trials and filtered 0.5-75 Hz.

To further characterize EEG signals during periods of motor imagery and rest/idling, signals were filtered between 2-50 Hz and artefacts were rejected using an automatic continuous rejection method (EEGLAB). Independent component analysis (ICA), followed by dipole clustering was used for source localization of cortical activation. Dipoles with residual variance values less than 15% were selected (Figure 5.4). Changes in activation maps were seen across areas of the motor cortex within sessions. However, the independent components corresponding to right hand movements

(those with equivalent dipoles near the area of the motor cortex related to right hand movements) were present and stable in all of the subjects across all sessions. This suggests that the C3, C1, and Cz electrodes should contain the highest information content when subjects perform motor imagery of the right hand.

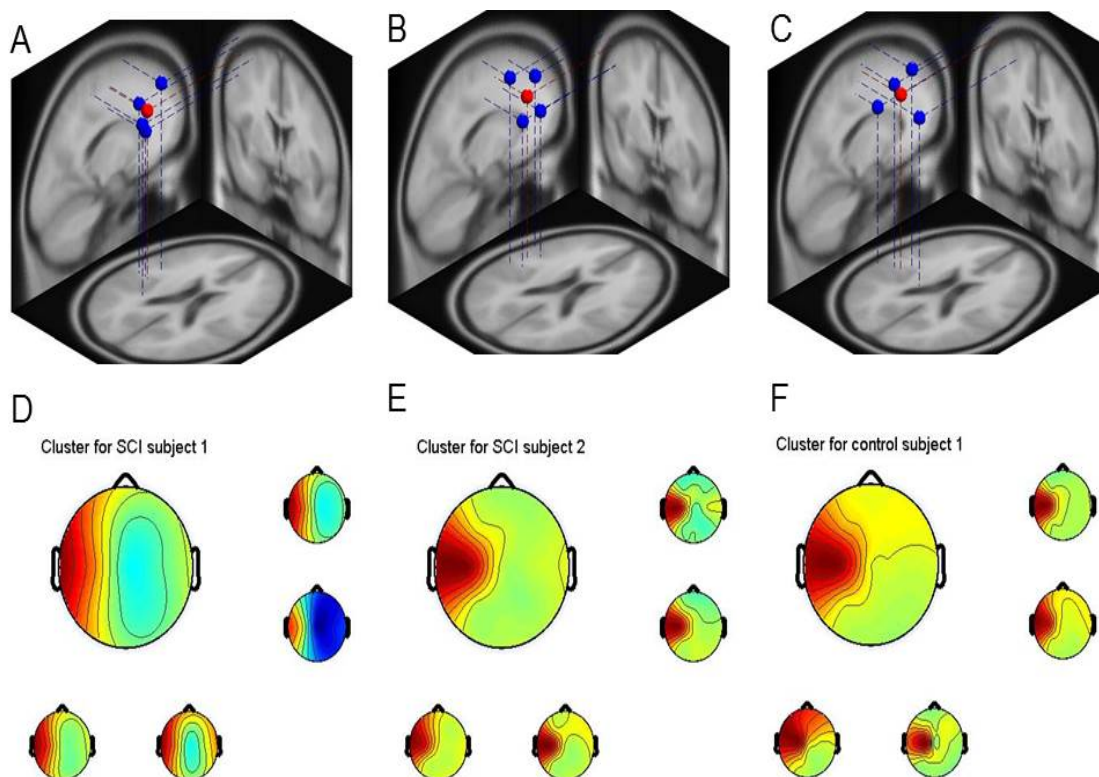


Figure 5.4 A-C) Fitted dipole positions of clustered independent components (blue dots) for SCI subject 1, SCI subject 2, and control subject 1, respectively. Red dots represent centroids of the clusters. D-F) Scalp maps of each clustered independent component. Upper left maps represent cluster averages.

ERD was observed in all subjects using spatial filters determined by the weights of the independent components (ICs). Normalized power spectral density (PSD) was then calculated for each IC, and the means of the normalized PSDs were found (Figure 5.5). Differences in the PSD can be seen during motor imagery vs periods of rest/idling, as

well as between healthy and SCI subjects. Peaks are apparent around 10 Hz in all subjects, with an additional peak in the 15-20 Hz range that is more apparent in the control subject. This analysis suggests that features should be chosen from within the mu frequency range (8-12 Hz), which is reactive over multiple experiment sessions during motor imagery in both SCI and control subjects.

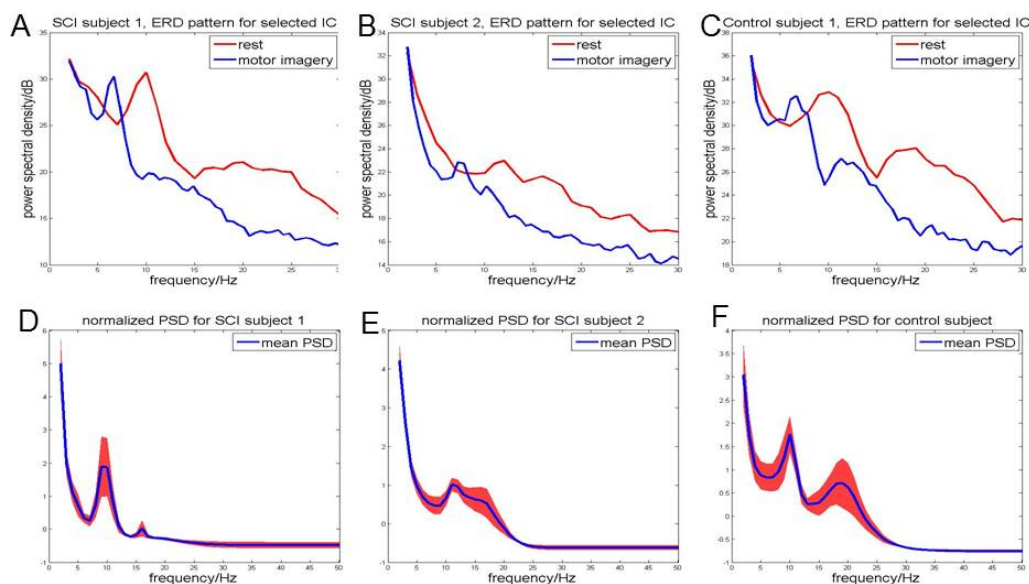


Figure 5.5 A-C) Power spectral density during periods of motor imagery and periods of rest/idling for SCI subject 1, SCI subject 2, and control subject 1. D-F) Normalized mean power spectral density calculated by selected independent components for all sessions in each subject. Red region represents the range of \pm one standard deviation.

The time course of ERD during imagery of right hand movements or imagery of bilateral leg movements was evaluated. ERD is present during imagery of movements in both the right hand and legs averaged over the C3, C1, Cz, C2, and C4 electrodes (Figure 5.6). Raw data were filtered 5-35 Hz (5th order Butterworth), squared, moving average filtered (125 ms), averaged across all trials, and referenced to a 1 second “rest” time period. The most extensive ERD is present starting from 2 seconds following the visual

command. The ERD continues throughout the remainder of the period, while the subject continues to imagine the movement. During the first 1 second following the cue, the power is just starting to decrease and ERD is not apparent. This could suggest why ERD was not clearly identifiable during previous experiments, where only a 1 second window of time was used for imagined movements of the right hand.

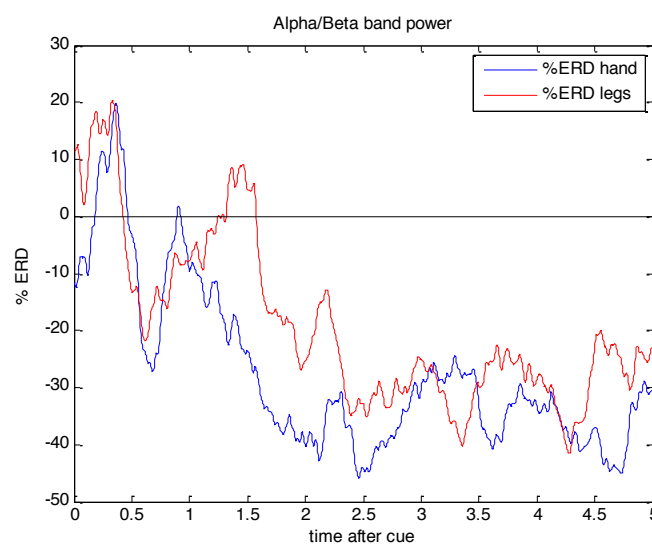


Figure 5.6 Time course of ERD during right hand (blue) or bilateral leg (red) motor imagery averaged over the C3, C1, Cz, C2, and C4 electrodes, averaged over 10 trials, with respect to the cue in one subject with SCI.

We then explored whether we could distinguish between imagery of two different muscle groups, rather than between movement and rest. There were no differences in power spectral densities from the C3, C1, Cz, C2, and C4 electrodes in either SCI subject (Figure 5.7). In addition, no frequency-based differences were present when subjects performed motor imagery of the left and right hands (Figure 5.8).

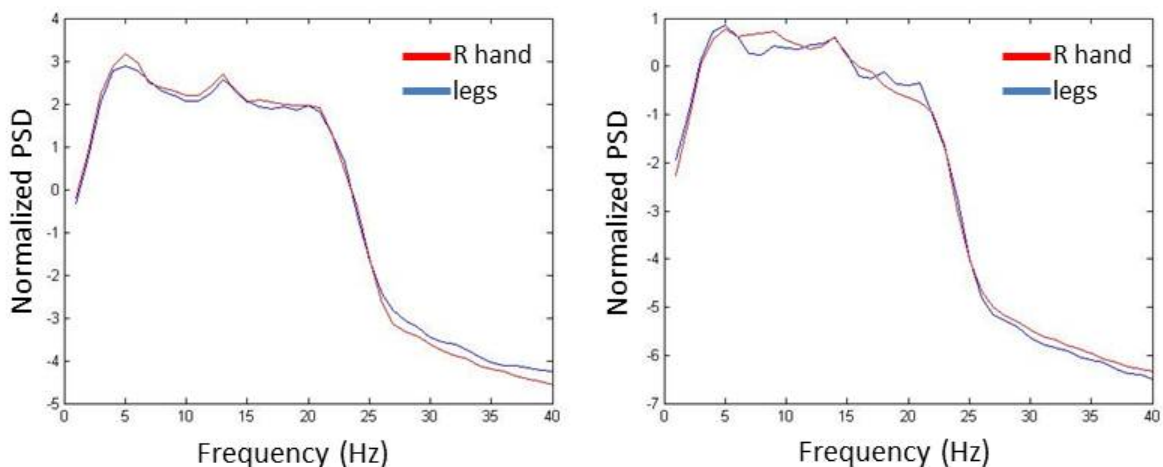


Figure 5.7 Normalized power spectral density averaged over the C3, C1, Cz, C2, and C4 electrodes for SCI subject 1 (left) and SCI subject 2 (right) during right hand and bilateral leg motor imagery, averaged over 100 trials.

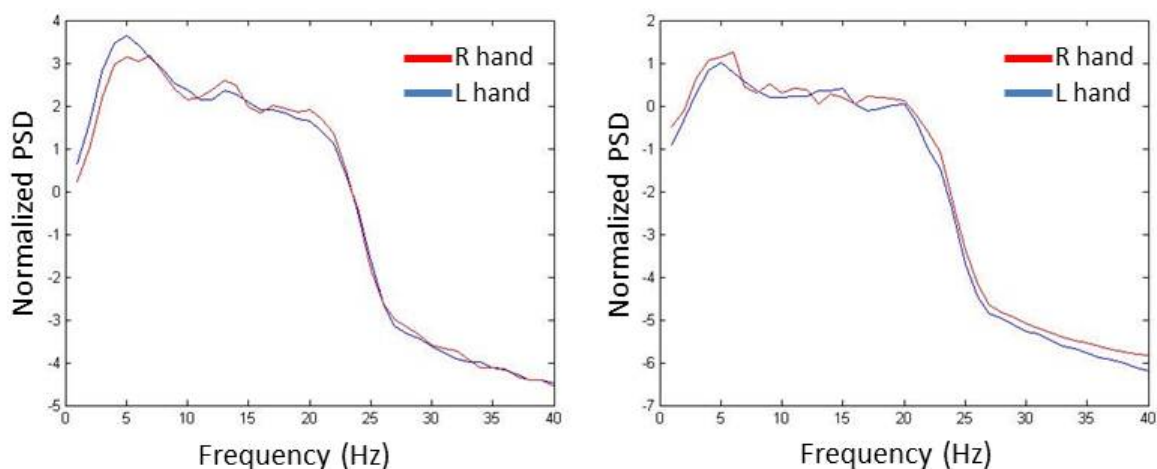


Figure 5.8 Normalized power spectral density averaged over the C3, C1, Cz, C2, and C4 electrodes for SCI subject 1 (left) and SCI subject 2 (right) during right hand and left hand motor imagery, averaged over 100 trials.

EEG signals generated in response to “wrong” and “correct” feedback were similar when averaged across 50 trials (Figure 5.9). Although the positive peak around 300 ms was slightly higher in response to “wrong” feedback, the average

waveform shapes and characteristics did not differ. According to previous studies [9], interaction errPs would be expected to have a large negative peak around 400 ms. The clearest error signals were generated by the control subject, and two examples of errPs are shown (Figure 5.10).

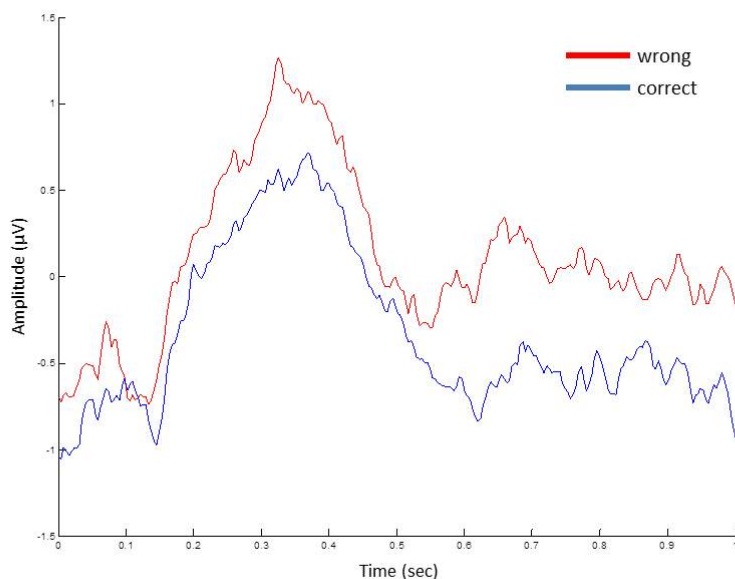


Figure 5.9 Error signals generated in response to wrong (red) and correct (blue) feedback in an uninjured, control subject. Each trace represents an average of 50 trials.

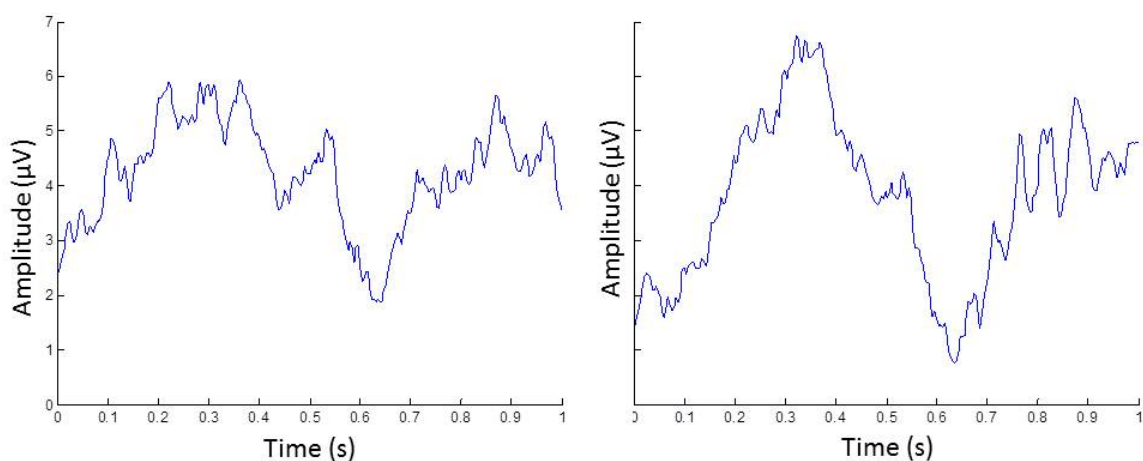


Figure 5.10 Two examples of error signals generated in response to wrong feedback in an uninjured, control subject. Each trace represents a single trial.

We then attempted to classify error potentials using a Gaussian mixture classifier, similar to the one described in [9]. For SCI subject 1, classification accuracies did not reach over the level of chance (50%) on any of the 4 testing days. Accuracies in SCI subject 2 were slightly better on days 1 and 2, and reached a maximal accuracy of 59.4% on day 2. This was the maximal classification accuracy attained on any day in any subject. Accuracies for identifying errPs in single trials for the control subject were just around 50% on all 4 days, with a maximum of 54.8% on day 4.

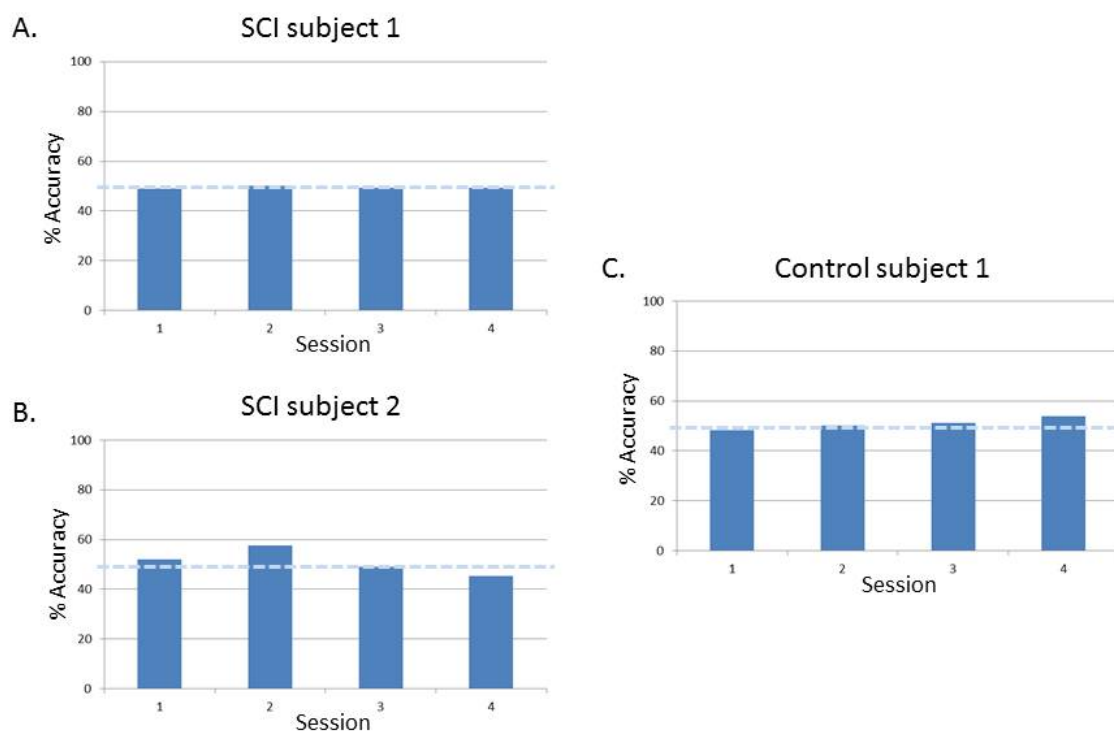


Figure 5.11 Error classification rates for two SCI subjects and one control subject using a Gaussian mixture model classifier. Accuracy rates were around 50% for all subjects.

5.4 Conclusion

Event-related desynchronization was clear during motor imagery of the right hand, left hand, and legs. However, power decreases were not apparent until at least 350 ms following the cue. For this reason, features input to classifiers should not incorporate signals before this time. In addition, the most meaningful frequency bands were in the mu range (8-12 Hz), which were reactive over multiple experiment sessions during motor imagery in both SCI and control subjects. Differences in power spectra were apparent when comparing actual hand movements and imagery of hand movements to rest. However, no differences could be seen when comparing imagined movements of different muscle groups, (right hand vs legs, or right hand vs left hand).

Error potentials could not be reliably identified in single trials. The maximum average classification accuracy attained using the Gaussian mixture model were approximately 60%. When incorporated in to the reinforcement learning BCI architecture (actor-critic), this caused the maximum actor accuracies to reach a plateau around 60% as well. For this reason we have decided not to incorporate a critic at this time. Further development of error potential classifiers may result in improved performance, and the critic could be reincorporated at that time. We have decided to use a SVM-based classifier to decode between rest vs movement states. This was also done so that the subject receives correct feedback most number of times. To make the experimental design more interactive, we have incorporated correct/wrong visual and auditory cues as well as showing cues on a laptop screen. The subject's also receive feedback on the laptop screen about how well they are modulating their EEG in near real-time by showing them the percent changes in the event related desynchronization (ERD). The SVM

classifies data based on past “move” and “rest” periods. Average power in 5 Hz bins for the frequency range 5-35 Hz is used for 3 seconds of data. For the “move” class, this is 0.5 – 3.5 s following the command. For the rest period, this is 3s before the “move” command. The average power from 5-35 Hz is found for electrodes C3, C1, Cz, C2, and C4 in 5 Hz bins. These features are input to the standard Matlab SVM classifier.

CHAPTER 6 ASSESSMENT OF FUNCTION

6.1 Subjects

One SCI subject and three uninjured, control subjects participated in this set of experiments. The SCI subject was a 30 year old male with a C6 complete SCI, who had been injured for 15 years at the time of testing. His hand muscles were responsive to electrical stimulation with the Bioness and Digitimer stimulators.

6.2 Experiment Protocol

Aim 3 of this project was to assemble a battery of rehab metrics to quantify improvements in hand function over time. During preliminary closed-loop experiments (Chapter 3), function was not assessed. Moving forward, grip strength will be assessed at the beginning of each testing session using a microFET4 grip and pinch force gauge dynamometer (Figure 6.1). Testing of the grip strength will be evaluated here in three uninjured, control subjects. Functional performance of the task will also be evaluated in the same group of subjects by the Grasp and Release Test (GRT).



Figure 6.1 The microFET4 dynamometer is used for quantifying grip strength.

To be effective in transferring an object from one position to another, the grip strength achieved during stimulation with the Digitimer/relay configuration should be similar to that achieved during stimulation with the Bioness. In order to assess the grip strength produced by the Digitimer/relay configuration, grip strength was tested in three healthy control subjects during maximal voluntary contractions, stimulation of the muscles of the right hand with the Digitimer/relay, and stimulation with the Bioness. The average grip strength resulting from each of these conditions is reported.

Control subjects were instructed to voluntarily contract the muscles of the right hand while grasping the microFET4 dynamometer for 4 seconds. The researcher held the dynamometer in a vertical position in front of the subject, who sat comfortably in a stable chair. Then, the subjects were instructed to relax their muscles, i.e. not to produce any voluntary activity. Either the Bioness H200 or the Digitimer/relay was used to apply electrical stimulation to the muscles of the right hand. With either device, stimulation intensity was set by holding the pulse duration (200 μ s) and frequency (35Hz) constant, while slowly increasing the current amplitude. Once a maximal contraction was attained

in the flexor muscles of the hand (increases in current intensity did not result in additional force production), the current amplitude was increased an additional 25% in order to maintain consistent muscle contractions. Three separate trials were conducted for each control subject and for each condition, with contraction duration of 4 seconds and one minute rest between consecutive trials. The SCI subject participated in 4 days of muscle testing. He also participated in some BCI testing on those days. Grip strength was tested at the beginning and end of each day in the three conditions (voluntary, Bioness, and Digitimer).

To assess function of the stimulation sequence for completing the Grasp and Release Test, activation of hand muscles was achieved by stimulation with the Digitimer/relay configuration. Stimulation was delivered to the extensors and flexors in a predetermined sequence so that the hand opened for 4 seconds, closed for 4 seconds, and then opened again for 2 seconds. Subjects were tasked with moving objects from one side of the table to another (Figure 6.2). Subjects made 5 attempts with 3 objects: a wooden shot glass, a large diameter plastic cup, and a heavy unopened can. Control subjects participated in one day of testing, while the SCI subject completed 4 days of testing.



Figure 6.2 Subject readying to perform the Grasp and Release Test. Stimulation is delivered to the muscles responsible for opening and closing of the hand, so that the subject may grasp the object, pick it up, and move it from one side of the table to the other.

6.3 Results

An average of the maximum grip strength (+/- standard error) achieved during Bioness and Digitimer/relay use was calculated for each control subject (Figure 6.3). Maximal grip strength was highest during voluntary contraction, followed by Digitimer/relay stimulation, and lowest during Bioness stimulation for all three subjects. The grip strength achieved during the two stimulation conditions was significantly lower than that measured during maximal voluntary contraction ($p < 0.05$). This could be due to either non-maximal stimulation intensity or insufficient activation of all muscles that may contribute to hand closing. However, the average grip strengths attained during both stimulation conditions were similar. The SCI subject performed 4 days of grip strength testing, before and after BCI-FES testing, similar to the testing that will be done during the full experiment. The force produced by the SCI subject was significantly lower than the force produced by the control subjects ($p < 0.05$) for both stimulation conditions. The

force achieved with both types of stimulation was higher at the beginning (pre) of each experiment day when compared to the end (post) (Figure 6.4), suggesting some muscle fatigue due to BCI-FES testing. No differences in average force were seen between the Bioness and Digitimer stimulation. Therefore, the Digitimer/relay configuration was determined to be comparable to the Bioness in terms of activating paralyzed muscles for a grasp and release task. The SCI subject was not able to produce any voluntary force at the beginning or end of any testing days.

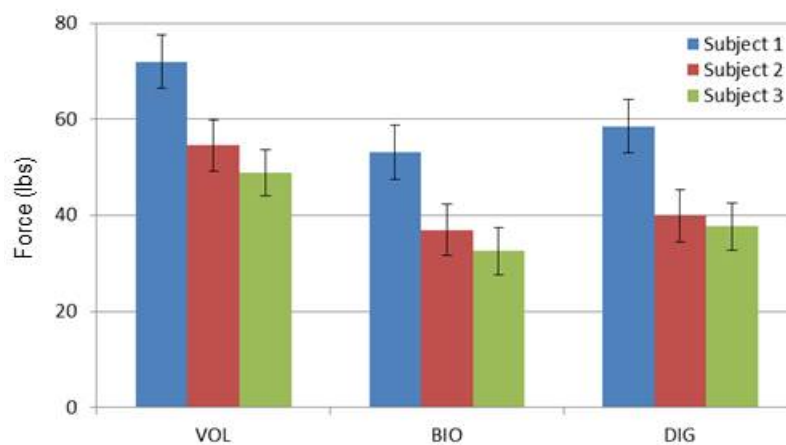


Figure 6.3 In control subjects, average grip strength/force (\pm standard error) achieved during voluntary contraction of the muscles of the right hand, Bioness stimulation, or stimulation with the custom Digitimer/relay configuration. Stimulation parameters: 35 Hz, 200 μ s, 20-25 mA.

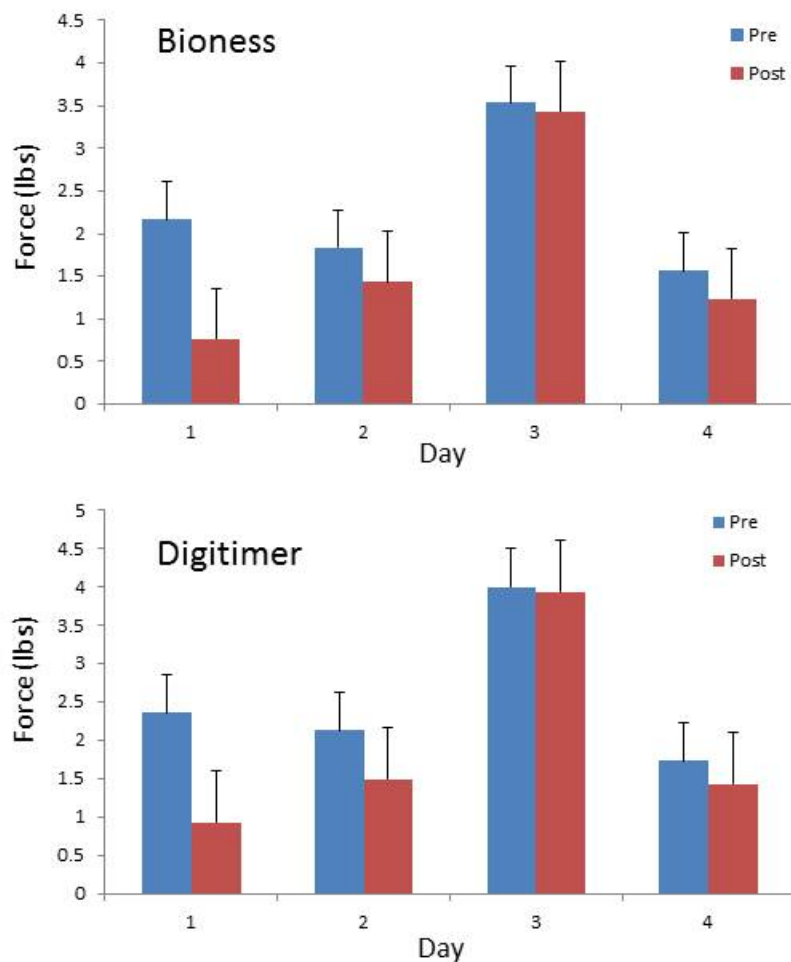


Figure 6.4 Average grip strength/force (+ standard error) achieved during electrical stimulation of paralyzed hand muscles in SCI subject with Bioness (top) and Digitimer (bottom) stimulators. Stimulation parameters: 35 Hz, 200 μ s, 40 mA.

All three control subjects were able to pick up, move, and release all three objects successfully, both with and without (voluntary) the application of FES. The SCI subject was able to pick up the shot glass using tenodesis every day, 100% of the time (Figure 6.5). On the first day of testing, he failed during one attempt (80% success rate). Throughout the rest of the testing he was always able to pick up the shot glass with stimulation. He was never able to pick up the wide-diameter empty cup using only voluntary control. Only on the third day of testing was the subject able to pick up the cup

with stimulation with 80% success (4 out of 5 trials). It is unknown why he was able to perform this task on this day but not on the others. The subject was usually able to pick up the heavy can using tenodesis (60-100% success throughout testing). However, the stimulation enabled him to always be successful in picking up the heavy can.

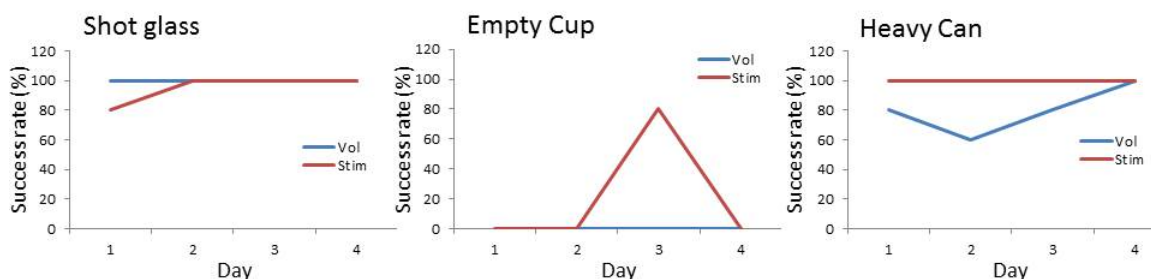


Figure 6.5 Average success rate (%) of grasp and release task with a small diameter shot glass, a large diameter, lightweight, empty plastic cup, and a heavy can. The SCI subject performed 5 attempts with each object using voluntary control (blue) and stimulation (red) at the beginning of each session.

6.4 Conclusion

We have successfully developed and tested a protocol for assessing muscle strength and fatigability, as well as performance of a functional task (grasp and release test). In future testing with SCI subjects (Chapter 7), grip strength and the performance of the grasp and release task will be assessed before any training (baseline) and throughout the experiment (at the beginning of each session). Before each subject completes any training, a pretest will be administered, in which the subject will be tasked with moving 3 objects with and without use of FES. The stimulation will be triggered automatically, without use of the BCI. The subject will be given 5 attempts to pick up and move each object with and without FES. Each trial will last 30 seconds. If the subject is unable to move the object in that time, that trial will be counted as a failure. The three objects will

consist of a small diameter wooden shot glass, a large diameter empty plastic cup, and a heavy, unopened soup can. This period of time will also allow the subject to practice the task before closed-loop testing, when the stimulation sequence will be triggered by neural activity.

CHAPTER 7: BCI-FES FOR GRASP AND RELEASE

7.1 Subjects

Five subjects with spinal cord injury (ages 19-49, mean \pm SD: 33.6 \pm 11.4) and five uninjured, control subjects (ages 18-31, mean \pm SD: 22.6 \pm 4.9) participated in this study. Subjects participated in six experimental sessions (2-3 hours each) scheduled at their convenience over a 2-6 week period. SCI subject details are included in Table 7.1.

Subject #	Age (years)	Sex	Time Since Injury (years)	Cause of Injury	Motor Level
1	35	M	13.2	MVA	C6
2	27	M	8.2	Diving	C6
3	38	F	14.8	Fall	C5
4	49	M	1.2	Diving	C5
5	19	M	1.6	Sports	C5

Table 7.1 SCI subject details. Age (in years), time since injury (in years), cause of injury, and right side motor level. MVA = motor vehicle accident.

7.2 Experiment Protocol

During each session, subjects performed 120 trials of BCI training with FES of the right hand, which was the dominant hand for all participants. Each subject completed a total of 720 BCI-FES trials over the 6 days of training. Each training session lasted 2-3 hours. Subjects were seated comfortably either in their wheelchair (SCI subjects) or a stationary chair (control subjects) in front of a computer monitor (Figure 7.1 A). A trial (Figure 7.1 C) began with a fixation cross, which was displayed for 1 second to minimize eye movements. This was followed by a 3 second “relax/don’t move” cue on screen during which the subjects were instructed to rest and look straight ahead with eyes open.

A 5 second “move” period followed, during which subjects were instructed to imagine movements of the right hand while avoiding any body or eye movements. Feedback during the motor imagery period was displayed in the form of a scrolling plot showing the inverse instantaneous power from the C3 electrode. Online decoding of the motor imagery period was then performed. If decoded correctly (features classified as intended movement), the screen displayed “correct” and the subject received FES for grasp and release (Figure 7.1 C, i). If decoded incorrectly (features classified as rest), the screen displayed “wrong” and the subject did not receive FES. Different auditory cues accompanied both feedback outcomes (Figure 7.1 C, ii).

At the beginning of the first session, the support vector machine (SVM) was trained when the user was instructed to perform motor imagery by following cues on the screen. The binary SVM model was initially trained using 40 trials of rest and 40 trials of motor imagery. Subsequent trials were added to the training set until it was composed of the most recent 120 trials from each class. The user was instructed to either “rest” (do nothing) or perform “motor imagery” (imagine moving right hand) by following “Rest” and “Move” commands on the screen. Three second segments of data were extracted from the rest (0-3 seconds following rest cue) and motor imagery (0.5-3.5 seconds following motor imagery cue) periods. From each segment, the average power from 5-35 Hz in 5Hz bins from the C3, C1, Cz, C2, and C4 electrodes was input to the classifier. These features were input to a SVM classifier with linear kernel function in Matlab. The purpose was to train the SVM classifier to distinguish between “Rest” and “Move (motor imagery of imagined movements)” states from the input features of the EEG signal. Since SVM learns a hyperplane in a high dimensional space, the signal can be seen as a single

point in this space. The classifier gives classification according to which side the point lies alongside the hyperplane. If this output was the same as the cue, then the output was classified as "correct".

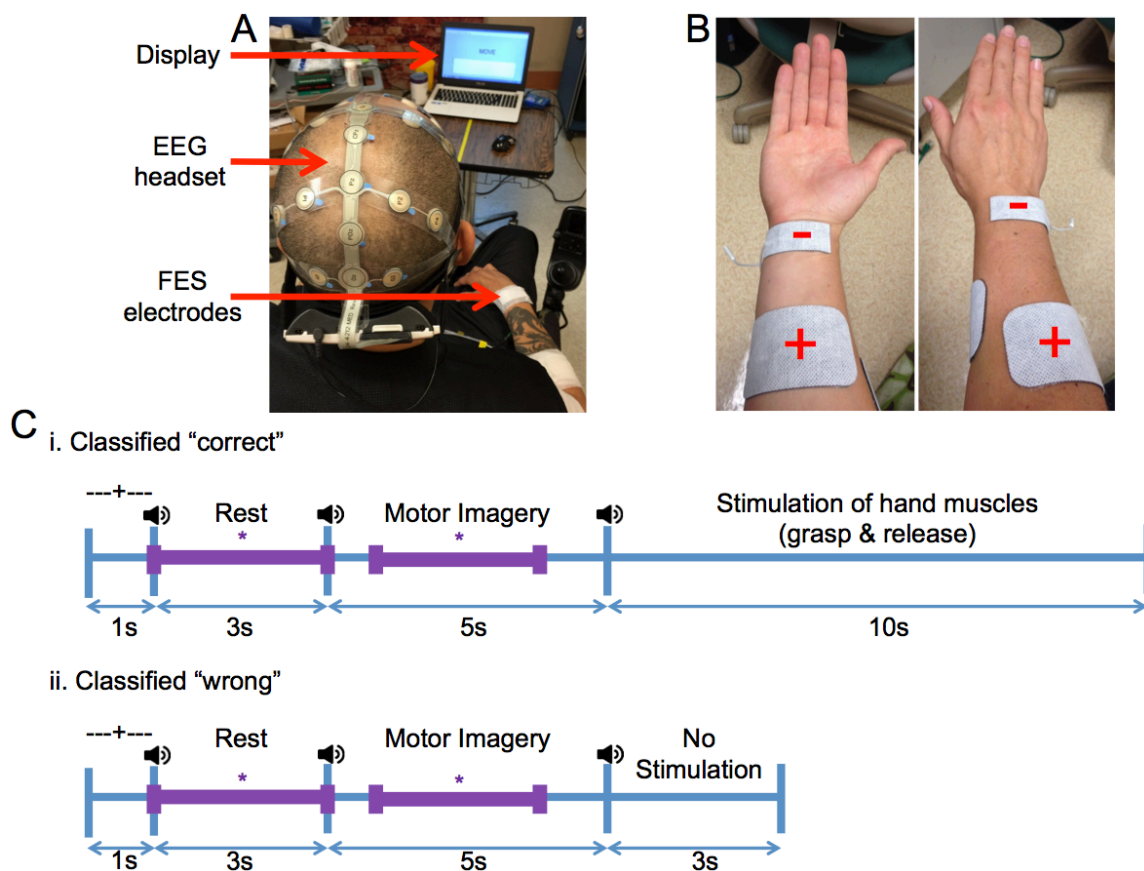


Figure 7.1 Experimental setup. A) EEG headset transmits neural data to computer as subject responds to commands displayed on screen. FES is delivered to the muscles via surface electrodes during feedback. B) FES electrodes span the flexor and extensor muscles responsible for hand closing and opening. C) Cue-based experimental timeline for trials classified as correct (i) and wrong (ii). Audio cues sound at the beginning of the rest, motor imagery, and feedback periods. 3 seconds of data from the rest (0-3 seconds following cue) and motor imagery (0.5-3.5 seconds following cue) are used to create features for input to the classifier.

During closed-loop (CL) sessions, the user performed a trial by following cues on the screen similar to the above session in which the classifier was being trained. However, in the CL session, the following things happen: “Move” cue on screen → user imagined movement of their right hand → EEG features (power in frequency bands) were input to the SVM classifier during the motor imagery period → the SVM classifier classified features as either the “Rest” class or “Move” class based upon when it was trained. If the classifier classified the input EEG features during this trial as “Move”, then the output of the classifier matched that of the cue and the result of the trial would be “Correct”, which would then trigger stimulation of the hand. On the other hand, if the classifier classified the EEG features in that trial as “Rest”, then there was a mismatch between the cue that was shown (which was Move) and the classifier output, thus the trial output was regarded as “Wrong”, which resulted in no stimulation of hand. For the “Rest” cue, the user was instructed not to perform any motor imagery. In both types of cue, the user was provided a feedback of how they are performing in the form of real-time ERD and “Correct” or “Wrong” commands on the screen, which the users said helped them in improving future performance.

To examine differences in neural signals between the rest and motor imagery states, the percentage of event-related desynchronization during motor imagery as compared to rest was found from the C3, C1, Cz, C2, and C4 electrodes. Raw data were bandpass filtered (5-35 Hz, 4th order Butterworth), squared, and smoothed (0.5 second span). Three second segments for rest (0-3 seconds following cue) and motor imagery (0.5-3.5 seconds following cue) were extracted from each trial and averaged. The percentage of event-related desynchronization, corresponding to a decrease in power in

the 5-35 Hz range was calculated as the change in power between motor imagery and rest. %ERD was found overall (all trials performed by all subjects during all sessions), across subjects (720 trials performed across 6 days averaged for each subject), and across days (120 trials performed during a session by all subjects in each group averaged for each day). Decoding accuracies were calculated by dividing the number of trials decoded correctly by the total number of attempted trials in each session.

A one-way analysis of variance (ANOVA) was computed in order to determine whether there were significant differences ($p < 0.05$) in %ERD and decoding accuracies between SCI and control groups and within subjects. Tukey's post-hoc test was used to determine significant differences between multiple groups ($p < 0.05$). Mean \pm standard error values are used to show average values for ERD and BCI decoding accuracies.

Grip strength was assessed at the beginning and end of each testing session using a microFET4 grip and pinch force gauge dynamometer (Hoggan Scientific, West Jordan, UT). The subject's right hand was positioned around the handle of the dynamometer, which was supported by the researcher, with the shoulder adducted and neutrally rotated, elbow flexed at 90° , and forearm in neutral position [127]. Three trials were performed under voluntary control only, during which the subject was encouraged to attempt to squeeze the handle for 4 seconds. Although all subjects had completely paralyzed hand muscles, some were able to generate grip force using compensatory mechanisms, such as tenodesis (extension of the wrist). Three additional trials of grip strength were performed with electrical stimulation of the flexor muscles of the forearm, during which the subject was instructed to relax. The average grip strengths (force in lbs) achieved using voluntary

effort and stimulation were calculated for each subject at the beginning (pre) and end (post) of each session.

In addition, a modified grasp and release test (Wuolle, Van Doren et al. 1994, Mulcahey, Smith et al. 2004) was performed at the beginning of each session to assess the subjects' functional ability to pick up and release different objects. The subject was instructed to attempt to pick up and release three objects of varying weight and size (small diameter shot glass, a large diameter, lightweight plastic cup, and a heavy soup can) using only the right hand. Five attempts were made with each object using only voluntary control, followed by five attempts with electrical stimulation only of the muscles for hand opening for object positioning, closing for grasping, and opening for release. Success/failure data were recorded for each attempt. The percentage of successful attempts with each object was calculated.

7.3 Results

7.3.1 Neural Features for Decoding

Both SCI and control subjects were able to modulate their neural activity during motor imagery. Examples from two individual subjects (SCI subject #2 and control subject #1) who were able to modulate their neural signals effectively are shown below. Alpha and low beta band power (5-35 Hz) from the 5 electrodes used for decoding (C3, C1, Cz, C2, and C4) was decreased during motor imagery when compared to resting state (Figure 2A, B). Within that range, the greatest desynchronization occurred below 20 Hz for all tested subjects. For example, the SCI subject exhibited the strongest

desynchronization at 7Hz (Figure 7.2 A) with ERD of $24.6\% \pm 4.88\%$. ERD was strongest in the control subject at 10Hz (Figure 7.2 B) with ERD of $31.7\% \pm 3.8\%$. On average, power in the range used for neural decoding (5-30Hz) began to decrease with similar latencies following the cue for motor imagery, at 390 ms in the SCI subject and 380 ms in the control subject (Figure 7.2 C, D). The SCI subject achieved an average ERD of $30.2\% \pm 2.2\%$ during the time period used for decoding (0.5-3.5 seconds following imagery cue), and the control subject ERD averaged $29.2 \pm 1.3\%$. EEG data convolved by a Morlet wavelet transform confirms the decrease in power following the motor imagery cue after 380-390 ms, as shown (Figure 7.2 E, F). In addition, it is clear that the strongest ERD occurs in the lower end of the frequency range used for decoding, with the greatest desynchronization occurring at 7 Hz in the SCI subject and 10 Hz in the control subject. Power spectral density curves to show differences between rest and motor imagery states for all subjects are shown in Figure 7.3.

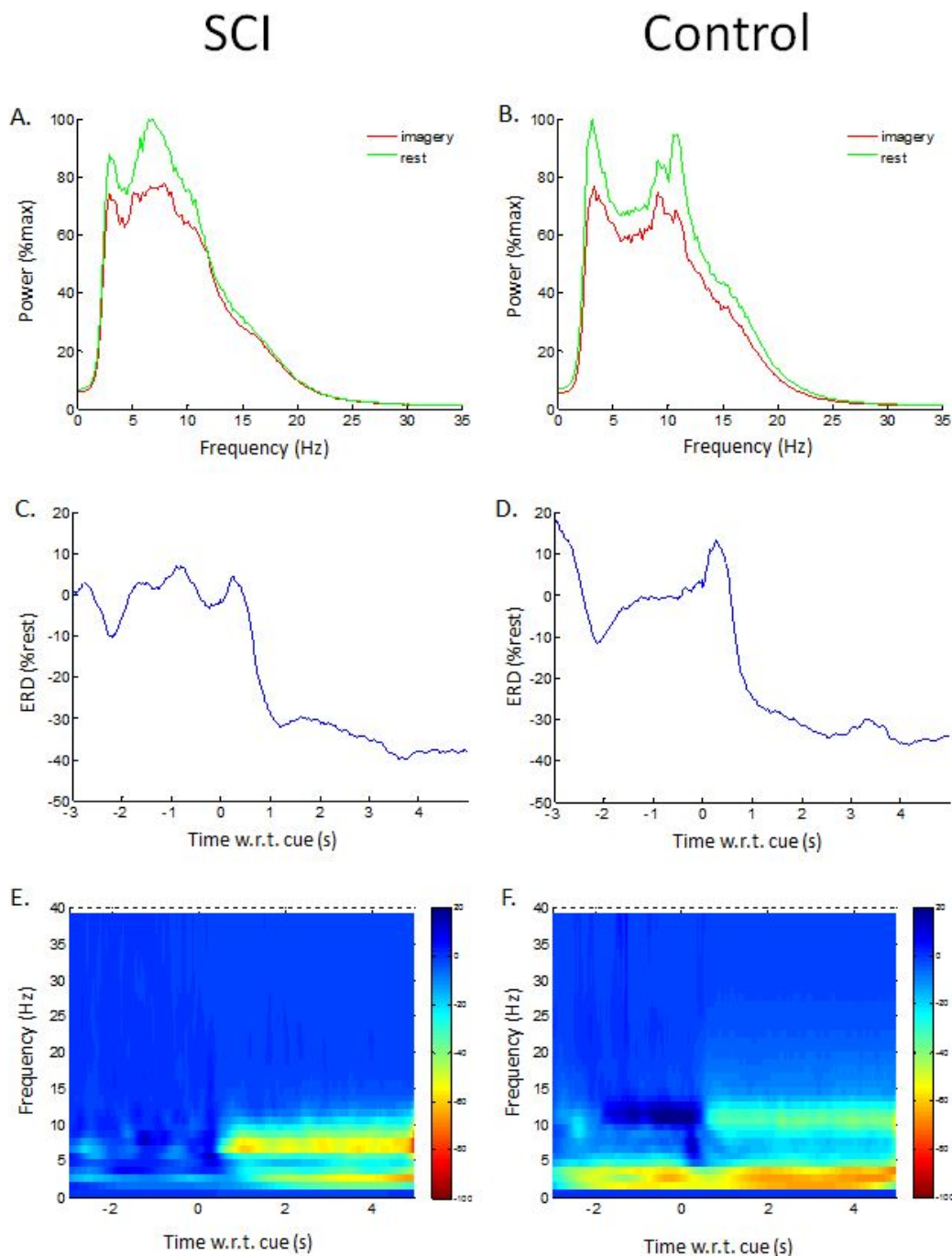
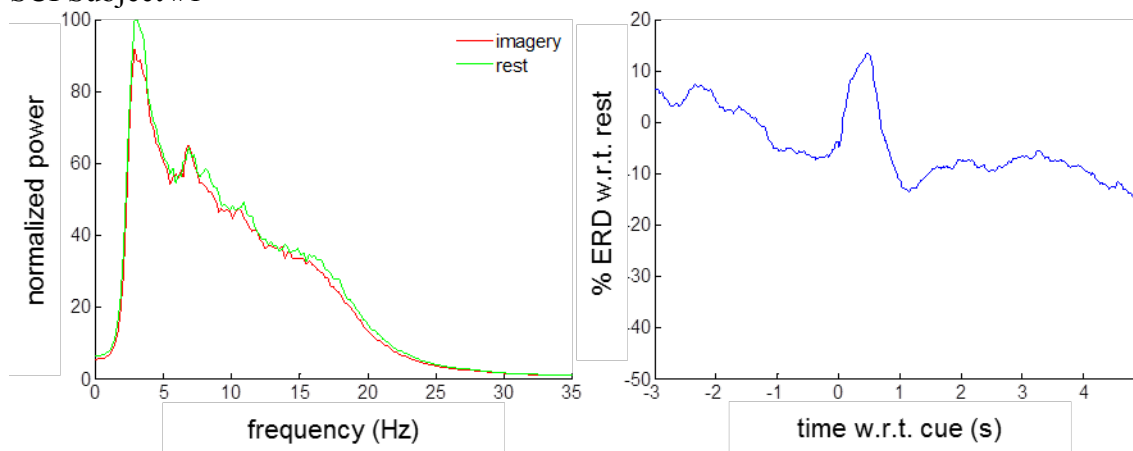
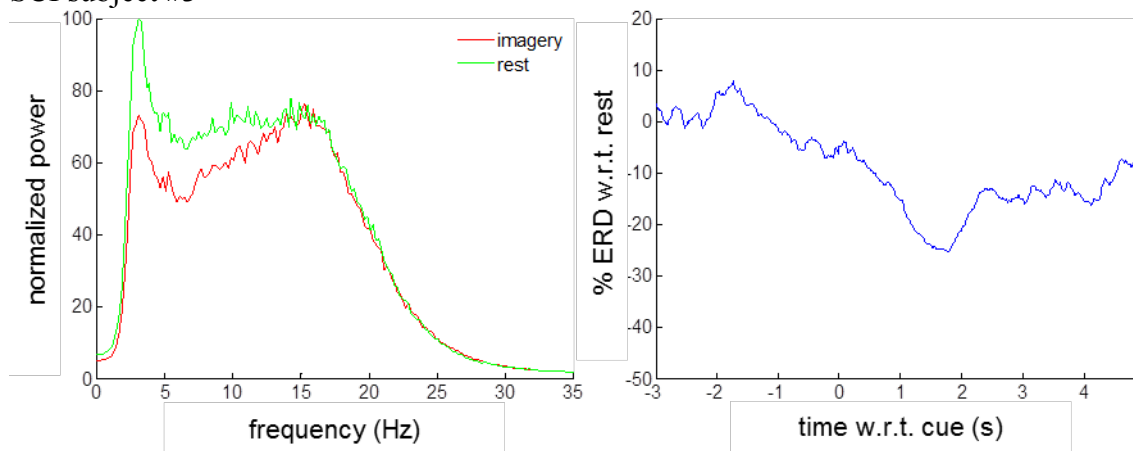


Figure 7.2 Control signals used for decoding from one SCI (SCI subject #1) and one control subject (Control subject #2). Power spectral density averaged across 5 motor strip electrodes (C3, C1, Cz, C2, and C4) for SCI (A) and control (B) subject, averaged across 720 trials during motor imagery and rest periods (3 sec). Time course of ERD in same subset of electrodes averaged over 720 trials with respect to the motor imagery cue in SCI (C) and control (D) subject. (E,F) Morlet wavelet time-frequency plots showing ERD/ERS during rest and motor imagery. Color scale ranges from 20% ERS to 100% ERD.

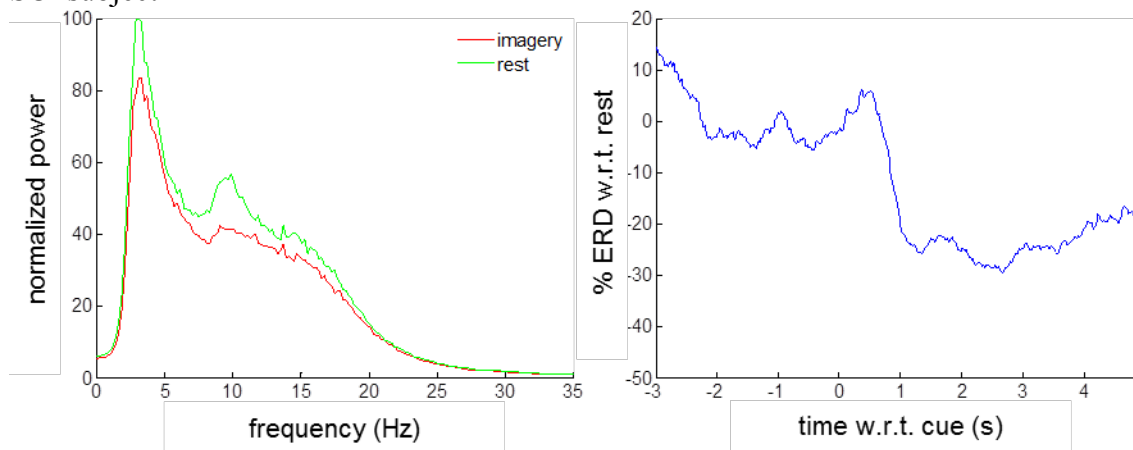
SCI Subject #1



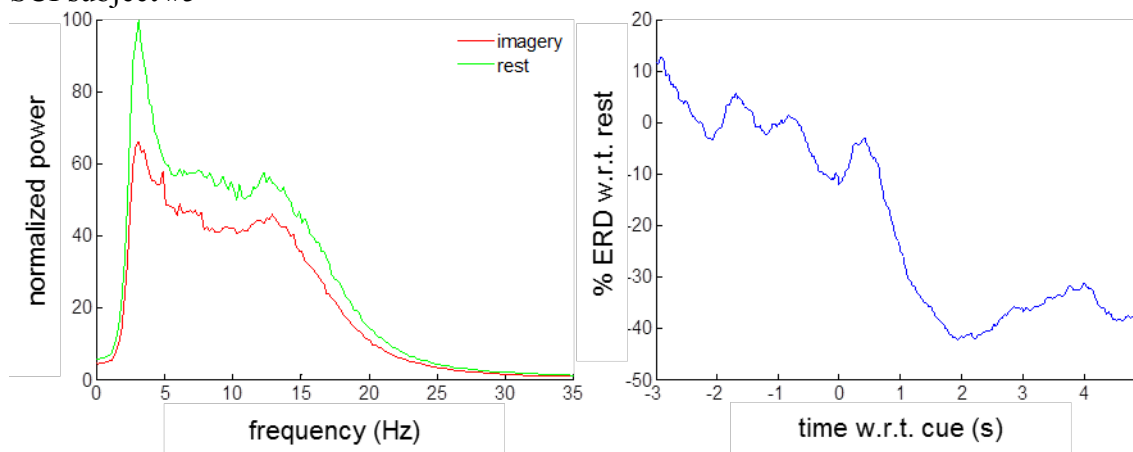
SCI subject #3



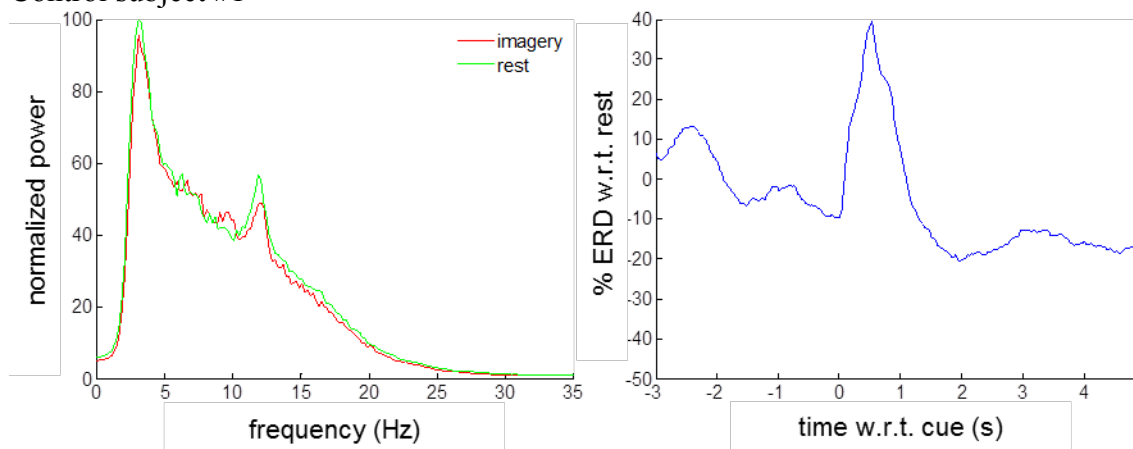
SCI subject #4



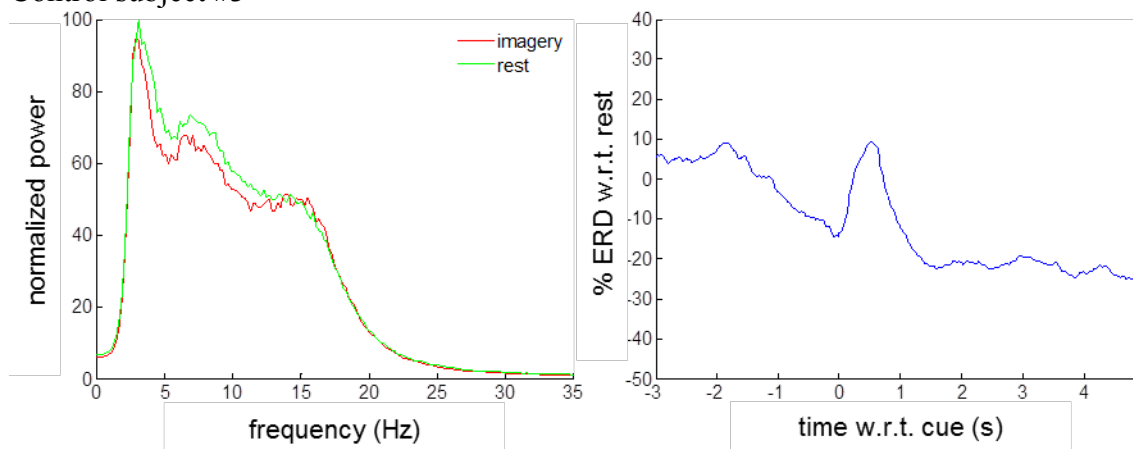
SCI subject #5



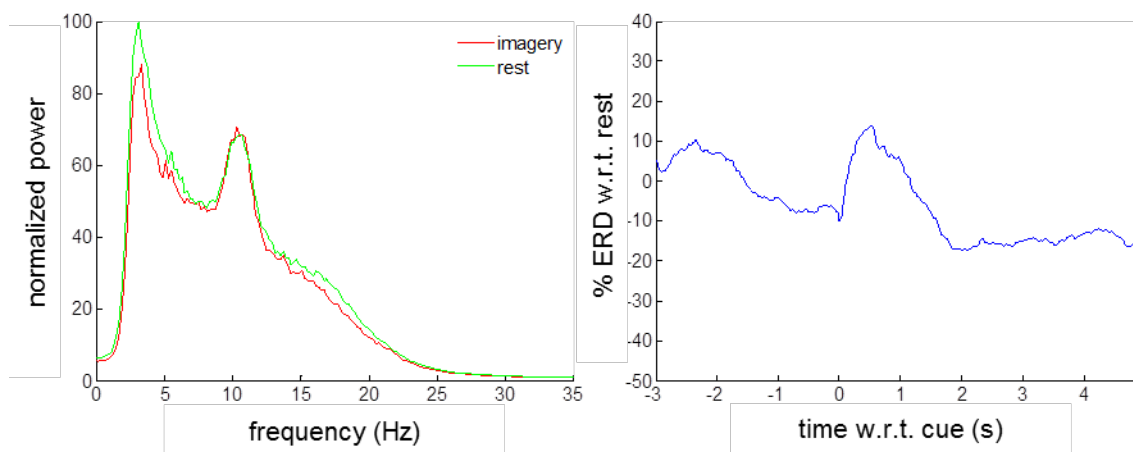
Control subject #1



Control subject #3



Control subject #4



Control subject #5

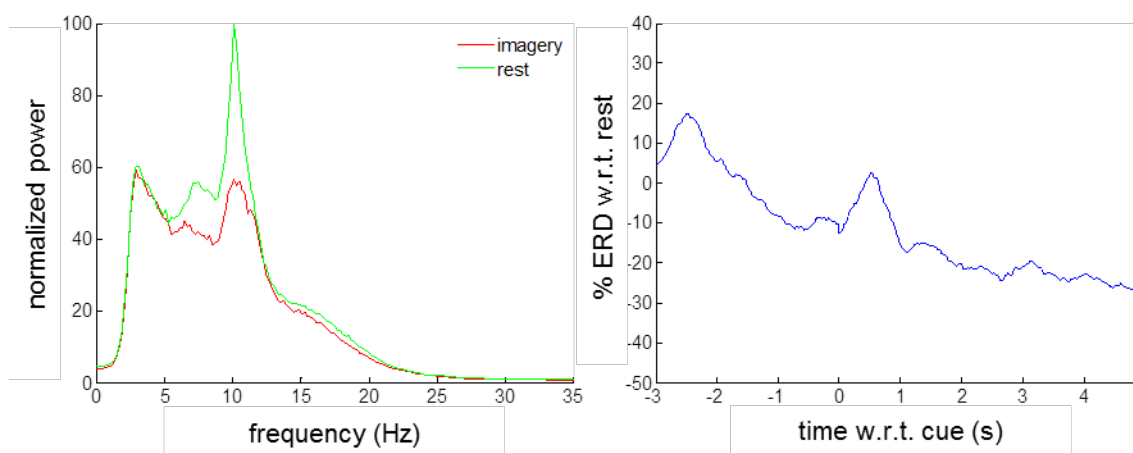


Figure 7.3 Control signals used for decoding from the remainder of SCI and Control subjects. Power spectral density averaged across 5 motor strip electrodes (C3, C1, Cz, C2, and C4), averaged across 720 trials during motor imagery and rest periods (3 sec) (left panel for each subject). Time course of ERD in same subset of electrodes averaged over 720 trials with respect to the motor imagery cue (right panel for each subject).

Average power decreased during motor imagery in individual SCI subjects between 6.9% to 31.1%, and -0.5% (event-related synchronization) to 28.2% in control subjects (Figure 7.4 A). Significant differences in ERD were observed between individual subjects in both groups ($p < 0.05$), due to the drastic range of neural modulation

achieved by different individuals. Average event-related desynchronization with respect to the baseline activity during the resting state across the 5 motor strip electrodes (C3, C1, Cz, C2, and C4) decreased by $21.0\% \pm 3.9\%$ in the SCI group and $13.5\% \pm 3.2\%$ (difference not statistically significant) in the control group during motor imagery (Figure 7.4 B).

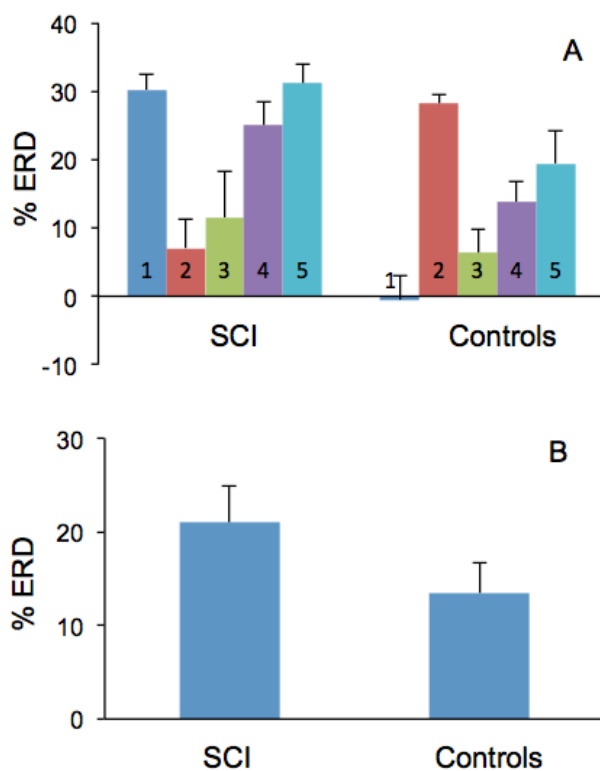


Figure 7.4 A) Average event-related desynchronization (as a $\% \pm SE$) averaged across 5 motor strip electrodes (C3, C1, Cz, C2, and C4) during motor imagery as compared to rest in each subject (each bar represents an individual subject). B) Average ERD (as a $\% \pm SE$) in SCI and control subject groups, averaged across all subjects during full experiment.

7.3.2 BCI Decoding Accuracy

Decoding accuracies were calculated by dividing the number of trials correctly classified by the total number of trials in each session. Average decoding accuracies varied between the subjects in both groups, and some subjects performed significantly better than others ($p=0.05$, Figure 7.5 A). Accuracies in individual subjects in the SCI group ranged from $62.5\% \pm 10.1\%$ to $87.2\% \pm 1.4\%$. In the control group, the range across subjects was from $65.3\% \pm 2.6\%$ to $90.5\% \pm 2.4\%$. Overall, the online decoding accuracies were similar between the SCI ($73.3\% \pm 4.2\%$) and control ($73.6\% \pm 4.8\%$) groups (Figure 7.5 B).

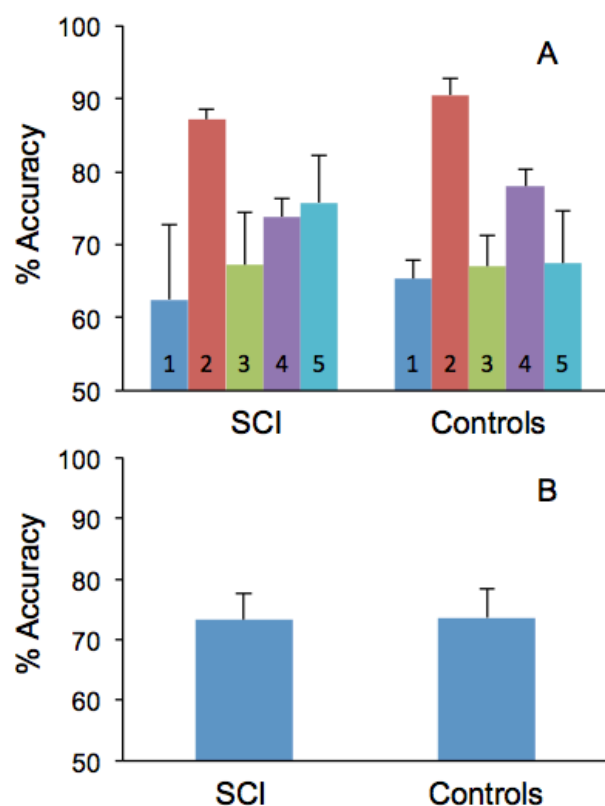


Figure 7.5 A) Average decoder accuracy (as a mean \pm SE) in 5 SCI and 5 control subjects over the entire duration of training (each bar represents an individual subject). B) Average decoder accuracy during closed-loop experiments in SCI and control groups, averaged across subjects.

7.3.3 ERD Changes and Decoder Performance over Time

Over the course of training, ERD strength improved in both groups, but the increase was only significant for the SCI group (Figure 7.6 A). On the first day of training, ERD in the SCI and control groups was $6.5\% \pm 9.7\%$ and $14.3\% \pm 6.9\%$ respectively. On day 2, ERD increased significantly in the SCI group to $26.5\% \pm 6.3\%$ ($p < 0.05$). A less dramatic increase to $16.1\% \pm 5.3\%$ was observed for the control group. ERD remained relatively constant throughout the remainder of the training period with an average ERD of $19.3\% \pm 5.5\%$ in the SCI group and $8.0\% \pm 5.9\%$ in the control group during the last BCI session. Over time, decoding accuracy increased over time in both groups, although variability between subjects was high (Figure 7.6 B). On the first day of training, accuracies in the SCI and control groups were similar, at $63.8\% \pm 12.5\%$ and $64.2\% \pm 9.3\%$ respectively. Accuracies increased over time with some variation between days. By day 6, decoding accuracy in the SCI group averaged $80.7\% \pm 3.7\%$ and $72.3\% \pm 4.4\%$ in the control group.

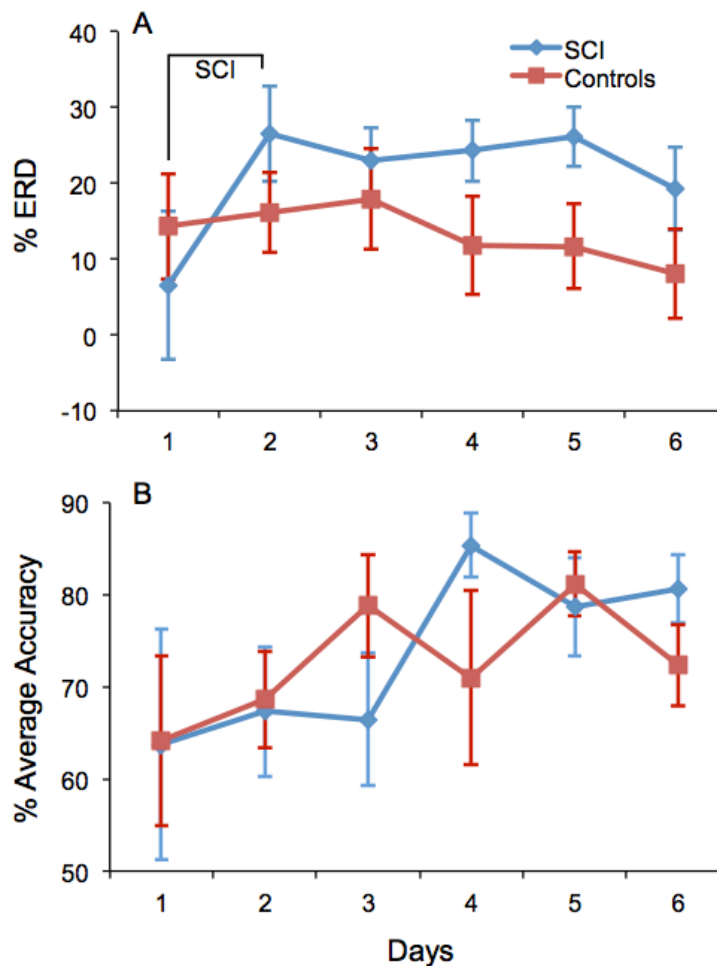


Figure 7.6 A) Average ERD (as a % \pm SE) in SCI (blue) and control (red) subjects over the 6 training days (120 trials/day). B) Average decoder accuracy (as a % \pm SE) during closed-loop experiments in SCI (blue) and control (red) subjects.

7.3.4 Functional Assessment and Muscle Fatigue in SCI Group

Average grip strength in the SCI subjects was higher when stimulation was applied to paralyzed muscles (4.1 ± 0.5 lbs) compared to attempted grasping using only voluntary efforts (0.7 ± 0.1 lbs) at the beginning of each session. Average grip strength was similar at the end of each session, with average force of 3.7 ± 0.5 lbs during stimulation and 0.7 ± 0.1 lbs with voluntary effort. For all 5 SCI subjects, average grip strength improved when stimulation was applied to the muscles (Figure 7.7 B, D)

compared to when the SCI subjects tried to grasp using voluntary control (Figure 7.7 A, C). On the first 3 days of training, only 2 SCI subjects (#1 and #2) were able to voluntarily produce force using voluntary compensatory mechanisms (Figure 7.7 A, C). On days 4 and 6, an additional SCI subject (#3) was able to produce a small amount of force using tenodesis. Two SCI subjects (#4 and #5) were not able to produce any force using compensatory mechanisms during any measurement. In response to maximal stimulation, the paralyzed muscles were able to generate force in all SCI subjects (Figure 7.7 B, D). Three subjects (#1, #2, and #3) had consistently stronger muscles than the other two subjects (#4 and #5), with forces registering above 1 lb (on average) during each stimulation trial. At the end of each training session (Post-BCI), the average grip strengths did not decrease when compared to the beginning of the session (Pre-BCI), suggesting that muscle fatigue did not occur. In addition, grip strength did not improve over the 6 days of training, so there were no training effects or strengthening of muscles that occurred during the 6 days of BCI-FES training.

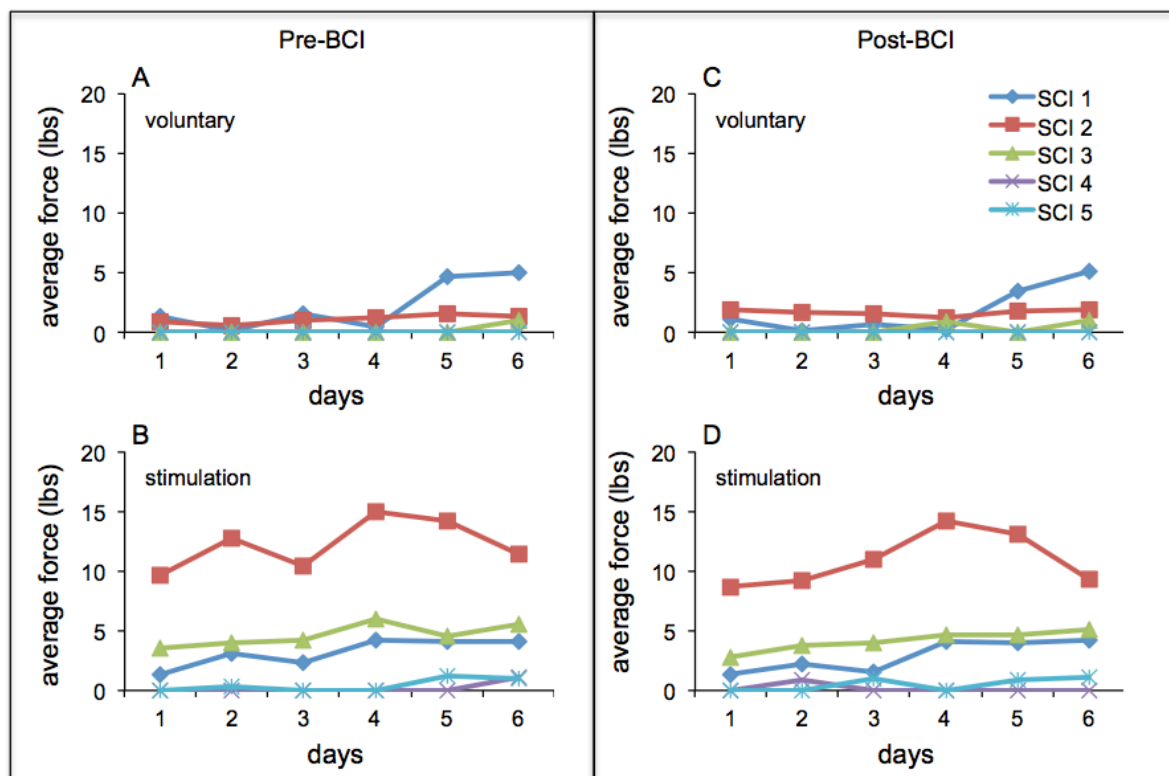


Figure 7.7 A) Average grip strength ($n=3$ trials) in SCI subjects ($n=5$). A) Force generated during voluntary contractions using residual compensatory mechanisms before BCI training (Pre-BCI). B) Force generated during application of maximal stimulation before BCI-training. C) Force generated during voluntary contractions using compensatory mechanisms after BCI training (Post-BCI). D) Force generated during application of maximal stimulation after BCI-training.

Successful performance of the grasp and release task with three different objects (a large diameter, lightweight, empty plastic cup, a heavy full can, and a small diameter shot glass) for one SCI subject (#2) is shown in Figure 7.8. Results from the other 4 subjects are included in the Supplemental material. Subject 2 was never able to pick up any of the three objects using tenodesis. In addition, this subject was not able to pick up the large-diameter empty cup with stimulation (Figure 7.8), due to the hand being unable to open wide enough to get around the cup. However, the subject was able to pick up the

other two objects on days 5 and 6 with success rates of 60% (heavy can) and 80% (shot glass). Results from the other 4 subjects are shown in Figure 7.9.

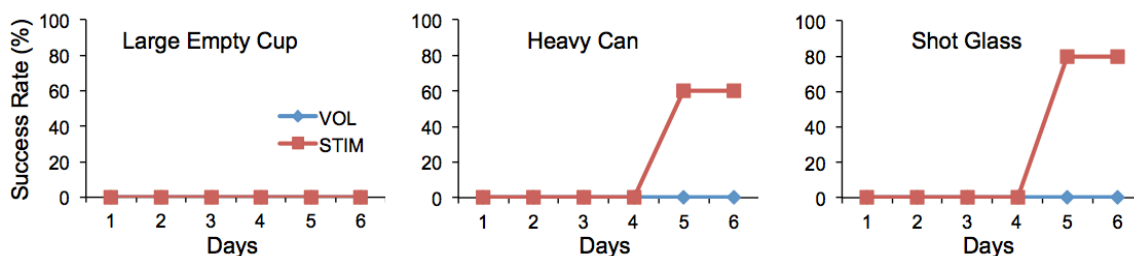
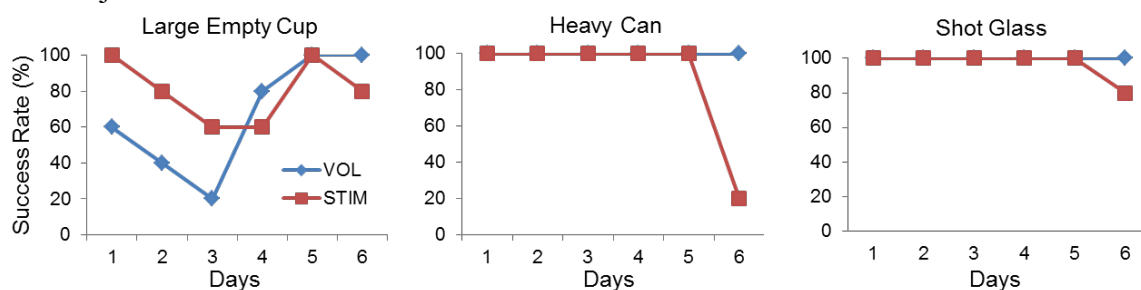
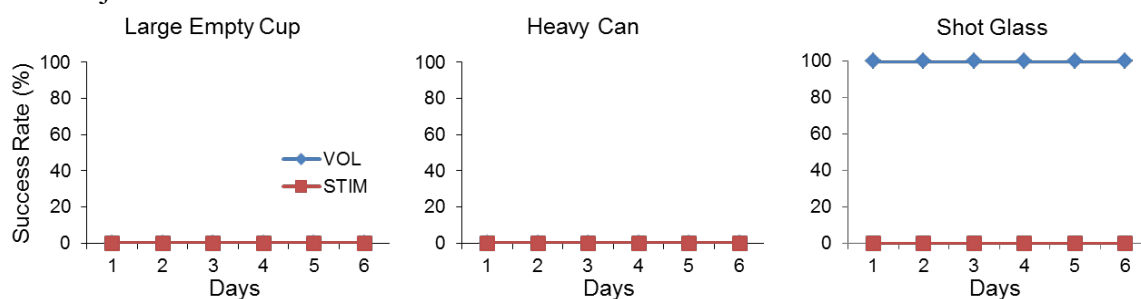


Figure 7.8. Average success rate (%) of grasp and release task with a large diameter, lightweight, empty plastic cup (A), a heavy can (B), and a small diameter shot glass (C) in one SCI subject. Subjects performed 5 attempts with each object using voluntary control (blue) and stimulation (red) at the beginning of each session.

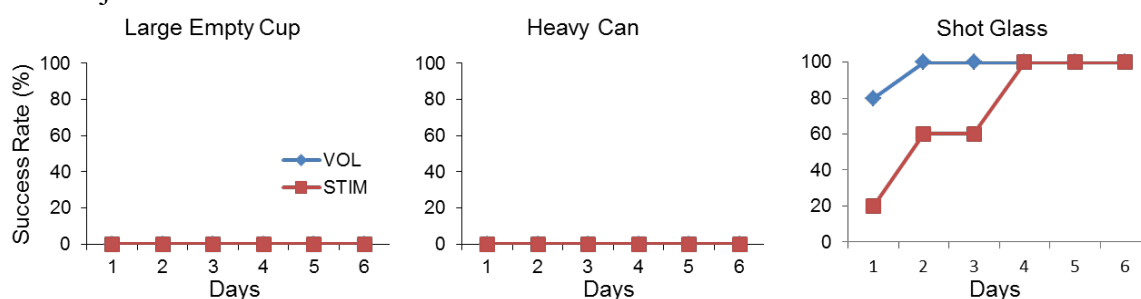
SCI subject #1



SCI subject #3



SCI subject #4



SCI subject #5

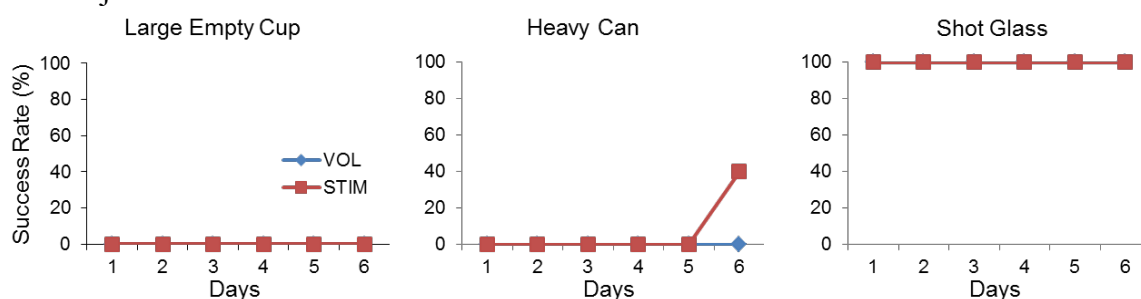


Figure 7.9 Average success rate (%) of grasp and release task with a large diameter, lightweight, empty plastic cup (A), a heavy can (B), and a small diameter shot glass (C) in remaining 4 SCI subjects.

7.4 Conclusion

In this study, we developed a BCI-FES system and demonstrated effective control of a grasp and release task in 5 subjects with chronic (>1 year post-injury), complete, cervical SCI and compared results with 5 uninjured, control subjects (see supplementary videos). Subjects with SCI were able to control the BCI-FES system just as well as uninjured subjects despite living with a complete SCI for at least 1 and up to 15 years post-injury. We also evaluated the functional aspects of the FES by testing grip strength as well as performance of a grasp and release task.

Subjects with SCI and control subjects were able to effectively modulate their neural activity in order to produce ERD across the 5 central electrodes during motor imagery with SCI subjects producing an average of $21 \pm 3.9\%$ ERD and control subjects averaging $13.5 \pm 3.2\%$ ERD. Previous studies have established the pattern of ERD that results in the motor cortex of uninjured, healthy subjects during motor imagery [77, 128]. Although SCI subjects are capable of modulating their neural activity during motor imagery [22, 56, 85, 88-90, 129], contradicting ERD patterns have been shown in previous studies. Results from an earlier study show weaker ERD patterns in SCI subjects during imagination of movements than uninjured subjects [87]. In contrast, other studies have actually shown stronger ERD patterns after SCI [85, 88, 130]. Another study showed decreased alpha and increased beta activation in SCI subjects [131]. In addition, ERD patterns are more diffused and widely distributed throughout the primary motor cortex after an injury to the spinal cord [21, 22, 56, 85, 87]. Often after a neurological injury, reorganization of cortical networks occurs in regions connected to the affected and surrounding areas in order to compensate for sensorimotor loss [132, 133]. In our results,

ERD patterns were more widely distributed across the central electrodes in the SCI group, contributing to an overall stronger modulation. Some have suggested that a broader network of neurons is recruited from neighboring areas after a SCI once the brain realizes that paralyzed muscles are unable to be controlled using previous strategies [21, 130]. In addition, SCI subjects have reported a higher degree of “vividness” during motor imagery, which is strongly correlated to the extent of ERD [88].

Subjects in the SCI group had more difficulty modulating their neural activity during the first session compared to subsequent sessions. SCI subjects on average had only $6.5 \pm 9.7\%$ ERD across compared to $14.3 \pm 6.9\%$ in the control group. However, by the second session ERD in SCI subjects was significantly greater ($26.5 \pm 6.3\%$, $p < 0.05$) compared to the first session and remained high throughout the rest of the sessions. In contrast, ERD in the control group on session 2 did not increase significantly and averaged $16.1 \pm 5.3\%$ across subjects. The initially poor neural modulation by the SCI group during session 1 may be linked to subjects’ feelings of being unaccustomed to the motor imagery task and the length of time they had not attempted to move their hands. During the first session, SCI subjects expressed feeling awkward and unsure of how to perform the motor imagery. By the second session after some practice (approximately 100 trials), subjects reported feeling more comfortable with the task and were better able to modulate their sensorimotor rhythms. A similar trend was not observed in the control group data. Uninjured control subjects were able to modulate their sensorimotor rhythms from the first session, which did not change across sessions.

We also observed that some subjects were better able to modulate their neural activity compared to others. In both groups, some subjects achieved high levels of ERD

(>30%) and some averaged low (<10%). In uninjured healthy subjects, approximately 70-85% of the population is thought to be able to modulate their neural signals to control a BCI [79, 134]. It is unclear what percentage of the population living with a complete, cervical SCI would be considered capable of controlling a BCI. However, SCI subjects in our study were able to control the BCI-FES system just as well as uninjured subjects, despite having sustained their injuries from 1 to 15 years before participating in this study. In both groups, some subjects were able to control the BCI with accuracies over 80% while others had more difficulty and achieved accuracies below the level of control (<70%) [125]. However, average decoding accuracy on day 1 was less than 70% in both groups and rose to over 80% in the SCI group and 72% in the control group by the final session. Overall, SCI subjects appeared to be more engaged and motivated in the BCI-FES training than the control subjects, which could account for the higher performance in the SCI group. In experiments such as this that involve repetitive tasks, subject engagement is an important factor in determining BCI accuracy, as some subjects were more attentive than others during the testing. BCI coupled with FES also provided a positive reinforcement to the SCI subjects when they saw their hand move and perform functional tasks during stimulation.

Only a few previous studies developed and tested BCIs coupled with FES of completely paralyzed upper-limb muscles [8, 55-57, 66, 68]. There are several unique challenges in working with these types of systems in this population. First, SCI is an inherently complex type of injury and affects each individual in different ways. Varying motor and sensory function, involuntary muscle spasms, denervation, autonomic dysreflexia, and other complications contribute to a wide range of variability in subjects

with SCI, making it difficult to develop technologies applicable to a wide range of the SCI population. However, in this study we show a BCI-FES system based on a support vector machine classifier that could be generalized across subjects with a minimal training period for achieving high performance even in the SCI group (>70% accuracy).

Grip strength resulting from FES of muscles responsible for closing the hand varied between subjects in the SCI subject group. In a subset of subjects (SCI #1, #2, and #3), the flexor muscles were able to generate over 1lb of force in response to electrical stimulation while in others (SCI #4 and #5) were barely able to generate any force at all. Although potential subjects were screened out based on inclusion criteria, we suspect that some of the SCI subjects may have mild to moderate denervation of muscles in the hand and arm, which may have contributed to the low levels of force achieved during stimulation in some subjects. In addition, paralyzed muscles are weaker and more fatigable [135] and subjects in this study did not participate in any additional program to strengthen muscles before BCI training. Muscles could be stimulated to strengthen contractions and further minimize fatigue. The BCI training did not have any effect on the grip strength as the force values remained similar when measured before and after BCI sessions. This also suggests that the application of stimulation during the 120 trials of each BCI-FES session did not cause fatigue to the hand muscles. All subjects tested in this study were classified as cervical level, motor-complete spinal cord injury with variable residual function in the forearms and muscles located distally. None of the subjects had any voluntary control over hand opening and grasping function. Since the subjects had motor-complete SCI, we do not expect any improvement in muscle strength due to such a short-term BCI use. An increase in grip strength may be attributed to

improvement in residual muscle function or other voluntary compensatory mechanisms due to FES that is able to generate any measurable force (Figure 7.7). Additionally, in these subjects we also observed the ability to grasp and release a heavy can of beans with stimulation, otherwise not possible without FES (Figures 7.8 and 7.9). Nonetheless, it is encouraging to observe an increase in force generated and improvement in some hand function over a short duration study, even in a sub-population of tested subjects. In these SCI subjects, we did not expect an increase in grip strength, as these subjects had motor-complete injury with no hand function. However, our study shows that a BCI-FES system can be used as an assistive system to restore hand function in SCI subjects with cervical level motor-complete injury.

Further development of BCI-FES systems in subjects with motor complete SCI must consider end-user needs and preferences [136]. It is clear that people with tetraplegia rank restoration of hand function as an important goal [1, 136, 137]. However, many other considerations need to be addressed, including the functional benefits that the technology offers, the cosmetic look of the system, reliability, invasiveness, cost, the burden of maintaining the system, and the requirements of caregiver or technician help [136, 138]. By designing BCI-FES systems around the needs and preferences of people living with SCI, these new technologies will have a greater chance of being adopted and thus have a better opportunity to improve the quality of life for a larger number of people.

REFERENCES

1. Anderson, K.D., *Targeting recovery: priorities of the spinal cord-injured population*. J Neurotrauma, 2004. **21**(10): p. 1371-83.
2. Waters, R.L., et al., *Motor and sensory recovery following complete tetraplegia*. Arch Phys Med Rehabil, 1993. **74**(3): p. 242-7.
3. Hoffman, L.R. and E.C. Field-Fote, *Cortical reorganization following bimanual training and somatosensory stimulation in cervical spinal cord injury: a case report*. Phys Ther, 2007. **87**(2): p. 208-23.
4. Mortimer, J.T., *Motor Protheses*, in *Comprehensive Physiology*. 2011, John Wiley & Sons, Inc.
5. Peterchev, A.V., et al., *Electroconvulsive therapy stimulus parameters: rethinking dosage*. J ect, 2010. **26**(3): p. 159-74.
6. Wolpaw, J.R., et al., *Brain-computer interfaces for communication and control*. Clin Neurophysiol, 2002. **113**(6): p. 767-91.
7. Pfurtscheller, G., *Event-related synchronization (ERS): an electrophysiological correlate of cortical areas at rest*. Electroencephalogr Clin Neurophysiol, 1992. **83**(1): p. 62-9.
8. Pfurtscheller, G., et al., *'Thought'--control of functional electrical stimulation to restore hand grasp in a patient with tetraplegia*. Neurosci Lett, 2003. **351**(1): p. 33-6.
9. Ferrez, P.W. and R.M.J. del, *Error-related EEG potentials generated during simulated brain-computer interaction*. IEEE Trans Biomed Eng, 2008. **55**(3): p. 923-9.
10. N.S.C.I.S. Center, *Annual Report for the Model Spinal Cord Injury Systems for Care*. 2015: University of Alabama, Birmingham, AL.

11. McColl, M.A., et al., *Expectations of life and health among spinal cord injured adults*. Spinal Cord, 1997. **35**(12): p. 818-28.
12. Kirshblum, S.C., et al., *International standards for neurological classification of spinal cord injury (revised 2011)*. J Spinal Cord Med, 2011. **34**(6): p. 535-46.
13. Fawcett, J.W., et al., *Guidelines for the conduct of clinical trials for spinal cord injury as developed by the ICCP panel: spontaneous recovery after spinal cord injury and statistical power needed for therapeutic clinical trials*. Spinal Cord, 2007. **45**(3): p. 190-205.
14. Donoghue, J.P., *Plasticity of adult sensorimotor representations*. Curr Opin Neurobiol, 1995. **5**(6): p. 749-54.
15. Bareyre, F.M., et al., *The injured spinal cord spontaneously forms a new intraspinal circuit in adult rats*. Nat Neurosci, 2004. **7**(3): p. 269-77.
16. Bruehlmeier, M., et al., *How does the human brain deal with a spinal cord injury?* Eur J Neurosci, 1998. **10**(12): p. 3918-22.
17. Cohen, L.G., et al., *Magnetic stimulation of the human cerebral cortex, an indicator of reorganization in motor pathways in certain pathological conditions*. J Clin Neurophysiol, 1991. **8**(1): p. 56-65.
18. Levy, W.J., Jr., et al., *Focal magnetic coil stimulation reveals motor cortical system reorganized in humans after traumatic quadriplegia*. Brain Res, 1990. **510**(1): p. 130-4.
19. Raineteau, O. and M.E. Schwab, *Plasticity of motor systems after incomplete spinal cord injury*. Nat Rev Neurosci, 2001. **2**(4): p. 263-73.
20. Wall, P.D. and M.D. Egger, *Formation of new connexions in adult rat brains after partial deafferentation*. Nature, 1971. **232**(5312): p. 542-5.
21. Green, J.B., et al., *Cortical sensorimotor reorganization after spinal cord injury: an electroencephalographic study*. Neurology, 1998. **50**(4): p. 1115-21.

22. Green, J.B., et al., *Cortical motor reorganization after paraplegia: an EEG study*. Neurology, 1999. **53**(4): p. 736-43.
23. Kokotilo, K.J., J.J. Eng, and A. Curt, *Reorganization and preservation of motor control of the brain in spinal cord injury: a systematic review*. J Neurotrauma, 2009. **26**(11): p. 2113-26.
24. Hebb, D.O., *The Organization of Behavior: A Neuropsychological Theory*. 1949, New York: Wiley and Sons.
25. Beekhuizen, K.S. and E.C. Field-Fote, *Sensory stimulation augments the effects of massed practice training in persons with tetraplegia*. Arch Phys Med Rehabil, 2008. **89**(4): p. 602-8.
26. Conner, J.M., A.A. Chiba, and M.H. Tuszynski, *The basal forebrain cholinergic system is essential for cortical plasticity and functional recovery following brain injury*. Neuron, 2005. **46**(2): p. 173-9.
27. Hoffman, L.R. and E.C. Field-Fote, *Functional and corticomotor changes in individuals with tetraplegia following unimanual or bimanual massed practice training with somatosensory stimulation: a pilot study*. J Neurol Phys Ther, 2010. **34**(4): p. 193-201.
28. Conforto, A.B., A. Kaelin-Lang, and L.G. Cohen, *Increase in hand muscle strength of stroke patients after somatosensory stimulation*. Ann Neurol, 2002. **51**(1): p. 122-5.
29. Beekhuizen, K.S. and E.C. Field-Fote, *Massed practice versus massed practice with stimulation: effects on upper extremity function and cortical plasticity in individuals with incomplete cervical spinal cord injury*. Neurorehabil Neural Repair, 2005. **19**(1): p. 33-45.
30. Ridding, M.C. and J.C. Rothwell, *Afferent input and cortical organisation: a study with magnetic stimulation*. Exp Brain Res, 1999. **126**(4): p. 536-44.
31. Rossini, P.M. and F. Pauri, *Neuromagnetic integrated methods tracking human brain mechanisms of sensorimotor areas 'plastic' reorganisation*. Brain Res Brain Res Rev, 2000. **33**(2-3): p. 131-54.

32. Khaslavskaja, S., M. Ladouceur, and T. Sinkjaer, *Increase in tibialis anterior motor cortex excitability following repetitive electrical stimulation of the common peroneal nerve*. *Exp Brain Res*, 2002. **145**(3): p. 309-15.
33. Knash, M.E., et al., *Electrical stimulation of the human common peroneal nerve elicits lasting facilitation of cortical motor-evoked potentials*. *Exp Brain Res*, 2003. **153**(3): p. 366-77.
34. Rushton, D.N., *Functional electrical stimulation and rehabilitation--an hypothesis*. *Med Eng Phys*, 2003. **25**(1): p. 75-8.
35. Peckham, P.H. and J.S. Knutson, *Functional electrical stimulation for neuromuscular applications*. *Annu Rev Biomed Eng*, 2005. **7**: p. 327-60.
36. Popovic, M.R., et al., *Functional electrical stimulation therapy of voluntary grasping versus only conventional rehabilitation for patients with subacute incomplete tetraplegia: a randomized clinical trial*. *Neurorehabil Neural Repair*, 2011. **25**(5): p. 433-42.
37. Bryden, A.M., et al., *Triceps denervation as a predictor of elbow flexion contractures in C5 and C6 tetraplegia*. *Arch Phys Med Rehabil*, 2004. **85**(11): p. 1880-5.
38. Thomas, C.K. and I. Zijdwind, *Fatigue of muscles weakened by death of motoneurons*. *Muscle Nerve*, 2006. **33**(1): p. 21-41.
39. Kilgore, K.L., et al., *An implanted upper-extremity neuroprosthesis. Follow-up of five patients*. *J Bone Joint Surg Am*, 1997. **79**(4): p. 533-41.
40. Kilgore, K.L., et al., *Synthesis of hand grasp using functional neuromuscular stimulation*. *IEEE Trans Biomed Eng*, 1989. **36**(7): p. 761-70.
41. Mangold, S., et al., *Transcutaneous functional electrical stimulation for grasping in subjects with cervical spinal cord injury*. *Spinal Cord*, 2005. **43**(1): p. 1-13.
42. Chiou, Y.H., et al., *Patient-driven loop control for hand function restoration in a non-invasive functional electrical stimulation system*. *Disabil Rehabil*, 2008. **30**(19): p. 1499-505.

43. Fuglevand, A.J. and D.A. Keen, *Re-evaluation of muscle wisdom in the human adductor pollicis using physiological rates of stimulation*. J Physiol, 2003. **549**(Pt 3): p. 865-75.
44. Doucet, B.M., A. Lam, and L. Griffin, *Neuromuscular electrical stimulation for skeletal muscle function*. Yale J Biol Med, 2012. **85**(2): p. 201-15.
45. Peckham, P.H., J.T. Mortimer, and E.B. Marsolais, *Controlled prehension and release in the C5 quadriplegic elicited by functional electrical stimulation of the paralyzed forearm musculature*. Ann Biomed Eng, 1980. **8**(4-6): p. 369-88.
46. Keith, M.W., et al., *Functional neuromuscular stimulation neuroprostheses for the tetraplegic hand*. Clin Orthop Relat Res, 1988(233): p. 25-33.
47. Handa, Y., et al., *Functional electrical stimulation (FES) systems for restoration of motor function of paralyzed muscles--versatile systems and a portable system*. Front Med Biol Eng, 1992. **4**(4): p. 241-55.
48. Johnson, M.W., et al., *Implantable transducer for two-degree of freedom joint angle sensing*. IEEE Trans Rehabil Eng, 1999. **7**(3): p. 349-59.
49. Handa, Y., R. Yagi, and N. Hoshimiya, *Application of functional electrical stimulation to the paralyzed extremities*. Neurol Med Chir (Tokyo), 1998. **38**(11): p. 784-8.
50. Smith, B.T., M.J. Mulcahey, and R.R. Betz, *Development of an upper extremity FES system for individuals with C4 tetraplegia*. IEEE Trans Rehabil Eng, 1996. **4**(4): p. 264-70.
51. Hart, R.L., K.L. Kilgore, and P.H. Peckham, *A comparison between control methods for implanted FES hand-grasp systems*. IEEE Trans Rehabil Eng, 1998. **6**(2): p. 208-18.
52. Moss, C.W., K.L. Kilgore, and P.H. Peckham, *A novel command signal for motor neuroprosthetic control*. Neurorehabil Neural Repair, 2011. **25**(9): p. 847-54.
53. Scott, T.R. and M. Haugland, *Command and control interfaces for advanced neuroprosthetic applications*. Neuromodulation, 2001. **4**(4): p. 165-75.

54. Daly, J.J., et al., *Feasibility of a new application of noninvasive Brain Computer Interface (BCI): a case study of training for recovery of volitional motor control after stroke*. J Neurol Phys Ther, 2009. **33**(4): p. 203-11.
55. Lauer, R.T., P.H. Peckham, and K.L. Kilgore, *EEG-based control of a hand grasp neuroprosthesis*. Neuroreport, 1999. **10**(8): p. 1767-71.
56. Muller-Putz, G.R., et al., *EEG-based neuroprosthesis control: a step towards clinical practice*. Neurosci Lett, 2005. **382**(1-2): p. 169-74.
57. Rohm, M., et al., *Hybrid brain-computer interfaces and hybrid neuroprostheses for restoration of upper limb functions in individuals with high-level spinal cord injury*. Artif Intell Med, 2013. **59**(2): p. 133-42.
58. Wolpaw, J.R., *Brain-computer interfaces (BCIs) for communication and control: a mini-review*. Suppl Clin Neurophysiol, 2004. **57**: p. 607-13.
59. Akcakaya, M., et al., *Noninvasive brain-computer interfaces for augmentative and alternative communication*. IEEE Rev Biomed Eng, 2014. **7**: p. 31-49.
60. Farwell, L.A. and E. Donchin, *Talking off the top of your head: toward a mental prosthesis utilizing event-related brain potentials*. Electroencephalogr Clin Neurophysiol, 1988. **70**(6): p. 510-23.
61. Leeb, R., et al., *Self-paced (asynchronous) BCI control of a wheelchair in virtual environments: a case study with a tetraplegic*. Comput Intell Neurosci, 2007: p. 79642.
62. Wang, Y. and T.P. Jung, *A collaborative brain-computer interface for improving human performance*. PLoS One, 2011. **6**(5): p. e20422.
63. King, C.E., et al., *Operation of a brain-computer interface walking simulator for individuals with spinal cord injury*. J Neuroeng Rehabil, 2013. **10**: p. 77.
64. King, C.E., et al., *Noninvasive brain-computer interface driven hand orthosis*. Conf Proc IEEE Eng Med Biol Soc, 2011. **2011**: p. 5786-9.

65. Fok, S., et al., *An EEG-based brain computer interface for rehabilitation and restoration of hand control following stroke using ipsilateral cortical physiology*. Conf Proc IEEE Eng Med Biol Soc, 2011. **2011**: p. 6277-80.
66. Kreilinger, A., et al., *BCI and FES Training of a Spinal Cord Injured End-User to Control a Neuroprosthesis*. Biomed Tech (Berl), 2013.
67. Mulcahey, M.J., B.T. Smith, and R.R. Betz, *Psychometric rigor of the Grasp and Release Test for measuring functional limitation of persons with tetraplegia: a preliminary analysis*. J Spinal Cord Med, 2004. **27**(1): p. 41-6.
68. Roset, S.A., et al., *An adaptive brain actuated system for augmenting rehabilitation*. Front Neurosci, 2014. **8**: p. 415.
69. Takahashi, M., et al., *Event related desynchronization-modulated functional electrical stimulation system for stroke rehabilitation: a feasibility study*. J Neuroeng Rehabil, 2012. **9**: p. 56.
70. Do, A.H., et al., *Brain-computer interface controlled functional electrical stimulation system for ankle movement*. J Neuroeng Rehabil, 2011. **8**: p. 49.
71. Do, A.H., et al., *Brain-computer interface controlled functional electrical stimulation device for foot drop due to stroke*. Conf Proc IEEE Eng Med Biol Soc, 2012. **2012**: p. 6414-7.
72. Neuper, C., et al., *Motor imagery and EEG-based control of spelling devices and neuroprostheses*. Prog Brain Res, 2006. **159**: p. 393-409.
73. Cincotti, F., et al., *EEG-based Brain-Computer Interface to support post-stroke motor rehabilitation of the upper limb*. Conf Proc IEEE Eng Med Biol Soc, 2012. **2012**: p. 4112-5.
74. Barsi, G.I., et al., *Cortical excitability changes following grasping exercise augmented with electrical stimulation*. Exp Brain Res, 2008. **191**(1): p. 57-66.
75. Chatrian, G.E., M.C. Petersen, and J.A. Lazarte, *The blocking of the rolandic wicket rhythm and some central changes related to movement*. Electroencephalogr Clin Neurophysiol, 1959. **11**(3): p. 497-510.

76. Jasper, H. and W. Penfield, *Electrocorticograms in man: Effect of voluntary movement upon the electrical activity of the precentral gyrus*. *Archiv für Psychiatrie und Nervenkrankheiten*. **183**(1): p. 163-174.
77. Neuper, C., A. Schlogl, and G. Pfurtscheller, *Enhancement of left-right sensorimotor EEG differences during feedback-regulated motor imagery*. *J Clin Neurophysiol*, 1999. **16**(4): p. 373-82.
78. Pfurtscheller, G. and A. Aranibar, *Evaluation of event-related desynchronization (ERD) preceding and following voluntary self-paced movement*. *Electroencephalogr Clin Neurophysiol*, 1979. **46**(2): p. 138-46.
79. Dickhaus, T., et al., *Predicting BCI performance to study BCI illiteracy*. *BMC Neuroscience*, 2009. **10**(1): p. 1-2.
80. Pfurtscheller, G., *Functional topography during sensorimotor activation studied with event-related desynchronization mapping*. *J Clin Neurophysiol*, 1989. **6**(1): p. 75-84.
81. Blankertz, B., et al., *Neurophysiological predictor of SMR-based BCI performance*. *Neuroimage*, 2010. **51**(4): p. 1303-9.
82. Wolpaw, J.R., et al., *Timing of EEG-based cursor control*. *J Clin Neurophysiol*, 1997. **14**(6): p. 529-38.
83. Wolpaw, J.R., et al., *An EEG-based brain-computer interface for cursor control*. *Electroencephalogr Clin Neurophysiol*, 1991. **78**(3): p. 252-9.
84. Castro, A., F. Diaz, and G.J. van Boxtel, *How does a short history of spinal cord injury affect movement-related brain potentials?* *Eur J Neurosci*, 2007. **25**(9): p. 2927-34.
85. Gourab, K. and B.D. Schmit, *Changes in movement-related beta-band EEG signals in human spinal cord injury*. *Clin Neurophysiol*, 2010. **121**(12): p. 2017-23.
86. Green, J.B., et al., *Bereitschaft (readiness potential) and supplemental motor area interaction in movement generation: spinal cord injury and normal subjects*. *J Rehabil Res Dev*, 2003. **40**(3): p. 225-34.

87. Muller-Putz, G.R., et al., *Event-related beta EEG-changes during passive and attempted foot movements in paraplegic patients*. Brain Res, 2007. **1137**(1): p. 84-91.
88. Alkadhi, H., et al., *What disconnection tells about motor imagery: evidence from paraplegic patients*. Cereb Cortex, 2005. **15**(2): p. 131-40.
89. Onose, G., et al., *On the feasibility of using motor imagery EEG-based brain-computer interface in chronic tetraplegics for assistive robotic arm control: a clinical test and long-term post-trial follow-up*. Spinal Cord, 2012. **50**(8): p. 599-608.
90. Pfurtscheller, G., et al., *Discrimination of motor imagery-induced EEG patterns in patients with complete spinal cord injury*. Comput Intell Neurosci, 2009: p. 104180.
91. Lauer, R.T., et al., *Applications of cortical signals to neuroprosthetic control: a critical review*. IEEE Trans Rehabil Eng, 2000. **8**(2): p. 205-8.
92. Pfurtscheller, G., et al., *Brain oscillations control hand orthosis in a tetraplegic*. Neurosci Lett, 2000. **292**(3): p. 211-4.
93. Collinger, J.L., et al., *High-performance neuroprosthetic control by an individual with tetraplegia*. Lancet, 2013. **381**(9866): p. 557-64.
94. Gilja, V., et al., *A high-performance neural prosthesis enabled by control algorithm design*. Nat Neurosci, 2012. **15**(12): p. 1752-7.
95. Hochberg, L.R., et al., *Reach and grasp by people with tetraplegia using a neurally controlled robotic arm*. Nature, 2012. **485**(7398): p. 372-5.
96. Guger, C., et al., *Rapid prototyping of an EEG-based brain-computer interface (BCI)*. IEEE Trans Neural Syst Rehabil Eng, 2001. **9**(1): p. 49-58.
97. Guger, C., et al., *Design of an EEG-based brain-computer interface (BCI) from standard components running in real-time under Windows*. Biomed Tech (Berl), 1999. **44**(1-2): p. 12-6.

98. Pfurtscheller, G., et al., *Separability of EEG signals recorded during right and left motor imagery using adaptive autoregressive parameters*. IEEE Trans Rehabil Eng, 1998. **6**(3): p. 316-25.
99. Wolpaw, J.R., et al., *EEG-based communication: improved accuracy by response verification*. IEEE Trans Rehabil Eng, 1998. **6**(3): p. 326-33.
100. Blankertz, B., et al., *Boosting bit rates and error detection for the classification of fast-paced motor commands based on single-trial EEG analysis*. IEEE Trans Neural Syst Rehabil Eng, 2003. **11**(2): p. 127-31.
101. Schalk, G., et al., *EEG-based communication: presence of an error potential*. Clin Neurophysiol, 2000. **111**(12): p. 2138-44.
102. Holroyd, C.B. and M.G. Coles, *The neural basis of human error processing: reinforcement learning, dopamine, and the error-related negativity*. Psychol Rev, 2002. **109**(4): p. 679-709.
103. Falkenstein, M., et al., *ERP components on reaction errors and their functional significance: a tutorial*. Biol Psychol, 2000. **51**(2-3): p. 87-107.
104. Carter, C.S., et al., *Anterior cingulate cortex, error detection, and the online monitoring of performance*. Science, 1998. **280**(5364): p. 747-9.
105. Chavarriaga, R. and R. Millan Jdel, *Learning from EEG error-related potentials in noninvasive brain-computer interfaces*. IEEE Trans Neural Syst Rehabil Eng, 2010. **18**(4): p. 381-8.
106. Zhang, H., et al., *Improved recognition of error related potentials through the use of brain connectivity features*. Conf Proc IEEE Eng Med Biol Soc, 2012. **2012**: p. 6740-3.
107. Zhang, H., et al., *EEG-based decoding of error-related brain activity in a real-world driving task*. J Neural Eng, 2015. **12**(6): p. 066028.
108. Dunn, J.A., et al., *Measurement issues related to upper limb interventions in persons who have tetraplegia*. Hand Clin, 2008. **24**(2): p. 161-8, v.

109. Bryden, A., et al., *Assessing activity of daily living performance after implantation of an upper extremity neuroprosthesis*. Topics in Spinal Cord Injury Rehabilitation, 2008. **13**(4): p. 37-53.
110. Jebsen, R.H., et al., *An objective and standardized test of hand function*. Arch Phys Med Rehabil, 1969. **50**(6): p. 311-9.
111. Sollerman, C. and A. Ejeskar, *Sollerman hand function test. A standardised method and its use in tetraplegic patients*. Scand J Plast Reconstr Surg Hand Surg, 1995. **29**(2): p. 167-76.
112. Wuolle, K.S., et al., *Development of a quantitative hand grasp and release test for patients with tetraplegia using a hand neuroprosthesis*. J Hand Surg Am, 1994. **19**(2): p. 209-18.
113. Peckham, P.H., et al., *Efficacy of an implanted neuroprosthesis for restoring hand grasp in tetraplegia: a multicenter study*. Arch Phys Med Rehabil, 2001. **82**(10): p. 1380-8.
114. Stroh, K.C.V.D., C. L., *An ADL test to assess hand function with tetraplegic patients*. Journal of Hand Therapy, 1994. **7**(1): p. 47-48.
115. Waring, W.P., 3rd, et al., *2009 review and revisions of the international standards for the neurological classification of spinal cord injury*. J Spinal Cord Med, 2010. **33**(4): p. 346-52.
116. DiGiovanna, J., et al., *Coadaptive brain-machine interface via reinforcement learning*. IEEE Trans Biomed Eng, 2009. **56**(1): p. 54-64.
117. Taylor, D.M., S.I. Tillery, and A.B. Schwartz, *Direct cortical control of 3D neuroprosthetic devices*. Science, 2002. **296**(5574): p. 1829-32.
118. Orsborn, A.L., et al., *Closed-loop decoder adaptation on intermediate time-scales facilitates rapid BMI performance improvements independent of decoder initialization conditions*. IEEE Trans Neural Syst Rehabil Eng, 2012. **20**(4): p. 468-77.
119. Mahmoudi, B. and J.C. Sanchez, *A symbiotic brain-machine interface through value-based decision making*. PLoS One, 2011. **6**(3): p. e14760.

120. LeCun, Y., et al., *Efficient backprop*. Neural Networks: Tricks of the Trade, 1998. **1524**: p. 9-50.
121. P. Trappenberg, T., *Fundamentals of Computational Neuroscience*. 2002: Oxford University Press UK.
122. Qin, L., L. Ding, and B. He, *Motor imagery classification by means of source analysis for brain-computer interface applications*. J Neural Eng, 2004. **1**(3): p. 135-41.
123. Pohlmeier, E.A., et al., *Brain-Machine Interface control of a robot arm using actor-critic reinforcement learning*. Conf Proc IEEE Eng Med Biol Soc, 2012. **2012**: p. 4108-11.
124. Cramer, S.C., et al., *Effects of motor imagery training after chronic, complete spinal cord injury*. Exp Brain Res, 2007. **177**(2): p. 233-42.
125. Kübler, A., et al., *Predictability of Brain-Computer Communication*. Journal of Psychophysiology, 2004. **18**(2/3): p. 121-129.
126. Kubler, A., et al., *Brain-computer communication: self-regulation of slow cortical potentials for verbal communication*. Arch Phys Med Rehabil, 2001. **82**(11): p. 1533-9.
127. Fess, E. *The effects of Jaymar dynamometer handle position and test protocol on normal grip strength*. in *Journal of Hand Surgery-American Volume*. 1982. Churchill Livingstone Inc Medical Publishers, NY, NY 10011.
128. Neuper, C. and G. Pfurtscheller, *Event-related dynamics of cortical rhythms: frequency-specific features and functional correlates*. Int J Psychophysiol, 2001. **43**(1): p. 41-58.
129. Enzinger, C., et al., *Brain motor system function in a patient with complete spinal cord injury following extensive brain-computer interface training*. Exp Brain Res, 2008. **190**(2): p. 215-23.
130. Muller-Putz, G.R., I. Daly, and V. Kaiser, *Motor imagery-induced EEG patterns in individuals with spinal cord injury and their impact on brain-computer interface accuracy*. J Neural Eng, 2014. **11**(3): p. 035011.

131. Herbert, D., et al., *Altered brain wave activity in persons with chronic spinal cord injury*. Int J Neurosci, 2007. **117**(12): p. 1731-46.
132. Donoghue, J.P., S. Suner, and J.N. Sanes, *Dynamic organization of primary motor cortex output to target muscles in adult rats. II. Rapid reorganization following motor nerve lesions*. Exp Brain Res, 1990. **79**(3): p. 492-503.
133. Jain, N., K.C. Catania, and J.H. Kaas, *Deactivation and reactivation of somatosensory cortex after dorsal spinal cord injury*. Nature, 1997. **386**(6624): p. 495-8.
134. Vidaurre, C. and B. Blankertz, *Towards a cure for BCI illiteracy*. Brain Topogr, 2010. **23**(2): p. 194-8.
135. Thomas, C.K., et al., *Innervation and properties of the rat FDSBQ muscle: an animal model to evaluate voluntary muscle strength after incomplete spinal cord injury*. Exp Neurol, 1999. **158**(2): p. 279-89.
136. Blabe, C.H., et al., *Assessment of brain-machine interfaces from the perspective of people with paralysis*. J Neural Eng, 2015. **12**(4): p. 043002.
137. Snoek, G.J., et al., *Survey of the needs of patients with spinal cord injury: impact and priority for improvement in hand function in tetraplegics*. Spinal Cord, 2004. **42**(9): p. 526-32.
138. Gilja, V., et al., *Challenges and opportunities for next-generation intracortically based neural prostheses*. IEEE Trans Biomed Eng, 2011. **58**(7): p. 1891-9.

APPENDIX

Arduino Code for Muscle Stimulation

```
int incomingByte = 0; // for incoming serial data

// constants for RGB LED
const int TrigOut = 12; // Digital Output pin 12
const int Relay1 = 6; // Relay coil for First muscle stim
const int Relay2 = 8; // Relay coil for second muscle stim

void setup() {
  pinMode(TrigOut, OUTPUT); //Trigger going to Digitimer trigger input
  pinMode(Relay1, OUTPUT); //Relay1 to muscle1
  pinMode(Relay2, OUTPUT); //Relay2 to muscle2
  Serial.begin(9600); // Opens serial port, sets data rate to 9600 bps
  digitalWrite(Relay1, LOW);
  digitalWrite(Relay2, LOW);
}

int ii;
int jj;
void loop() {

  // send data only when you receive data:
  if (Serial.available() > 0) {
    // read the incoming byte:
    incomingByte = Serial.read();

    if (incomingByte==42){

      // send stimulation to the first muscle
      digitalWrite(Relay1,HIGH); //turn on relay coil 1
      for (ii=0;ii<70;ii++){
        digitalWrite(TrigOut,HIGH); //sends stim at 35 Hz for 140 cycles (4s), 70
cycles (2s)
        delay(0.02); //send trigger for stim for 20 microsec (0.02 ms) minimum
required is 5 microsec
        digitalWrite(TrigOut,LOW);
        delay(28.55); //send trigger pin low for 28.55 ms
      }
      digitalWrite(Relay1, LOW); //turn off relay coil 1

      // wait for a period of 200 ms
```

```

    delay(200);

    // send stimulation to the second muscle
    digitalWrite(Relay2,HIGH); //turn on relay coil 2
    for (jj=0;jj<100;jj++){
        digitalWrite(TrigOut,HIGH); //sends stim at 35 Hz for 140 cycles (4s), 120
cycles (3.43s)
        delay(0.02); //send trigger for stim for 20 microsec (0.02 ms) minimum
required is 5 microsec
        digitalWrite(TrigOut,LOW);
        delay(28.55); //send trigger pin low for 28.55 ms
        digitalWrite(TrigOut,LOW);
    }
    digitalWrite(Relay2, LOW); //turn off relay coil 2

    // wait for a period of 200 ms
    delay(200);

    // send stimulation to the first muscle
    digitalWrite(Relay1,HIGH); //turn on relay coil 1
    for (ii=0;ii<70;ii++){
        digitalWrite(TrigOut,HIGH); //sends stim at 35 Hz for 70 cycles (2s)
        delay(0.02); //send trigger for stim for 20 microsec (0.02 ms) minimum
required is 5 microsec
        digitalWrite(TrigOut,LOW);
        delay(28.55); //send trigger pin low for 28.55 ms
    }
    digitalWrite(Relay1, LOW); //turn off relay coil 1
}

else if (incomingByte==111){

    // send stimulation to the first muscle
    digitalWrite(Relay1,HIGH); //turn on relay coil 1
    for (ii=0;ii<140;ii++){
        digitalWrite(TrigOut,HIGH); //sends stim at 35 Hz for 140 cycles (4s)
        delay(0.02); //send trigger for stim for 20 microsec (0.02 ms) minimum
required is 5 microsec
        digitalWrite(TrigOut,LOW);
        delay(28.55); //send trigger pin low for 28.55 ms
    }
    digitalWrite(Relay1, LOW); //turn off relay coil 1

}

else if (incomingByte==99){

```

```
// send stimulation to the first muscle
  digitalWrite(Relay2,HIGH); //turn on relay coil 1
  for (ii=0;ii<140;ii++){
    digitalWrite(TrigOut,HIGH); //sends stim at 35 Hz for 140 cycles (4s)
    delay(0.02); //send trigger for stim for 20 microsec (0.02 ms) minimum
required is 5 microsec
    digitalWrite(TrigOut,LOW);
    delay(28.55); //send trigger pin low for 28.55 ms
  }
  digitalWrite(Relay2, LOW); //turn off relay coil 1
}

// say what you got:
Serial.print("I received: ");
Serial.println(incomingByte, DEC);
}
}
```


Matlab Code for Experiment: First Training Block

```

%Step 1: 3 seconds of rest, 5 seconds for motor imagery, 8 seconds for
stimulation. Given "correct"
%as feedback for each trialConfigured for X24 (ch mapping below)

%X10 Channel mapping: 123456 7EKG[1], 8POz[2], 9Fz[3], 10Cz[4],
11C3[5], 12C4[6], 13F3[7], 14F4[8], 15P3[9], 16P4[10]
%X24 Channel mapping: 123456 7F3[1], 8F1[2], 9Fz[3], 10F2[4], 11F4[5],
12C3[6],
%13C1[7], 14Cz[8], 15C2[9], 16C4[10], 17CPz[11], 18P3[12], 19P1[13],
%20Pz[14], 21P2[15], 22P4[16], 23POz[17], 24O1[18], 25Oz[19], 26O2[20],
%27ECG[21], 28AUX1[22],29AUX2[23],30AUX3[24]

function [action_start, action_end, action_recording, error_recording]
= robot_arm_step1_Amanda_Lauren_Amanda_2_25_15(subjID,trial_num)

%%%%%%%%%%%%%%%%%%%%%%%%%%%%%%%%%%%%%%%%%%%%%%%%%%%%%%%%%%%%%%%%%%%%%%%%
% HEADSET INITIALIZATION AND FILE DESTINATION SETTING
%%%%%%%%%%%%%%%%%%%%%%%%%%%%%%%%%%%%%%%%%%%%%%%%%%%%%%%%%%%%%%%%%%%%%%%%

    cd 'C:\ABM\B-Alert\SDK\SampleClients\TestSDKMatlab'
    %CheckImpedance = 1;

    timestamp = clock;
    subjID='HW';
    trial_num='1';
    filename = [subjID, '_', trial_num, '_', date, '_', num2str(timestamp(4)),
    '_', num2str(timestamp(5)), '_'];
    [devChN, devComPort, devNumCh, devEKGPos, devESUtp,
devTSp]=abmsdk('GetDeviceInfo');
    deviceType = (devNumCh<24)+1; %ABM_DEVICE_X10Standard=2
ABM_DEVICE_X24Standard=1
    [status]=abmsdk('SetDestinationFile',[cd '\\' filename '.eps']);
    [status]=abmsdk('InitSession',deviceType,0,-1,0);
    [status]=abmsdk('StartAcquisition');

%%%%%%%%%%%%%%%%%%%%%%%%%%%%%%%%%%%%%%%%%%%%%%%%%%%%%%%%%%%%%%%%%%%%%%%%
% VARIABLE INITIALIZATION
%%%%%%%%%%%%%%%%%%%%%%%%%%%%%%%%%%%%%%%%%%%%%%%%%%%%%%%%%%%%%%%%%%%%%%%%

    total_trials =40;

    if deviceType == 2
        ChannelCoeff = 16;
    else
        ChannelCoeff = 30;
    end

%x24 setup 12C3[6], 14Cz[8]

```



```

%Get the EEG and ESU Time Data
clear eeg_ddata_current tsrdata_current
eeg_ddata_current = zeros(1,ChannelCoeff);
eeg_ddata_current = abmsdk('GetRawData');
tsrdata_current = abmsdk('GetTimeStampsStreamData',0);
while size(eeg_ddata_current,2) ~= ChannelCoeff
    eeg_ddata_current = abmsdk('GetRawData');
    tsrdata_current = abmsdk('GetTimeStampsStreamData',0);
end
eeg_ddata = vertcat(eeg_ddata,eeg_ddata_current(:,,:));
ESU_time = vertcat(ESU_time,tsrdata_current);
ESU_time_reshaped = reshape(ESU_time,4,[]);
ESU_time_reshaped = ESU_time_reshaped.';
ESU_time_reshaped = double(ESU_time_reshaped);
time = bsxfun(@times,ESU_time_reshaped,ESU_Coeff);
eeg_time = sum(time,2);

%Assigns the 'Rest Start' as the last passed ESU time stamp
rest_start(i)= eeg_time(end);

% While the last called ESU time is less than 8.1 seconds
% continue looping and collecting data

while eeg_time(end) <= rest_start(end)+3100

    figure(1)
    axis off
    str=sprintf('    RELAX \nDon''t Move!');
    text(.23,.5,str,'FontSize',80)
    text(.05, 0.9, ['Trial ' num2str(i) ' of '
num2str(total_trials)],'FontSize', 20)

    %Get the EEG and ESU Time Data
    eeg_ddata_current = abmsdk('GetRawData');
    tsrdata_current = abmsdk('GetTimeStampsStreamData',0);
    if size(eeg_ddata_current,2) == ChannelCoeff
        eeg_ddata = vertcat(eeg_ddata,eeg_ddata_current(:,,:));
        ESU_time = vertcat(ESU_time,tsrdata_current);
        ESU_time_reshaped = reshape(ESU_time,4,[]);
        ESU_time_reshaped = ESU_time_reshaped.';
        ESU_time_reshaped = double(ESU_time_reshaped);
        time = bsxfun(@times,ESU_time_reshaped,ESU_Coeff);
        eeg_time = sum(time,2);
    end

end

%%%%%%%%%%%%%%%%%%%%%%%%%%%%%%%%%%%%%%%%%%%%%%%%%%%%%%%%%%%%%%%%%%%%%%%%
% SAVE REST EEG DATA
%%%%%%%%%%%%%%%%%%%%%%%%%%%%%%%%%%%%%%%%%%%%%%%%%%%%%%%%%%%%%%%%%%%%%%%%

%Find the index of the 'Rest Start'

```

```

    find_rest_start(i) = find(eeg_time>=rest_start(i),1);
    %Create a EEG data entry for the error recording
    rest_recording(i,1:768,:) =
eeg_ddata(find_rest_start(i):find_rest_start(i)+767,:);
    n=5; %filter order
    Wn1 = [5 35]/fs; %pass signals between 0.5 and 75
    ftype = 'bandpass';
    [b,a] = butter(n,Wn1,ftype); %transfer function
    m=0;
    rest_filt(i,:)=filter(b,a,rest_recording(i,:,12));
    smoo=5;
    rest_power(i,:)=(rest_filt(i,:)).^2;
    rest_sm_power(i,:)=smooth(rest_power(i,:),smoo);
    while (m*50+50)<768
        rest_sm_power1(i,m+1)=mean(rest_sm_power(i,m*50+1:m*50+50));
        m=m+1;
    end
    rest_sm_power2=mean(rest_sm_power1);
    average_rest_power=mean(rest_sm_power2);
%
fft_rest(i,:)=abs(fftshift(fft(rest_recording(i,:,c3_electrode)))).^2;
%     f=-fs/2:fs/(size(rest_recording,2)-1):fs/2;
%     minbin=5;
%     maxbin=15;
%
mean_rest(i)=mean(fft_rest(i,find(floor(f)==minbin):find(floor(f)==maxb
in)));
%     average_rest_power=mean(mean_rest);

%%%%%%%%%%%%%%%%%%%%%%%%%%%%%%%%%%%%%%%%%%%%%%%%%%%%%%%%%%%%%%%%%%%%%%%%
% GOAL DISPLAY
%%%%%%%%%%%%%%%%%%%%%%%%%%%%%%%%%%%%%%%%%%%%%%%%%%%%%%%%%%%%%%%%%%%%%%%%

%Get the EEG and ESU Time Data
eeg_ddata_current = abmsdk('GetRawData');%abmsdk('GetRawData');
tsrdata_current = abmsdk('GetTimeStampsStreamData',0);
while size(eeg_ddata_current,2) ~= ChannelCoeff
    eeg_ddata_current = abmsdk('GetRawData');%abmsdk('GetRawData');
    tsrdata_current = abmsdk('GetTimeStampsStreamData',0);
end
size(eeg_ddata_current);
eeg_ddata = vertcat(eeg_ddata,eeg_ddata_current(:,,:));
ESU_time = vertcat(ESU_time,tsrdata_current);
ESU_time_reshaped = reshape(ESU_time,4,[]);
ESU_time_reshaped = ESU_time_reshaped.';
ESU_time_reshaped = double(ESU_time_reshaped);
time = bsxfun(@times,ESU_time_reshaped,ESU_Coeff);
eeg_time = sum(time,2);

%Assigns the 'Action Start' as the last passed ESU time stamp
action_start(i)= eeg_time(end);

eeg_time_current = 0;
tsrdata_current = zeros(4,1);

```

```

    %Assigns the 'Action End' for that trial (i) as 5100 MS post
    'Action
    %Start'
    action_end(i) = action_start(i)+5100;
    % While the last called ESU time is less than 5 seconds (1280
samples)
    % continue looping and collecting data
    power_z=[];

clear ERD mean_action
q=1;
sound_time=0:0.05:1000;
ready_sound=0.5*sin(1*pi*sound_time);
while eeg_time(end) <= action_end(i)

    if q==1
        sound(ready_sound,5e4)
    end
clear eeg_ddata_current tsrdata_current eeg_time_current

figure(1)
subplot(211)
axis off
subplot(211)
h1=text(.4,.2,'MOVE','FontSize',70,'Color','k');

%Get the EEG and ESU Time Data
eeg_ddata_current = abmsdk('GetRawData');%abmsdk('GetRawData');
tsrdata_current = abmsdk('GetTimeStampsStreamData',0);
%If new data is present:
if size(eeg_ddata_current,2) == ChannelCoeff
    eeg_ddata = vertcat(eeg_ddata,eeg_ddata_current);
    ESU_time = vertcat(ESU_time,tsrdata_current);

    figure(1)
    subplot(212)
    zero_line=zeros(1,30);
    plot(zero_line,'k')
    hold on
    e = size(eeg_ddata,1);
    z=[];

    if q==1
        z=eeg_ddata(find(eeg_time>=action_start(i),1)-
50:e,c3_electrode);
    %
        fft_action=abs(fftshift(fft(z))).^2;
    %
        f=-fs/2:fs/(length(z)-1):fs/2;
    %
        minbin=5;
    %
        maxbin=15;
    %
mean_action(q)=mean(fft_action(find(floor(f)==minbin):find(floor(f)==ma
xbin)));

    action_filt=filter(b,a,z);
    action_power=(action_filt).^2;
    action_sm_power=smooth(action_power,smoo);
    mean_action(q)=mean(action_sm_power);

```

```

        ERD(q)=-1*((mean_action(q)-
average_rest_power)/average_rest_power)*100;
        power_z=[power_z ERD(q)];
        if ERD(q)>0
            plot(power_z, 'g', 'LineWidth', 2)
        else
            plot(power_z, 'r', 'LineWidth', 2)
        end
        xlim([0 30])
        ylim([-200 200])
        drawnow
        q=q+1;
    end

    if eeg_time(end) > action_start(i) + 200*q
        z=eeg_ddata(e-150:e,c3_electrode);
        %         fft_action=abs(fftshift(fft(z))).^2;
        %         f=-fs/2:fs/(length(z)-1):fs/2;
        %         minbin=5;
        %         maxbin=15;
        %
mean_action(q)=mean(fft_action(find(floor(f)==minbin):find(floor(f)==ma
xbin)));

        action_filt=filter(b,a,z);
        action_power=(action_filt).^2;
        action_sm_power=smooth(action_power,smoo);
        mean_action(q)=mean(action_sm_power(end-100:end-50));
        ERD(q)=-1*((mean_action(q)-
average_rest_power)/average_rest_power)*100;
        power_z=[power_z ERD(q)];
        if ERD(q)>0
            plot(power_z, 'g', 'LineWidth', 2)
        else
            plot(power_z, 'r', 'LineWidth', 2)
        end
        xlim([0 30])
        ylim([-200 200])
        drawnow
        q=q+1;
    end

    %Get the EEG and ESU Time Data
    eeg_ddata_current =
abmsdk('GetRawData');%abmsdk('GetRawData');
    tsrdata_current = abmsdk('GetTimeStampsStreamData',0);
    while size(eeg_ddata_current,2) ~= ChannelCoeff
        eeg_ddata_current =
abmsdk('GetRawData');%abmsdk('GetRawData');
        tsrdata_current = abmsdk('GetTimeStampsStreamData',0);
    end
    size(eeg_ddata_current);
    eeg_ddata = vertcat(eeg_ddata,eeg_ddata_current(:,,:));
    ESU_time = vertcat(ESU_time,tsrdata_current);
    ESU_time_reshaped = reshape(ESU_time,4,[]);
    ESU_time_reshaped = ESU_time_reshaped.';

```

```

        ESU_time_resaped = double(ESU_time_resaped);
        time = bsxfun(@times,ESU_time_resaped,ESU_Coeff);
        eeg_time = sum(time,2);

        x = action_end(i) - eeg_time(end);
    end

    if x <120
        delete(h1)
        clf
    end
end

%Get the EEG and ESU Time Data
eeg_ddata_current = abmsdk('GetRawData');%abmsdk('GetRawData');
tsrdata_current = abmsdk('GetTimeStampsStreamData',0);
if size(eeg_ddata_current,2) == ChannelCoeff
    eeg_ddata = vertcat(eeg_ddata,eeg_ddata_current(:,:));
    ESU_time = vertcat(ESU_time,tsrdata_current);
    ESU_time_resaped = reshape(ESU_time,4,[]);
    ESU_time_resaped = ESU_time_resaped.';
    ESU_time_resaped = double(ESU_time_resaped);
    time = bsxfun(@times,ESU_time_resaped,ESU_Coeff);
    eeg_time = sum(time,2);
end

clf

%%%%%%%%%%%%%%%%%%%%%%%%%%%%%%%%%%%%%%%%%%%%%%%%%%%%%%%%%%%%%%%%%%%%%%%%
% SAVE ACTION EEG DATA
%%%%%%%%%%%%%%%%%%%%%%%%%%%%%%%%%%%%%%%%%%%%%%%%%%%%%%%%%%%%%%%%%%%%%%%%

    %Find the index of the 'Action Start'
    find_action_start(i) = find(eeg_time>=action_start(i),1);
    %Find the index of the 'Action End'
    end_of_action(i) = find_action_start(i)+1279;
    %Create a EEG data entry for the action recording
    action_recording(i,1:1280,:) =
eeg_ddata(find_action_start(i):end_of_action(i),:);

%%%%%%%%%%%%%%%%%%%%%%%%%%%%%%%%%%%%%%%%%%%%%%%%%%%%%%%%%%%%%%%%%%%%%%%%
% RESULTS DISPLAY
%%%%%%%%%%%%%%%%%%%%%%%%%%%%%%%%%%%%%%%%%%%%%%%%%%%%%%%%%%%%%%%%%%%%%%%%

clf

%Get the EEG and ESU Time Data
clear eeg_ddata_current tsrdata_current
eeg_ddata_current = zeros(1,ChannelCoeff);
eeg_ddata_current = abmsdk('GetRawData');
tsrdata_current = abmsdk('GetTimeStampsStreamData',0);
while size(eeg_ddata_current,2) ~= ChannelCoeff
    eeg_ddata_current = abmsdk('GetRawData');
    tsrdata_current = abmsdk('GetTimeStampsStreamData',0);
end

```

```

end
eeg_ddata = vertcat(eeg_ddata,eeg_ddata_current(:,:));
ESU_time = vertcat(ESU_time,tsrdata_current);
ESU_time_reshaped = reshape(ESU_time,4,[]);
ESU_time_reshaped = ESU_time_reshaped.';
ESU_time_reshaped = double(ESU_time_reshaped);
time = bsxfun(@times,ESU_time_reshaped,ESU_Coeff);
eeg_time = sum(time,2);

%Assigns the 'Error Start' as the last passed ESU time stamp
error_start(i)= eeg_time(end);
error_d(i) = 1;

% Sending '*' to Arduino (8 second stim)
fwrite(s,42,'int8');

% While the last called ESU time is less than 8.1 seconds
% continue looping and collecting data
q=1;
sound_time=0:0.05:300;
correct_sound=0.5*sin(5*pi*sound_time);
while eeg_time(end) <= error_start(end)+8100
    if q==1;
        sound(correct_sound)
    end
    figure(1)
    axis off
    text(.3,.5,'STOP','FontSize',70,'Color',[0,0.5,0])

    %Get the EEG and ESU Time Data
    eeg_ddata_current = abmsdk('GetRawData');
    tsrdata_current = abmsdk('GetTimeStampsStreamData',0);
    if size(eeg_ddata_current,2) == ChannelCoeff
        eeg_ddata = vertcat(eeg_ddata,eeg_ddata_current(:,:));
        ESU_time = vertcat(ESU_time,tsrdata_current);
        ESU_time_reshaped = reshape(ESU_time,4,[]);
        ESU_time_reshaped = ESU_time_reshaped.';
        ESU_time_reshaped = double(ESU_time_reshaped);
        time = bsxfun(@times,ESU_time_reshaped,ESU_Coeff);
        eeg_time = sum(time,2);
    end
    q=q+1;
end

%%%%%%%%%%%%%%%%%%%%%%%%%%%%%%%%%%%%%%%%%%%%%%%%%%%%%%%%%%%%%%%%%%%%%%%%
% SAVE ERROR EEG DATA
%%%%%%%%%%%%%%%%%%%%%%%%%%%%%%%%%%%%%%%%%%%%%%%%%%%%%%%%%%%%%%%%%%%%%%%%

%Find the index of the 'Error Start'
find_error_start(i) = find(eeg_time>=error_start(i),1);
%Create a EEG data entry for the error recording
error_recording(i,1:2048,:) =
eeg_ddata(find_error_start(i):find_error_start(i)+2047,:);

```



```
        i=i+1;

end

ESU_time_reshaped = reshape(ESU_time,4,[]);
ESU_time_reshaped = ESU_time_reshaped.';
ESU_time_reshaped = double(ESU_time_reshaped);
time = bsxfun(@times,ESU_time_reshaped,ESU_Coeff);
eeg_time = sum(time,2);

[status] = abmsdk('StopAcquisition');
save(fullfile(pwd,[filename,'_step1.mat']));

fclose(s);
close all

fprintf('\n\n*** EXPERIMENT COMPLETE ***\n\n');
```

Matlab Code for Experiment: Subsequent Training Blocks

```
%X10 Channel mapping: 123456 7EKG[1], 8POz[2], 9Fz[3], 10Cz[4],
11C3[5], 12C4[6], 13F3[7], 14F4[8], 15P3[9], 16P4[10]
%X24 Channel mapping: 123456 7F3[1], 8F1[2], 9Fz[3], 10F2[4], 11F4[5],
12C3[6],
%13C1[7], 14Cz[8], 15C2[9], 16C4[10], 17CPz[11], 18P3[12], 19P1[13],
%20Pz[14], 21P2[15], 22P4[16], 23POz[17], 24O1[18], 25Oz[19], 26O2[20],
%27ECG[21], 28AUX1[22],29AUX2[23],30AUX3[24]
```

```
function robot_arm_step3()
```

```
%%%%%%%%%%%%%%%%%%%%%%%%%%%%%%%%%%%%%%%%%%%%%%%%%%%%%%%%%%%%%%%%%%%%%%%%
% LOAD IN TRAINING DATA
%%%%%%%%%%%%%%%%%%%%%%%%%%%%%%%%%%%%%%%%%%%%%%%%%%%%%%%%%%%%%%%%%%%%%%%%
```

```
file={
'C:\ABM\B-Alert\SDK\SampleClients\TestSDKMatlab\MR_1_02-Mar-
2016_11_22__step3.mat',
'C:\ABM\B-Alert\SDK\SampleClients\TestSDKMatlab\MR_2_02-Mar-
2016_11_38__step3.mat',
'C:\ABM\B-Alert\SDK\SampleClients\TestSDKMatlab\MR_3_02-Mar-
2016_11_57__step3.mat',
'C:\ABM\B-Alert\SDK\SampleClients\TestSDKMatlab\MR_1_03-Mar-
2016_11_19__step3.mat',
'C:\ABM\B-Alert\SDK\SampleClients\TestSDKMatlab\MR_2_03-Mar-
2016_11_37__step3.mat'
}
```

```
move1 = [];
rest1 = [];
```

```
%Load data and clear
for filenum = 1 : length(file)
    load(file{filenum})
    move1 = cat(1,move1,action_recording(:,128:895,:));
    rest1 = cat(1,rest1,rest_recording(:, :, :));
end
```

```
clearvars -except move1 rest1
```

```
%Filter signal
eeg = cat(1,move1,rest1);
label = [ones(1,size(move1,1)), zeros(1,size(rest1,1))];
train=eeg;
train_label = label;
```

```
%Channels for SVM classification features
```

```
channels=[12 13 14 15 16];
fs=256;
disp('Extracting features...')
for m=1:size(train,1)
    c=1;
    for a=1:length(channels)
        for b=1:6
            p=abs(fftshift(fft(train(m, :, channels(a))))).^2;
```

```

        f=-fs/2:fs/(size(train,2)-1):fs/2;
        minbin=5*b+1;
        maxbin=5*b+5;
        %5Hz bin width average power features

power_bin(b)=mean(p(find(floor(f)==minbin):find(floor(f)==maxbin)));
        train_features(m,c)=power_bin(b);
        c=c+1;
    end
end
end
disp('Training...')
SVMStruct = svmtrain(train_features,train_label,'Kernel_Function',
'linear'); %train
clearvars -except train train_label eeg train_features SVMStruct

%%%%%%%%%%%%%%%%%%%%%%%%%%%%%%%%%%%%%%%%%%%%%%%%%%%%%%%%%%%%%%%%%%%%%%%%
% HEADSET INITIALIZATION AND FILE DESTINATION SETTING
%%%%%%%%%%%%%%%%%%%%%%%%%%%%%%%%%%%%%%%%%%%%%%%%%%%%%%%%%%%%%%%%%%%%%%%%

cd 'C:\ABM\B-Alert\SDK\SampleClients\TestSDKMatlab'

timestamp = clock;
subjID='MR';
trial_num='3';
filename = [subjID,'_',trial_num,'_',date, '_',num2str(timestamp(4)),
'_', num2str(timestamp(5)), '_'];

[devChN, devComPort, devNumCh, devEKGPos, devESUtp,
devTSp]=abmsdk('GetDeviceInfo');
deviceType = (devNumCh<24)+1; %ABM_DEVICE_X10Standard=2
ABM_DEVICE_X24Standard=1
[status]=abmsdk('SetDestinationFile',[cd '\ ' filename '.ebs']);
[status]=abmsdk('InitSession',deviceType,0,-1,0);
[status]=abmsdk('StartAcquisition');

%x24 setup 10C3[6], 12Cz[8]
c3_electrode = 12;
cz_electrode = 14;

%Sampling frequency
fs=256;

%Channels for SVM classification features
channels=[12 13 14 15 16];

total_trials = 40;

if deviceType == 2
    ChannelCoeff = 16;
else
    ChannelCoeff = 30;
end

%Initialize variables to store data

```

```

clear eeg_ddata
clear eeg_time
ESU_time = zeros(4,1);
eeg_time = 0;
eeg_time_current = 0;
eeg_ddata = zeros(1,ChannelCoeff);
eeg_ddata_current = zeros(1,ChannelCoeff);
tsrdata_current = zeros(4,1);
ESU_Coeff = [16777216,65536,256,1];

%Loop through all trials
i = 1;

%delete serial ports so that they can be defined and used
delete(instrfind);

s = serial('COM3','BaudRate', 9600,'timeout',.05);
fopen(s);

% Calls ABM twice to clear data in registers
decon_clear = abmsdk('GetRawData');
tsrdata_current = abmsdk('GetTimeStampsStreamData',0);
decon_clear = abmsdk('GetRawData');
tsrdata_current = abmsdk('GetTimeStampsStreamData',0);

%%%%%%%%%%%%%%%%%%%%%%%%%%%%%%%%%%%%%%%%%%%%%%%%%%%%%%%%%%%%%%%%%%%%%%%%
%%%%%%%%%%%%%%%%%%%%%%%%%%%%%%%%%%%%%%%%%%%%%%%%%%%%%%%%%%%%%%%%%%%%%%%%
% EXPERIMENT BEGIN
%%%%%%%%%%%%%%%%%%%%%%%%%%%%%%%%%%%%%%%%%%%%%%%%%%%%%%%%%%%%%%%%%%%%%%%%
%%%%%%%%%%%%%%%%%%%%%%%%%%%%%%%%%%%%%%%%%%%%%%%%%%%%%%%%%%%%%%%%%%%%%%%%

figure(1)
set(figure(1),'Units', 'Normalized', 'OuterPosition', [0 0 1 1]);
axis off
text(.125,.5,'-----+-----','FontSize',40)
waitforbuttonpress

while (i <= total_trials);

    fprintf('\n\n*** TRIAL: %d ***\n\n', i);
    clf

%%%%%%%%%%%%%%%%%%%%%%%%%%%%%%%%%%%%%%%%%%%%%%%%%%%%%%%%%%%%%%%%%%%%%%%%
% REST DISPLAY
%%%%%%%%%%%%%%%%%%%%%%%%%%%%%%%%%%%%%%%%%%%%%%%%%%%%%%%%%%%%%%%%%%%%%%%%

    %Get the EEG and ESU Time Data
    clear eeg_ddata_current tsrdata_current

```

```

eeg_ddata_current = abmsdk('GetRawData');
tsrdata_current = abmsdk('GetTimeStampsStreamData',0);
while size(eeg_ddata_current,2) ~= ChannelCoeff
    eeg_ddata_current = abmsdk('GetRawData');
    tsrdata_current = abmsdk('GetTimeStampsStreamData',0);
end
eeg_ddata = vertcat(eeg_ddata,eeg_ddata_current(:,,:));
ESU_time = vertcat(ESU_time,tsrdata_current);
ESU_time_reshaped = reshape(ESU_time,4,[]);
ESU_time_reshaped = ESU_time_reshaped.';
ESU_time_reshaped = double(ESU_time_reshaped);
time = bsxfun(@times,ESU_time_reshaped,ESU_Coeff);
eeg_time = sum(time,2);

%Assigns the 'Rest Start' as the last passed ESU time stamp
rest_start(i)= eeg_time(end);

% While the last called ESU time is less than 8.1 seconds
% continue looping and collecting data

while eeg_time(end) <= rest_start(end)+3100

    figure(1)
    axis off
    str=sprintf('    RELAX \nDon''t Move!');
    text(.23,.5,str,'FontSize',80)
    text(.05, 0.9, ['Trial ' num2str(i) ' of '
num2str(total_trials)], 'FontSize', 20)
    %Get the EEG and ESU Time Data
    eeg_ddata_current = abmsdk('GetRawData');
    tsrdata_current = abmsdk('GetTimeStampsStreamData',0);
    if size(eeg_ddata_current,2) == ChannelCoeff
        eeg_ddata = vertcat(eeg_ddata,eeg_ddata_current(:,,:));
        ESU_time = vertcat(ESU_time,tsrdata_current);
        ESU_time_reshaped = reshape(ESU_time,4,[]);
        ESU_time_reshaped = ESU_time_reshaped.';
        ESU_time_reshaped = double(ESU_time_reshaped);
        time = bsxfun(@times,ESU_time_reshaped,ESU_Coeff);
        eeg_time = sum(time,2);
    end
end

%%%%%%%%%%%%%%%%%%%%%%%%%%%%%%%%%%%%%%%%%%%%%%%%%%%%%%%%%%%%%%%%%%%%%%%%
% SAVE REST EEG DATA
%%%%%%%%%%%%%%%%%%%%%%%%%%%%%%%%%%%%%%%%%%%%%%%%%%%%%%%%%%%%%%%%%%%%%%%%

%Find the index of the 'Rest Start'
find_rest_start(i) = find(eeg_time>=rest_start(i),1);
%Create a EEG data entry for the error recording
rest_recording(i,1:768,:) =
eeg_ddata(find_rest_start(i):find_rest_start(i)+767,:);
n=5; %filter order
Wn1 = [5 20]/fs; %pass signals between 5 and 20
ftype = 'bandpass';
[b1,a1] = butter(n,Wn1,ftype); %transfer function
m=0;

```

```

smoo=5;
rest_filt(i,:)=filter(b1,a1,rest_recording(i,:,12));
rest_power(i,:)=(rest_filt(i,:)).^2;
rest_sm_power(i,:)=smooth(rest_power(i,:),smoo);
while (m*50+50)<768
    rest_sm_power1(i,m+1)=mean(rest_sm_power(i,m*50+1:m*50+50));
    m=m+1;
end
rest_sm_power2=mean(rest_sm_power1);
average_rest_power=mean(rest_sm_power2);
test_eeg_rest=rest_recording(i,:,:);

test_features_rest=[];
for m=1:size(test_eeg_rest,1)
    c=1;
    for a=1:length(channels)
        for b=1:6

p=abs(fftshift(fft(test_eeg_rest(1,:,channels(a))))).^2;
        f=-fs/2:fs/(size(test_eeg_rest,2)-1):fs/2;
        minbin=5*b+1;
        maxbin=5*b+5;
        %5Hz bin width average power features

power_bin_rest(b)=mean(p(find(floor(f)==minbin):find(floor(f)==maxbin)
));
        test_features_rest(m,c)=power_bin_rest(b);
        c=c+1;
        end
    end
end

clear p power_bin_rest
%Result = 1 for expected movement, result = 0 for expected rest
svm_result_rest=svmclassify(SVMStruct,test_features_rest)
if svm_result_rest==0
    rest_classification_performance_over_iterations(i)=1;
end
if svm_result_rest==1
    rest_classification_performance_over_iterations(i)=0;
end

%%%%%%%%%%%%%%%%%%%%%%%%%%%%%%%%%%%%%%%%%%%%%%%%%%%%%%%%%%%%%%%%%%%%%%%%
% GOAL DISPLAY
%%%%%%%%%%%%%%%%%%%%%%%%%%%%%%%%%%%%%%%%%%%%%%%%%%%%%%%%%%%%%%%%%%%%%%%%

%Get the EEG and ESU Time Data
eeg_ddata_current = abmsdk('GetRawData');%abmsdk('GetRawData');
tsrdata_current = abmsdk('GetTimeStampsStreamData',0);
while size(eeg_ddata_current,2) ~= ChannelCoeff
    eeg_ddata_current = abmsdk('GetRawData');%abmsdk('GetRawData');
    tsrdata_current = abmsdk('GetTimeStampsStreamData',0);
end
eeg_ddata = vertcat(eeg_ddata,eeg_ddata_current(:,:,));

```

```

ESU_time = vertcat(ESU_time,tsrdata_current);
ESU_time_reshaped = reshape(ESU_time,4,[]);
ESU_time_reshaped = ESU_time_reshaped.';
ESU_time_reshaped = double(ESU_time_reshaped);
time = bsxfun(@times,ESU_time_reshaped,ESU_Coeff);
eeg_time = sum(time,2);

%Assigns the 'Action Start' as the last passed ESU time stamp
action_start(i)= eeg_time(end);

eeg_time_current = 0;
tsrdata_current = zeros(4,1);
%Assigns the 'Action End' for that trial (i) as 5100 MS post
'Action
%Start'
action_end(i) = action_start(i)+5100;

% While the last called ESU time is less than 5 seconds (1280
samples)
% continue looping and collecting data
power_z=[];
q=1;
sound_time=0:0.05:1000;
ready_sound=0.5*sin(1*pi*sound_time);
while eeg_time(end) <= action_end(i)
    if q==1
        sound(ready_sound,5e4)
    end
    clear eeg_ddata_current tsrdata_current eeg_time_current

    figure(1)
    subplot(211)
    axis off
    subplot(211)
    h1=text(.4,.2,'MOVE','FontSize',70,'Color','k');

    %Get the EEG and ESU Time Data
    eeg_ddata_current = abmsdk('GetRawData');
    tsrdata_current = abmsdk('GetTimeStampsStreamData',0);
    if size(eeg_ddata_current,2) == ChannelCoeff
        eeg_ddata = vertcat(eeg_ddata,eeg_ddata_current(:,,:));
        ESU_time = vertcat(ESU_time,tsrdata_current);

        figure(1)
        subplot(212)
        zero_line=zeros(1,30);
        plot(zero_line,'k')
        hold on
        e = size(eeg_ddata,1);
        z=[];

        if q==1
            z=eeg_ddata(find(eeg_time>=action_start(i),1)-
50:e,c3_electrode);

            action_filt=filter(b1,a1,z);

```

```

        action_power=(action_filt).^2;
        action_sm_power=smooth(action_power,smoo);
        mean_action(q)=mean(action_sm_power);
        ERD(q)=-1*((mean_action(q)-
average_rest_power)/average_rest_power)*100;
        power_z=[power_z ERD(q)];
        if ERD(q)>0
            plot(power_z,'g','LineWidth',2)
        else
            plot(power_z,'r','LineWidth',2)
        end
        xlim([0 30])
        ylim([-200 200])
        drawnow
        q=q+1;
    end

    if eeg_time(end) > action_start(i) + 200*q
        z=eeg_ddata(e-150:e,c3_electrode);

        action_filt=filter(b1,a1,z);
        action_power=(action_filt).^2;
        action_sm_power=smooth(action_power,smoo);
        mean_action(q)=mean(action_sm_power(end-100:end-50));
        ERD(q)=-1*((mean_action(q)-
average_rest_power)/average_rest_power)*100;
        power_z=[power_z ERD(q)];
        if ERD(q)>0
            plot(power_z,'g','LineWidth',2)
        else
            plot(power_z,'r','LineWidth',2)
        end
        xlim([0 30])
        ylim([-200 200])
        drawnow
        q=q+1;
    end

    %Get the EEG and ESU Time Data
    eeg_ddata_current =
abmsdk('GetRawData');%abmsdk('GetRawData');
    tsrdata_current = abmsdk('GetTimeStampsStreamData',0);
    while size(eeg_ddata_current,2) ~= ChannelCoeff
        eeg_ddata_current =
abmsdk('GetRawData');%abmsdk('GetRawData');
        tsrdata_current = abmsdk('GetTimeStampsStreamData',0);
    end
    size(eeg_ddata_current);
    eeg_ddata = vertcat(eeg_ddata,eeg_ddata_current(:,,:));
    ESU_time = vertcat(ESU_time,tsrdata_current);
    ESU_time_reshaped = reshape(ESU_time,4,[]);
    ESU_time_reshaped = ESU_time_reshaped.';
    ESU_time_reshaped = double(ESU_time_reshaped);
    time = bsxfun(@times,ESU_time_reshaped,ESU_Coeff);
    eeg_time = sum(time,2);
    x = action_end(i) - eeg_time(end);

```



```

end

if x <120
    delete(h1)
    clf
end
end

clf

%Get the EEG and ESU Time Data
eeg_ddata_current = abmsdk('GetRawData');%abmsdk('GetRawData');
tsrdata_current = abmsdk('GetTimeStampsStreamData',0);
if size(eeg_ddata_current,2) == ChannelCoeff
    eeg_ddata = vertcat(eeg_ddata,eeg_ddata_current(:, :));
    ESU_time = vertcat(ESU_time,tsrdata_current);
    ESU_time_reshaped = reshape(ESU_time,4, []);
    ESU_time_reshaped = ESU_time_reshaped.';
    ESU_time_reshaped = double(ESU_time_reshaped);
    time = bsxfun(@times,ESU_time_reshaped,ESU_Coeff);
    eeg_time = sum(time,2);
end

%%%%%%%%%%%%%%%%%%%%%%%%%%%%%%%%%%%%%%%%%%%%%%%%%%%%%%%%%%%%%%%%%%%%%%%%
% SAVE ACTION EEG DATA
%%%%%%%%%%%%%%%%%%%%%%%%%%%%%%%%%%%%%%%%%%%%%%%%%%%%%%%%%%%%%%%%%%%%%%%%

%Find the index of the 'Action Start'
    find_action_start(i) = find(eeg_time>=action_start(i),1);
%Find the index of the 'Action End'
    end_of_action(i) = find_action_start(i)+1279;
%Create a EEG data entry for the action recording
    action_recording(i,1:1280,:) =
eeg_ddata(find_action_start(i):end_of_action(i),:);

%%%%%%%%%%%%%%%%%%%%%%%%%%%%%%%%%%%%%%%%%%%%%%%%%%%%%%%%%%%%%%%%%%%%%%%%
% SVM CLASSIFICATION
%%%%%%%%%%%%%%%%%%%%%%%%%%%%%%%%%%%%%%%%%%%%%%%%%%%%%%%%%%%%%%%%%%%%%%%%

test_eeg_move=action_recording(i,128:895,:);

test_features_move=[];
for m=1:size(test_eeg_move,1)
    c=1;
    for a=1:length(channels)
        for b=1:6

p=abs(fftshift(fft(test_eeg_move(1, :, channels(a))))).^2;
        f=-fs/2:fs/(size(test_eeg_move,2)-1):fs/2;
        minbin=5*b+1;
        maxbin=5*b+5;
        %5Hz bin width average power features

```

```

power_bin_move(b)=mean(p(find(floor(f)==minbin):find(floor(f)==maxbin)
);
        test_features_move(m,c)=power_bin_move(b);
        c=c+1;
    end
end
end
clear p power_bin_move svm_result_move
%Result = 1 for expected movement, result = 0 for expected rest
svm_result_move=svmclassify(SVMStruct,test_features_move)

if svm_result_move==1
    action_classifier_performance=1;
elseif svm_result_move==0
    action_classifier_performance=0;
end

%%%%%%%%%%%%%%%%%%%%%%%%%%%%%%%%%%%%%%%%%%%%%%%%%%%%%%%%%%%%%%%%%%%%%%%%
% RESULTS DISPLAY
%%%%%%%%%%%%%%%%%%%%%%%%%%%%%%%%%%%%%%%%%%%%%%%%%%%%%%%%%%%%%%%%%%%%%%%%

clf

%Get the EEG and ESU Time Data
clear eeg_ddata_current tsrdata_current
eeg_ddata_current = abmsdk('GetRawData');
tsrdata_current = abmsdk('GetTimeStampsStreamData',0);
while size(eeg_ddata_current,2) ~= ChannelCoeff
    eeg_ddata_current = abmsdk('GetRawData');
    tsrdata_current = abmsdk('GetTimeStampsStreamData',0);
end
eeg_ddata = vertcat(eeg_ddata,eeg_ddata_current(:,,:));
ESU_time = vertcat(ESU_time,tsrdata_current);
ESU_time_reshaped = reshape(ESU_time,4,[]);
ESU_time_reshaped = ESU_time_reshaped.';
ESU_time_reshaped = double(ESU_time_reshaped);
time = bsxfun(@times,ESU_time_reshaped,ESU_Coeff);
eeg_time = sum(time,2);

%Assigns the 'Error Start' as the last passed ESU time stamp
error_start(i)= eeg_time(end);

if action_classifier_performance == 1;
    fwrite(s,42,'int8');
end

    action_classifier_performance_over_iterations(i) =
action_classifier_performance;

eeg_time_current = 0;
tsrdata_current = zeros(4,1);

% While the last called ESU time is less than 2.1 seconds
% continue looping and collecting data

```

```

q=1;
sound_time=0:0.05:1000;
correct_sound=0.5*sin(3*pi*sound_time);
wrong_sound=10*sin(0.05*pi*sound_time);
if action_classifier_performance == 1;
    error_d(i) = 1;
    while eeg_time(end) <= error_start(end)+8100
        if q==1
            sound(correct_sound,5e4)
        end
        figure(1)
        axis off
        text(.3,.5,'CORRECT','FontSize',70,'Color',[0,0.5,0])

        %Get the EEG and ESU Time Data
        eeg_ddata_current = abmsdk('GetRawData');
        tsrdata_current = abmsdk('GetTimeStampsStreamData',0);
        if size(eeg_ddata_current,2) == ChannelCoeff
            eeg_ddata = vertcat(eeg_ddata,eeg_ddata_current(:,,:));
            ESU_time = vertcat(ESU_time,tsrdata_current);
            ESU_time_reshaped = reshape(ESU_time,4,[]);
            ESU_time_reshaped = ESU_time_reshaped.';
            ESU_time_reshaped = double(ESU_time_reshaped);
            time = bsxfun(@times,ESU_time_reshaped,ESU_Coeff);
            eeg_time = sum(time,2);
        end
        q=q+1;
    end
end

if action_classifier_performance == 0;
    error_d(i) = -1;
    while eeg_time(end) <= error_start(end)+3100
        if q==1
            sound(wrong_sound,5e4)
        end
        figure(1)
        axis off
        text(.3,.5,'WRONG','FontSize',70,'Color','r')

        %Get the EEG and ESU Time Data
        eeg_ddata_current = abmsdk('GetRawData');
        tsrdata_current = abmsdk('GetTimeStampsStreamData',0);
        if size(eeg_ddata_current,2) == ChannelCoeff
            eeg_ddata = vertcat(eeg_ddata,eeg_ddata_current(:,,:));
            ESU_time = vertcat(ESU_time,tsrdata_current);
            ESU_time_reshaped = reshape(ESU_time,4,[]);
            ESU_time_reshaped = ESU_time_reshaped.';
            ESU_time_reshaped = double(ESU_time_reshaped);
            time = bsxfun(@times,ESU_time_reshaped,ESU_Coeff);
            eeg_time = sum(time,2);
        end
        q=q+1;
    end
end
end

```

```

%%%%%%%%%%%%%%%%%%%%%%%%%%%%%%%%%%%%%%%%%%%%%%%%%%%%%%%%%%%%%%%%%%%%%%%%
% SAVE ERROR EEG DATA
%%%%%%%%%%%%%%%%%%%%%%%%%%%%%%%%%%%%%%%%%%%%%%%%%%%%%%%%%%%%%%%%%%%%%%%%

    %Find the index of the 'Error Start'
    find_error_start(i) = find(eeg_time>=error_start(i),1);
    %Create a EEG data entry for the error recording
    error_recording(i,1:2048,:)=zeros(2048,ChannelCoeff);

    if action_classifier_performance == 1;
        error_recording(i,1:2048,:) =
eeg_ddata(find_error_start(i):find_error_start(i)+2047,:);
    end

    if action_classifier_performance == 0;
        error_recording(i,1:768,:) =
eeg_ddata(find_error_start(i):find_error_start(i)+767,:);
    end

%%%%%%%%%%%%%%%%%%%%%%%%%%%%%%%%%%%%%%%%%%%%%%%%%%%%%%%%%%%%%%%%%%%%%%%%
clear new_data
clf
figure(1)
axis off
pause(0.1)
text(.125,.5,'-----+-----')
', 'FontSize', 40)
pause(0.1)

m=size(train,1);

new_data=cat(1,action_recording(i,128:895,:),rest_recording(i,:,:));
for new=1:2
    train(m+new,:,:)= new_data(new,:,:);
end

train_label=[train_label 1 0];

for new=1:2
    c=1;
    for a=1:length(channels)
        for b=1:6
            p=abs(fftshift(fft(train(m+new,:,channels(a))))).^2;
            f=-fs/2:fs/(size(train,2)-1):fs/2;
            minbin=5*b+1;
            maxbin=5*b+5;
            %5Hz bin width average power features

power_bin(b)=mean(p(find(floor(f)==minbin):find(floor(f)==maxbin)));
            train_features(m+new,c)=power_bin(b);
            c=c+1;
        end
    end
end
clear p power_bin test_eeg test_eeg_filt

```

```
        SVMStruct = svmtrain(train_features,train_label,'Kernel_Function',  
'linear'); %train  
        i=i+1;  
  
end  
  
ESU_time_reshaped = reshape(ESU_time,4,[]);  
ESU_time_reshaped = ESU_time_reshaped.';  
ESU_time_reshaped = double(ESU_time_reshaped);  
time = bsxfun(@times,ESU_time_reshaped,ESU_Coeff);  
eeg_time = sum(time,2);  
  
% Saves data recorded  
save(fullfile(pwd,[filename,'_step3.mat']));  
  
[status] = abmsdk('StopAcquisition');  
  
fclose(s);  
close all  
  
fprintf('\n\n*** EXPERIMENT COMPLETE ***\n\n');
```